JUNE 2026 | VOLUME 24 | ISSUE 6

BioProcess International
by informa

COVERING THE WHOLE DEVELOPMENT PROCESS
FOR THE GLOBAL BIOTECHNOLOGY INDUSTRY

Special Edition

The Best of BPI

- Interoperability and Big Data at the 2025 NIIMBL National Meeting
- Blood Centers Support Reliable Supply Chains for Cell and Gene Therapies
- Integrating Quality by Design Principles for Gene-Therapy Programs
- Development of a Closed-System Approach for Downstream Processing of Large Viruses
- Monitoring and Control of Adenovirus Processes with Real-Time Multiangle Light Scattering
- Sterilization-Lethality Calculations Are Not Enough
- Empowering Safe and Sterile Environments for Biomanufacturing
- Sponsored Contributions on Mesenchymal Stem Cells, Host-Cell Protein Quantification, Antibody–Drug Conjugate Process Development, and Controlled Freezing for Biologics

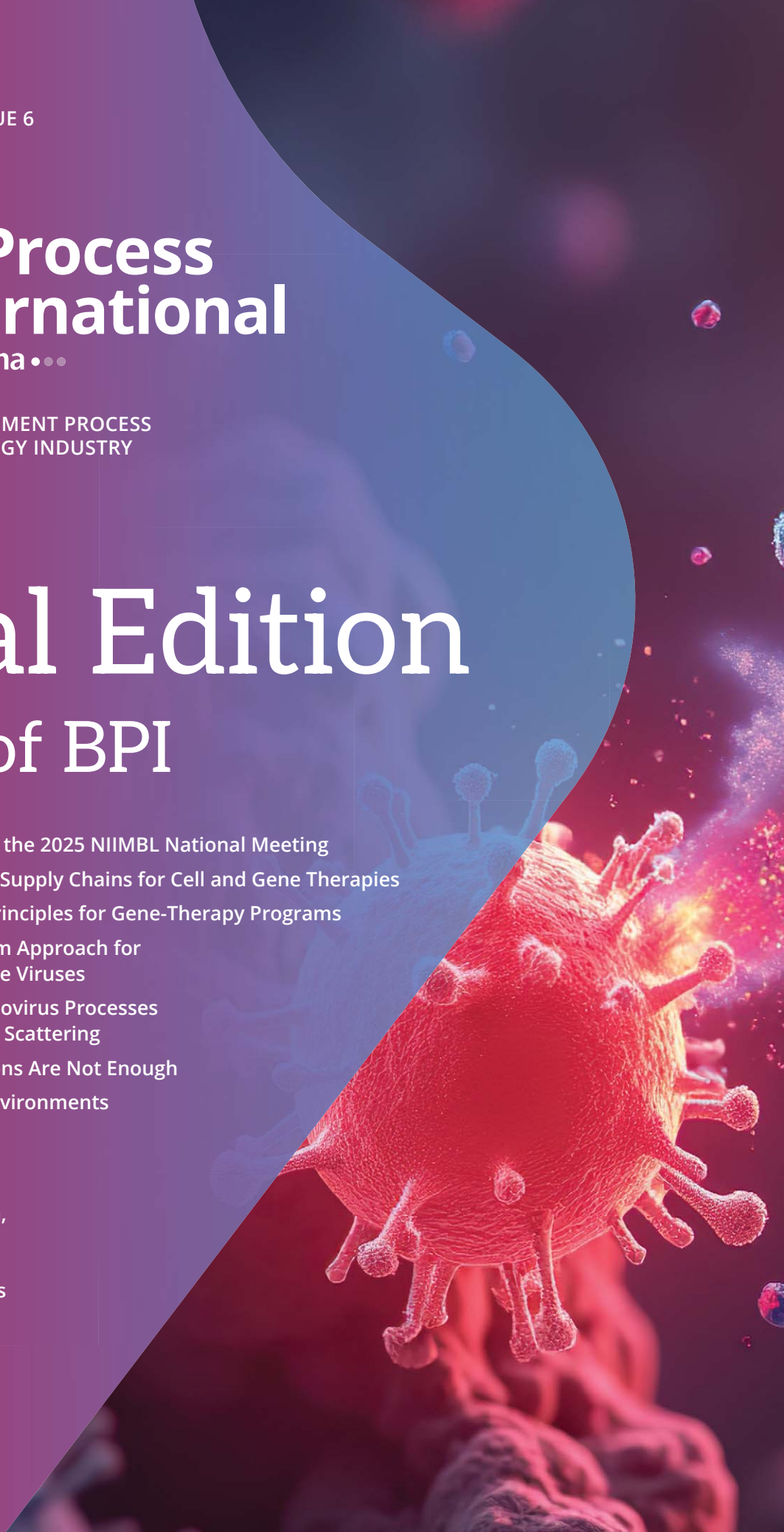

BioProcessIntl.com

WuXi Biologics
Global Solution Provider

Every biologic can be made

As a leading CRDMO, WuXi Biologics integrates biologics services from concept through commercialization, delivering quality at every stage. We perform under the most demanding conditions, advancing programs at unmatched speed with expertise and assurance.

Multi-modality discovery generates development-ready assets built for continuity. DNA reaches IND in as little as 6 months, fueling a growing pipeline that supports over 660 IND approvals and 25 commercial manufacturing programs.

RESEARCH
From Target to Lead Identification

DEVELOPMENT
6 Months from DNA to IND

MANUFACTURING
Global Dual Sourcing

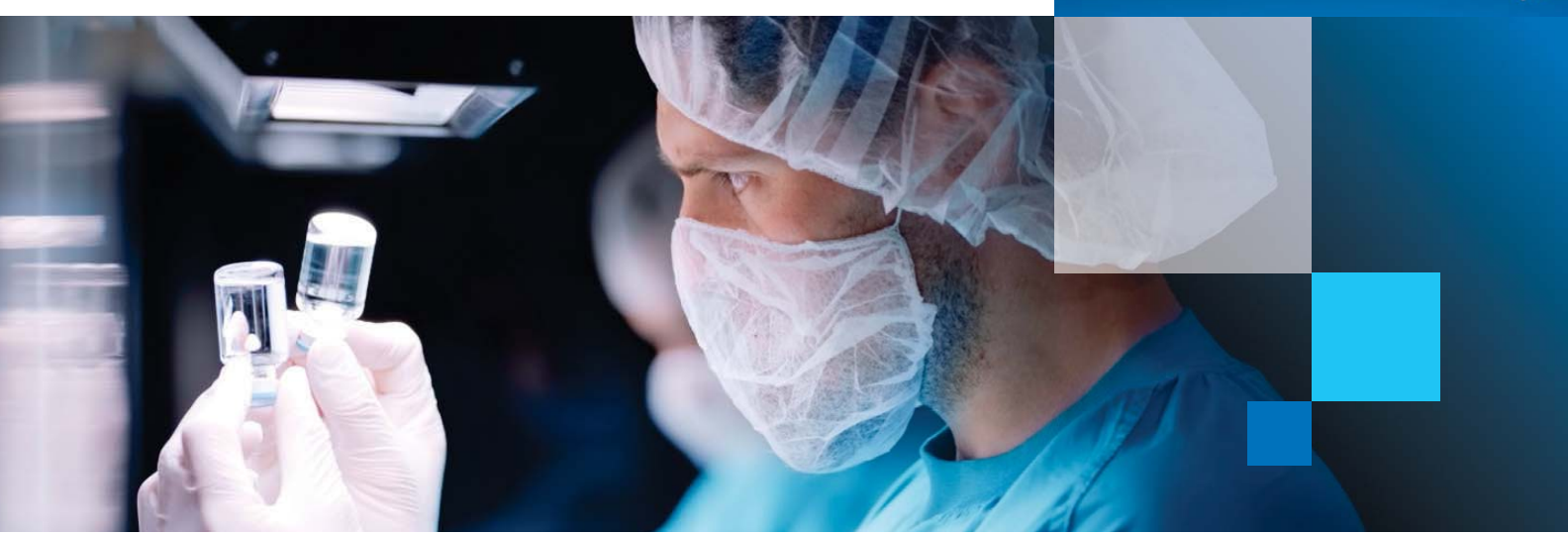

CRDMO
EVERY BIOLOGIC CAN BE MADE

The world's leading global single-source platform from concept to commercialization.

Connect with Us
wuxibiologics.com

BioProcess International

JUNE 2026
VOLUME 24 ISSUE 6

On the Cover Advanced therapies such as treatments leveraging chimeric antigen receptor (CAR) T cells, pictured below, face unique manufacturing and supply-chain obstacles (HTTPS://STOCK.ADOBE.COM). *Find us online at https://www.bioprocessintl.com.*

NANO PAUSE

Chris Spivey
Industry Relations and Strategic Partnerships Director, BPI

Entering a new era in biologics creates a need to pause, reflect, and rethink what we know. My aim, as the new Industry Relations and Strategic Partnerships Director for BioProcess International, is to foster and cultivate stronger partnerships and alliances for our media and events. Along with the scientific and commercial rationale for enabling alignment and productivity for the industry, there is also an inherent cross-pollination of ideas and perspectives between BPI's media and events audiences that can enhance and elevate what we can achieve collectively.

The gordian knot of translating new therapies into patient access abandons silos and vacates insular thinking. The concept of "community" should not fade as we leave a conference or a symposium, but persist through new structures, services, and associations. Somewhat ironically, social media, while a menace in many contexts, might well be an ally and a lubricant in the context of holding our community together a full 365 days each year.

At Informa, we are in the process of reengineering our media arm to more closely align with current consumption modes, styles, and tastes. Thus, BPI's, peer-reviewed technical articles and business-focused nontechnical pieces will more naturally combine with event-created content and discovery. This fusion of expected and unexpected connected content will gather us in mutual advancement with a sustainable sense of focus and purpose. We need to do better year long, not just during event gatherings. And we will.

This new era for our industry sets previously unimaginable goals. Former US President Joe Biden called for a cancer moonshot in 2022 to reduce "age-standardized [cancer] mortality rates by at least 50% over the next 25 years in the US." The Coalition for Epidemic Preparedness Innovations (CEPI) has called for a similar paradigm shift, articulating a 100 Days Mission in which "vaccines should be ready for initial authorization and manufacturing at scale within 100 days of recognition of pathogen with pandemic potential, when appropriate."

Traditional biologics goals of producing large amounts of drug product for one-size-fits-all medications are now beginning their sunsets. Emerging are more effective goals that require smaller doses for a limited number of patients or even a single patient. This evolution transforms the connective tissue of not only drug discovery, development, and formulation, but also the supply chain and our methods and means of delivery. Some novel biologics need to be produced on site at a hospital or somewhere nearby — on the spoke of the wheel — then shipped expeditiously, as turnaround expectations from diagnosis to treatment are now measured in days and weeks, not months. Thus, modern modalities call for entirely new skillsets and organizational structures, which are barely yet invented. This is not "building the plane while you fly" and requires the kinds of insights and muscle memory seldom (if ever) seen inside one entity or organizational profile.

PROCESS DEVELOPMENT | ANALYTICS | PRODUCTION | QUALITY

BEST IN CLASS BIOLOGICS CDMO OVER 35 YEARS!

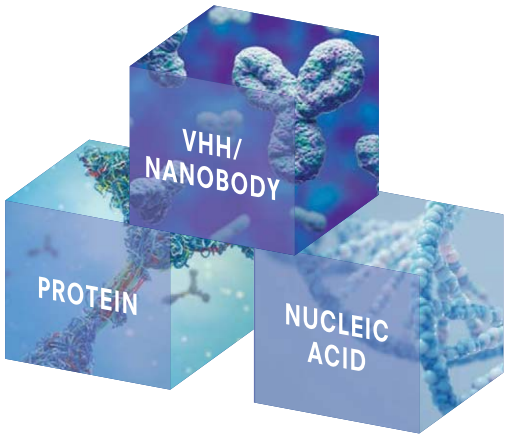

YOUR PRODUCT – OUR COMPETENCE AND DEDICATION

Richter Biologics is your professional and experienced partner offering CDMO solutions from gene to product all from one source.

Richter Biologics: your expert for late stage and commercial production.

RICHTER BIOLOGICS
Suhrenkamp 59, 22335 Hamburg, Germany
Phone: +49 40 55290-0
BusinessDevelopment@richterbiologics.eu

CONTACT US TO BRING YOUR PROJECT TO SUCCESS!

RICHTER BIOLOGICS

https://www.bioprocessintl.com/ebooks

BPI's June 2026 eBooks will discuss chromatography and manufacturing capacity. And look for our August 2026 featured report on cell lines and expression systems.

Focus on Data

The 2025 National Institute for Innovation in Manufacturing Biopharmaceuticals (NIIMBL) National Meeting featured sessions by the organization's Big Data Program on shared data challenges within the biopharmaceutical industry. A key focus was interoperability across diverse manufacturing technologies and information systems, as described on **page 6.** Presenters emphasized the importance of collaboration and shared data standards, which will help different systems and stakeholders to work together on platforms, data formats, and protocols.

Focus on CGTs

Because cell therapies are fragile, living, and often patient-specific products with time-sensitive logistics, drug developers will need to seek out collaborators to help scale such medicines safely and equitably. Thankfully, such partners might already be present. Writers from the blood-products industry highlight how community blood centers are uniquely suited to supporting cell-therapy supply chains on **page 12.** By leveraging experience as the backbone of transfusion medicine, blood centers could provide reliable starting-material supply, end-to-end chain of identity and custody, and other services that will be essential to the future of cell and gene therapy (CGT) scalability.

Focus on Quality

Some CGT-industry representatives repeat the misleading assertion that "the process is not the product" in the case of advanced therapies, implying that changes to manufacturing processes will be inconsequential so long as quality testing returns favorable results. But such testing neither fully predicts an advanced therapy's clinical performance nor captures subtle shifts in its biological activity. On **page 14,** industry consultant Mo Heidaran asserts that quality by design (QbD) principles must be extended to CGT products and implemented early in their development. He emphasizes the clinical relevance of critical quality attributes (CQAs), the challenges of correlating potency assays with product efficacy, and the need for statistical rigor when assessing comparability after manufacturing changes.

Development of a Closed-System Approach for Downstream Processing of Large Viruses

Ensuring sterility during manufacture of virus-based drug products is critical for patient safety, particularly when viral particles are too large to permit filtration through standard 0.2-µm sterilizing-grade filters. Large viruses such as poxviruses require bespoke process adaptations to meet current good manufacturing practice (CGMP) standards while maintaining process integrity. The authors describe their establishment of a fully closed system for downstream processing of poxvirus to minimize manual intervention and contamination risk. On **page 18,** they outline the design, implementation, and validation of the system; discuss associated challenges and solutions; and present key lessons learned through use of vaccinia virus as a model organism.

Monitoring and Control of Adenovirus Processes with RT-MALS

A primary difficulty in downstream development for adenovirus products is the lack of a means for rapid determination of identity, purity, titer, and other quality attributes. On **page 22,** the writers provide proof of concept for using real-time multiangle light scattering (RT-MALS) analysis for instantaneous measurements of viral-vector particle size and titer during downstream and fill–finish operations.

Sterilization Assurance Demands More

Achieving a sterilization lethality (F_0) value of ≥12 minutes at 121.1 °C long has been deemed the cornerstone of steam-in-place (SIP) validation. However, as the authors show, such an F_0 calculation does guarantee sufficient sterilization: Residual air can still prevent saturated steam from contacting all surfaces. The authors present recommendations for taking a holistic approach to sterilization assurance on **page 28.**

Surface Coatings in Cleanrooms

High-performance coatings are a foundational component of cleanroom design, promoting sterility, durability, and cleaning efficiency. By investing in such solutions, biopharmaceutical manufacturers can enhance facility safety, ensure regulatory compliance, and prevent costly process delays. Sharon L. Lee of Sherwin-Williams Protective & Marine discusses the advantages of such specialized coatings on **page 47.**

On the Supplier Side

An interview with Corning Life Sciences representatives on **page 36** covers engineered mesenchymal stem cells (MSCs) for targeted delivery of anticancer payloads. An article from Cygnus shares results of highly sensitive host-cell protein (HCP) quantification on **page 38.** Authors from Repligen present a case study for antibody–drug conjugate (ADC) process development on **page 40.** And an article from Single Use Support discusses controlled freezing of biologics on **page 44.**

Lonza
Integrated Biologics

DNA to IND in as little as 6 months*

Speed.
Not Setbacks.

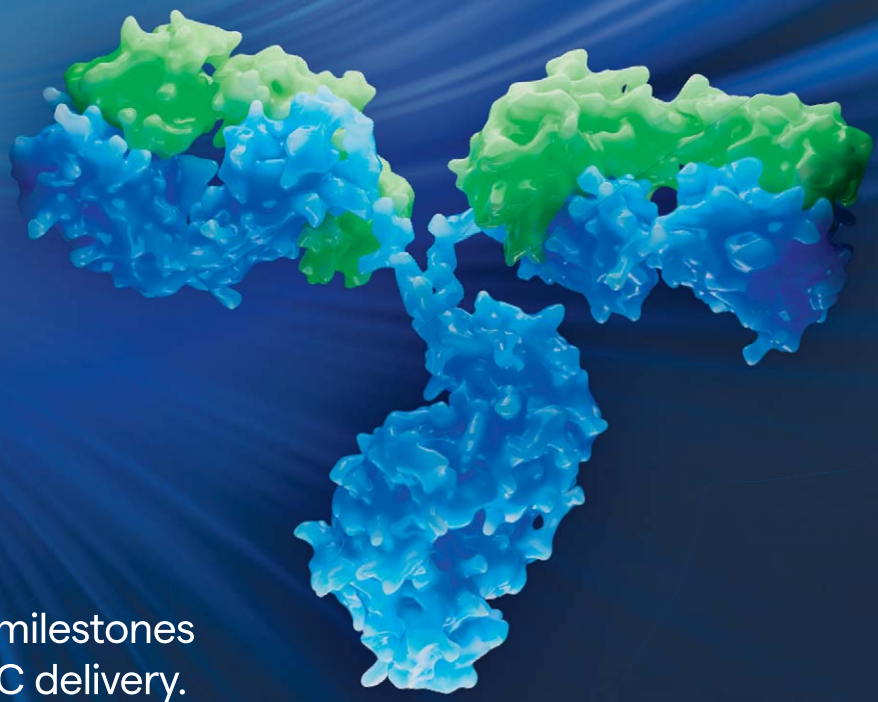

Power through preclinical milestones with certainty. Trusted CMC delivery. Decades of regulatory expertise. Reliable performance. All in one.

Visit us at BIO International in San Diego, 22–25 June 2026 Booth #4735

Find out more

*T&Cs apply.

Meeting the Challenge of Interoperability for Improved Process Performance in Biomanufacturing

Roger Hart, Emily Carson, Barry Buckland, and Kelvin H. Lee

Biopharmaceutical advancements across research, development, and manufacturing create increasingly large and complex datasets. The volume of data collected continues to grow in every biopharmaceutical laboratory, pilot plant, and manufacturing facility using new in-line and at-line detectors as well as multivariate analytical methods. Moreover, the industry continues to evolve, with electronic laboratory notebooks (ELNs), novel manufacturing recipes, enhanced process models, and improved integration of supply chains generating data throughout each product's life cycle.

The Big Data Program within the National Institute for Innovation in Manufacturing Biopharmaceuticals (NIIMBL) seeks to develop tools and systems that can manage such data to help companies optimize productivity, reduce costs, and realize novel therapeutic possibilities. One program goal is to improve the ability to manufacture biotherapeutics at low cost to meet high quality standards through both identifying and funding projects as well as leading initiatives that convene subject-matter experts (SMEs) from across the industrial base to answer urgent and complex problems.

As an industry-driven consortium, NIIMBL relies on its members to identify useful projects and to participate where they can contribute expertise. The diverse workstreams across NIIMBL's programs and member-funded projects encourage active engagement. Those workstreams also provide opportunities to coordinate efforts and address needs in process design, operations, quality control, supply chain and logistics, technology transfer, and facilities and engineering. One shared concern is how to use big data more effectively to enable application of sophisticated models, including machine learning/artificial intelligence (ML/AI) tools.

Through a 2023 roadmapping workshop that gathered more than 200 participants, the Big Data Program sought to develop an updated understanding of associated hurdles faced by the industry. Among issues expressed in detail through this industry-wide session, interoperability stood out as both a major need and a significant challenge. It could be made possible through standardization of data connectivity, data syntax, and data meaning expressed by an ontology.

Shared Interest in Advancing Big Data

The NIIMBL 2025 National Meeting was held in Washington, DC, on 23–27 June 2025. Restricted to members only, the annual gathering emphasizes engaged participation by SMEs. The active company membership includes large pharmaceutical companies, biotechnology innovators, contract manufacturing organizations (CMOs), contract development and manufacturing organizations (CDMOs), equipment and analytical-instrument vendors, developers of process-control systems, and data-handling companies. Leading academics and specialists from the US Food and Drug Administration (FDA) also attended the meeting, contributing to provide structure and using their expertise in developing a common framework for presenting process data. Much of the meeting was dedicated to discussion of projects funded by NIIMBL, particularly those

involving big data. Speakers from industry, academia, manufacturing, and the government addressed common big-data concerns about interoperability as well as data structure and management.

An Interoperability Conceptual Framework

Interoperability refers to the integration of diverse manufacturing technologies to achieve seamless data exchange and functionality across information systems. That goal is achieved through successful implementation of different levels of integration, ranging from technical to conceptual (Table 1). Thomas Cornish (senior manager and automation engineer at Pfizer) described first-level (L1) connectivity as "the ability of two or more systems or components to exchange information and to use the information that has been exchanged." The need for interoperability has increased with the volume of data relating to manufacturing processes and the need for its rapid dissemination to enable control and decisions.

Thomas Cornish (senior manager and automation engineer at Pfizer) discussed the need for rapid dissemination of interoperability to enable control and decisions in biomanufacturing.

"Data is the new oil," said Stephen Wing (principal business development manager, eData Exchange, at MilliporeSigma). "To implement ML and AI, we need access to data in the right format," Wing continued, referencing the common data structure (schema) achieved in a second level (L2) of interoperability (Table 1).

However, competition among technology suppliers remains a hurdle to interoperability. Vendors can enable interoperability within their vertically integrated systems when such systems comprise their equipment and use proprietary software. But end users might be compelled to use manufacturing and analytical equipment from more than one vendor. For example, the same Raman probe from different suppliers generates the same data, stored and transmitted in different formats, creating difficulty for digesting and analysis using different systems. Customer demand can drive coordination among those systems to implement interoperability. But biomanufacturing end users have

Table 1: The interoperability conceptual framework depicts cumulative maturity levels in which each level necessitates achieving the capabilities of the previous (adapted from **1**). BoM = bill of materials, COR-BA = common object request broker architecture, DEVS = discrete event system specification, DoDAF = US Department of Defense architecture framework, HLA-OMT = high-level architecture object model template, MDA = manufacturing data analytics, OWL = web ontology language, RPR-FOM = real-time platform reference federation object model, SOAP = simple object access protocol, SysML = systems modeling language, UML = unified modeling language, XML = explainable machine learning

Level	Name	Premise	Information Needed	Description	Prescriptive Requirements	Common Engineering Approaches
L6	Conceptual	Common conceptual model	Assumptions, constraints	Interoperating systems are aware of each other's information, processes, contexts, and modeling assumptions.	Shared understanding of a system's conceptual model (exposing its information, processes, states, and operations)	DoDAF, military missions to means framework, platform independent model-driven architecture, SysML
L5	Dynamic	Common execution model	Data effects	Interoperating systems reorient information production and consumption based on understood changes to meaning and context.	Ability to produce and understand definitions of meaning and context	Ontology for services, UML artifacts, DEVS, complete UML, BoM
Ontology						
L4	Pragmatic	Common workflow model	Data use	Interoperating systems are aware of context and meaning of information being exchanged.	Methods for sharing term definitions and anticipating context	Taxonomies, UML artifacts, in-particular-sequence diagrams, DEVS, OWL, MDA
L3	Semantic	Common reference model	Data meaning	Interoperating systems exchange sets of terms that can be parsed semantically.	Agreement among all systems on term sets that grammatically satisfies syntactic-level solution requirements	Common reference model, dictionaries, glossaries, protocol data units, RPR-FOM
Schema						
L2	Syntactic	Common data structure	Structured data	Systems have an agreed protocol to exchange the correct forms of data in the proper order; meaning of data elements is not yet established.	Protocol supported by technical-level solutions	XML, HLA-OMT, interface description language, COR-BA, SOAP
Connectivity						
L1	Technical	Common communication protocol	Bits, bytes	Systems have technical connections and can exchange data among each other.	Ability to produce and consume data in exchange with other systems	Network connection standards

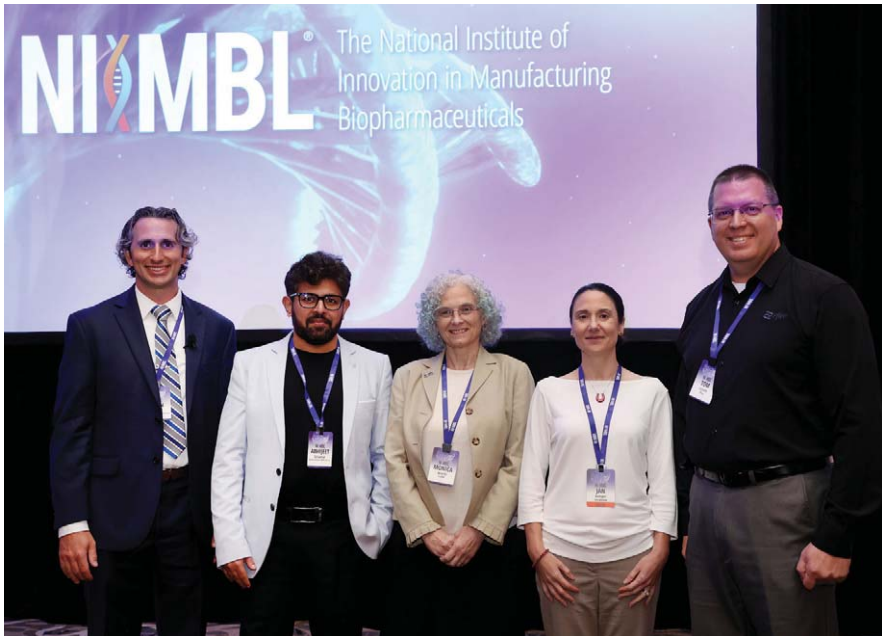

Speakers of the Interoperability session at NIIMBL's 2025 National Meeting (from left to right: Ryan Barton, Abhijeet Satwekar, Monica Acerbi, Jan Kemper, and Thomas Cornish)

yet to prioritize standardized interoperability, and technology providers have implemented proprietary protocols. As a result, biomanufacturing equipment from different suppliers often is not digitally compatible for data sharing and might require the work of software engineers to patch systems together. Achieving interoperability requires balancing the standardization needed for compatibility with the business interests of supplier differentiation. Cooperation benefits all stakeholders by accelerating innovation.

An Ontology To Structure Data Input and Exchange

The increasing complexity of generated data across diverse systems needs a common machine language to bridge gaps in understanding those data, representing the third level (L3) in achieving interoperability. Recently, industry leaders who are working together toward interoperability through the Big Data Program initiated an ontology to enable communication among computers from diverse manufacturing sites. "The ontology is a structured vocabulary and a formal, logic-based set of classes, properties, and axioms that computers can understand," explained Milos Drobnjakovic (research associate at NIST at the time of the meeting). After being in development for several years, the ontology was released in November 2025 in partnership with the Open Applications Group, Inc. (OAGi) as an open-source platform (**2**).

The ontology recognizes human vocabulary and enables users to engage it within their computers. That tool serves as a resource to ensure that vocabularies are shared and public and that no translators are needed to shift from one language or system to another. Just as a dictionary is useless if unshared, manufacturing cannot operate efficiently with private vocabularies. An ontology functions as a codebook: an open-source, common dictionary available for all users to consult.

Despite moves among different nonprofits to develop ontologies, uncoordinated efforts could move users toward private dictionaries instead. Collaboration will be critical for nonprofits working on such projects. The National Meeting ontology session served as a platform to promote such collaboration, with guest speakers from Johnson & Johnson and the Pistoia Alliance presenting different ontology work developed through another consortium. Such exchanges encourage partnerships among consortia toward the goal of one shared ontology.

A Use Case for Predictive Control

Model predictive control (MPC) is an advanced control strategy that uses process models to forecast future system behavior and optimize control actions within a moving time window. MPC combines prediction, real-time optimization, and feedback correction to handle dynamic and unpredictable systems effectively. Predictive control requires connectivity (e.g., among sensors) and seamless exchange across multiple communication modes. Process analytical technologies (PATs) benefit from test beds to identify and resolve gaps in connectivity. Ryan Barton and the Biomanufacturing Training and Education Center (BTEC) team at North Carolina State University (NCSU) created a test bed to implement MPC through advanced data connectivity. BTEC integrated at-line measurements — of cell density, metabolites, and glycan subunits — and autosampling systems for enhanced monitoring. Their MPC approach aimed to regulate glycan profiles (specifically galactosylation) using feed adjustments (e.g., galactose or glucosamine) that would be detected and corrected by the system automatically. The team's MPC sought dynamic updates to algorithms, with data ingested through connected instruments. If connectivity is interrupted during such an MPC test run, then updates stop, and real-time control is not achieved. Effective control also depends on rapid data exchange to detect deviations and correct perturbations, such as glycosylation shifts caused by nutrient additions. MPC represents a step toward *digital twins* — time-accurate representations that are based on rapid monitoring of physical processes — offering more sophisticated, dynamic control than that of traditional systems.

Although the goal of the BTEC galactosylation test run was real-time adaptive control, training was cyclic due to obstacles in hardware and software deployment. Ultraperformance liquid chromatography (UPLC) devices had unresolvable physical and connective gaps that required manual intervention. Predictable connectivity

among instruments could not be achieved. In that use case, instrument and connectivity limitations prevented true predictive control and made repetitive training necessary.

That use case revealed a standout need for PAT devices and analytical instruments in manufacturing laboratories. Unpredictable connectivity among instruments remains a major obstacle across the industry. The test bed exposed interoperability gaps and underscored the need for industry partnerships, such as with the US National Institute of Standards and Technology (NIST), to drive standards and collaboration. Using the NISTCHO Chinese hamster ovary cell line adds value for future experiments and workforce training, reinforcing the test bed's role as both an educational platform and a forum for additional development work to establish predictive control.

The 2025 National Meeting featured sessions on policy in innovation, national security, and industry studies.

A Need for Standardization

Standardization would facilitate interoperability and ensure that different systems and stakeholders can work together on platforms, data formats, and protocols. Although many platform-independent tools already are aligned with standards for secure and reliable industrial communication, so far no consensus or canonical framework has been applied within biomanufacturing and associated industries. Cornish remarked that "the concept is easy, but it is hard to implement." Standards for interoperability have been created to offer a general communication schema, but expectations have changed significantly with rapid acceleration in the field, rendering those standards ineffective. Both rapid and distributed computing now exist throughout factories. As increasing amounts of real-time data are generated from different sources, the diversity of sources continues to impede standardization for biomanufacturing. How can the industry ecosystem integrate major analytical systems such as laboratory information systems (LIMs), ELNs, manufacturing execution systems (MES), and quality management systems (QMS)? A typical biologic manufacturing process will use equipment from different vendors with no system to interconnect incoming data.

Digital twins have increased both the need for interoperability and the difficulty of achieving it. A digital twin requires interoperability, thus motivating vendors to use systems that are digitally compatible with those from other vendors. As a high-speed replica, a digital twin is similar to a self-driving car. An automation system in a self-driving car that is 10 minutes behind real time is useless. High speed and accurate measurement are necessary for a digital twin to replicate a system in the digital world. Thus, an array of sensors provides diversity of sensing. A communication protocol enables transmission. High-speed communication — most of which needs to be two-way — among the centralized computer and the devices, sensors, or control actuators keeps instruments under control. Such a complex system of devices can function and scale only with standard protocols. The digital twin thus exposes the deficiencies of the past as well as the needs of the future.

Standards have been issued that specifically call out the need for interoperability above all else for the creation of digital twins. The International Organization for Standardization (ISO) has published a set of standards (ISO23247) to provide a framework for digital-twin development (**3**). That standard includes general definitions, principles, reference models, functional information, and networking aspects, emphasizing the need for interoperable systems and infrastructure. Abhijeet Satwekar (innovation manager at MilliporeSigma/EMD Serono) summarized the different levels of standardization in the development of a digital twin for the purpose of interoperability (Table 1), completing integration of all levels from the interoperability conceptual framework to realize full interoperability as depicted in Figure 1.

Tim Berners-Lee (computer scientist and inventor of the World Wide Web information system) communicated similar levels of interoperability at the beginning of the World Wide Web in the early 1990s; thus, there is significant continuity in this conceptual view of interoperability over time and a clear logic for the importance of interoperability for advancing the efficiency and benefits of biopharmaceutical manufacturing.

Big Data's Future

As interoperability is addressed, we will run into additional challenges. From a regulatory point of view,

Abhijeet Satwekar (innovation manager at MilliporeSigma/EMD Serono) presented on the levels of standardization in the development of digital twins.

Figure 1: Shared capabilities and resources support individual enterprises in developing customized strategies that bring competitive advantage.

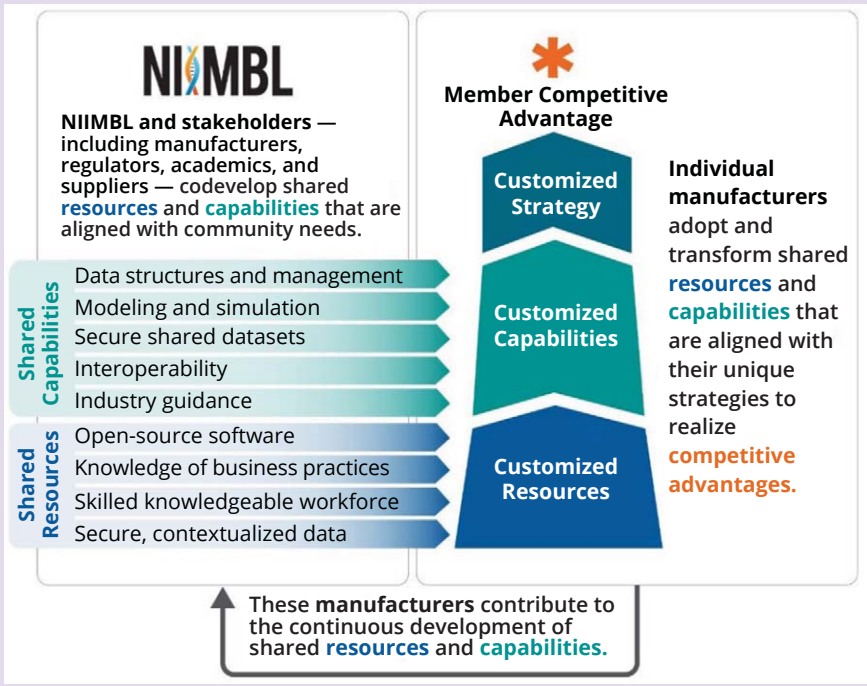

manufacturers must demonstrate that data are not being manipulated. From a cybersecurity perspective, data must be protected from theft. How can we ensure that data come from a trusted source?

Assembling a toolbox to realize practical benefits from big data is critical. A key goal is to generate complete integrated datasets as foundations for sophisticated process-control strategies. Availability of useful data can be increased through development of improved analytics. That becomes useful for building ML into biomanufacturing.

A standard format for presenting relevant manufacturing details would be most useful. We can learn from leading international regulatory authorities, including the FDA, which have established a common technical document (CTD) to describe a production process (**4**, **5**). Such documents have been used to summarize 10 years of process-development work.

The challenges are considerable and difficult for any individual company to make significant progress while working in isolation. Collaborating through a consortium spreads out the resource and cost demands while also making it more likely that the recommended path forward will be acceptable both to the broad biomanufacturing community and to international regulators.

Acknowledgments

NIIMBL is a public–private partnership whose mission is to accelerate biopharmaceutical innovation, support the development of standards that enable more efficient and rapid manufacturing capabilities, and educate and train a world-leading biomanufacturing workforce, fundamentally advancing US competitiveness in the industry. NIIMBL is part of Manufacturing USA, a diverse network of federally sponsored manufacturing innovation institutes, and is funded through a cooperative agreement (#70NANB21H086) from the National Institute of Standards and Technology (NIST) in the US Department of Commerce, with significant additional member support.

We gratefully acknowledge the speakers who participated in the 2025 NIIMBL National Meeting Big Data Program sessions, sharing their expertise and insights on big data and on the challenges and opportunity of interoperability. We thank NIST for their collaboration and contributions advancing the ontology.

References

1 Wang WG, Tolk A, Wang WP. *The Levels of Conceptual Interoperability Model: Applying Systems Engineering Principles to M&S*. Spring Simulation Multiconference: San Diego, CA, 2009; https://doi.org/10.48550/arXiv.0908.0191.

2 *Big Data Program*. National Institute for Innovation in Manufacturing Biopharmaceuticals: Newark, DE, 2026; https://www.niimbl.org/projects-programs/big-data.

3 ISO 23247-1:2021. *Automation Systems and Integration — Digital Twin Framework for Manufacturing, Part 1: Overview and General Principles*. International Organization for Standardization: Geneva, Switzerland, 2021; https://www.iso.org/standard/75066.html.

4 ICH M4Q(R1). *The Common Technical Document for the Registration of Pharmaceuticals for Human Use: Quality*. International Council on Harmonisation of Technical Requirements for Pharmaceuticals for Human Use: Geneva, Switzerland, 12 September 2002; https://database.ich.org/sites/default/files/M4Q_R1_Guideline.pdf.

5 *Providing Regulatory Submissions in Electronic Format — Certain Human Pharmaceutical Product Applications and Related Submissions Using the eCTD Specifications: Guidance for Industry*. US Food and Drug Administration: Silver Spring, MD, 2024; https://www.fda.gov/media/135373/download?attachment.

Roger Hart *is a senior fellow, corresponding author* ***Emily Carson*** *is a technical grant writer (ecarson@niimbl.org),* ***Barry Buckland*** *is executive director, and* ***Kelvin H. Lee*** *is institute director, all at NIIMBL, 590 Avenue 1743, Newark, DE 19713; https://www.niimbl.org.*

Is your project on the right path?

Don't get stuck in dead ends

Select the right partner.

Rezonbio

A European CDMO that is reliable, affordable and built to deliver high-quality biologics.

Booth#1411

Because your reason is our Rezon.

Explore our end-to-end CDMO services

Follow us
bd@rezonbio.com

Rezon Bio
Trzy Lipy 3, Building A
80-172 Gdansk, Poland

Blood Centers

A Ready Partner in Building Reliable Manufacturing Supply Chains for Cell and Gene Therapies

Lee Buckler, Jeff Wren, and Kate Fry

As cell and gene therapies (CGTs) move from promise to practice, the global biopharmaceutical industry must rethink its supply chains to ensure that these therapies can meet their commercial potential. Unlike traditional biologics, CGTs are fragile, living, and often patient-specific products with time-sensitive logistics. To scale those therapies safely and equitably, industry innovators are beginning to turn to collaborators with decades of experience collecting, processing, storing, and moving sensitive biologic materials under tight regulatory oversight. Those partners may exist already: community blood centers.

Blood centers are uniquely suited to solve obstacles in CGT supply chains. By leveraging their experience as a backbone of transfusion medicine, blood centers can provide reliable starting-material supply, end-to-end chain of identity and custody (CoI, CoC), site networks beyond major academic centers, and cost-disciplined scale. Some drug sponsors already are building partnerships with blood centers, filling out a model that could be replicated broadly.

Blood Centers Operating as Manufacturers

Blood-center systems can operate as regulated entities that provide cellular starting materials and services for clinical use. Such systems have evolved from whole-blood collection to support component isolation and separation, therapeutic apheresis, stem-cell transplantation, cord-blood and tissue banking, and cryopreservation, in addition to the logistical infrastructure and expertise required to ensure that

HTTPS://STOCK.ADOBE.COM

clinical-grade products are transported within specifications. That journey has built key capabilities that the biopharmaceutical industry requires for CGTs. Some centers have grown to offer true cell manufacturing, including expansion, differentiation, and transfection/transduction.

Blood centers collect, test, process, package, label, store, and transport biological materials under highly regulated and validated protocols. They maintain robust quality management systems, with traceability and compliance incorporated into daily operations. They also undergo continuous oversight from regulators, including the US Food and Drug Administration (FDA), state health departments, and accrediting organizations such as the Association for the Advancement of Blood and Biotherapies (AABB) and the College of American Pathologists. Blood centers' strong regulatory track records position them as natural partners for CGT developers that are seeking proven infrastructure without the cost or delay of building from scratch. Industry leaders have begun using blood centers to derisk launches, accelerate timelines, and scalable pilot distributed models (**1**).

Historically, blood centers have been an underused lever in the pharmaceutical industry's innovation model. Despite some change, uptake remains limited in part due to inertia. Teams that are used to working with hospitals might default to hospital-centric builds or vendor stacks that overlook other existing community infrastructure. Sponsors also might feel uncertainty about changing partners, with particular concerns related to variable information technology (IT) systems and documentation formats across centers. And depending on a biopharmaceutical company's development model and corporate structure, it might be unclear who owns the relationship: clinical operations teams; supply-chain managers; or chemistry, manufacturing, and controls (CMC) leads.

Those obstacles are not dealbreakers but rather integration challenges — issues that early adopters already are solving with clear specifications, joint qualifications, and service-level agreements.

Meeting Unique Demands of CGT Supply Chains

Blood centers now are slotting into several parts of CGT workflows, including sourcing starting material supply and supporting preinfusion product receipt, storage, and processing. Needs differ depending on therapy type, but blood centers are proving flexible enough to satisfy several requirements.

Autologous CGTs demand a high level of precision and CoC integrity compared to other medical products because they are patient-specific therapies that must be returned to the originating patient. On the other hand, allogeneic therapies have unique requirements for dealing with donors for starting-material procurement. Thus, allogeneic cell-therapy

manufacturing begins with complex large-scale prescreening logistics and scheduling. In blood centers, specialized staff members perform medically supervised patient apheresis, followed by initial processing, viability testing, and cryopreservation of collections.

Qualified release includes a thorough review of documentation by highly trained personnel and carefully planned cold-chain logistics. For shipment, that step requires strict labeling and shipping specifications to move biologic materials under controlled protocols. CoC documentation, controlled-rate freezing, shipper qualification, and exception handling are part of regular blood-center operations.

Blood centers also can handle final-product receipt and storage requirements in liquid-nitrogen containers, including temperature monitoring, controlled thawing, handling, and infusion preparation. All of those activities take place under time-sensitive, compliance-heavy conditions that must adhere to clinical protocols. Blood centers regularly oversee data capture and traceability requirements, including e-logs, equipment telemetry, and integration with sponsors' laboratory information management systems (LIMS) and/or electronic quality management systems (eQMS) for audit-ready traceability. Blood centers are prepared for such work because they have similar processes already embedded in their operations. Where some hospitals might lack the expertise or capacity to manage living biologics, blood centers can step in with proven systems, trained personnel, and inspection-ready facilities.

Enabling Access Beyond Advanced Treatment Centers

One shared challenge across the CGT field is expanding patient access. CGTs generally are confined to advanced treatment centers typically located in major urban hospitals with internal infrastructure to support advanced therapies. But as those therapeutics expand into broader indications, biopharmaceutical companies are under pressure to reach patients in community healthcare settings. Those sites rarely have the apheresis, cell-therapy laboratories, pharmacy infrastructure, or expertise required to manage CGTs. Blood centers already operate in those communities, and some biopharmaceutical partners have begun using them as essential nodes for equitable patient access (**2**).

The path from collection to treatment in CGT delivery is fragile, complex, and unforgiving. Any **BREAKDOWN** in a supply chain risks not only wasted product, but also lost treatment opportunities for patients who might have no alternative options.

The need to decentralize both apheresis activities and treatment delivery dovetails with another emerging development: distributed manufacturing. As the biopharmaceutical industry explores models in which elements of CGT production occur closer to a point of care, blood centers' proximity to treatment sites and ability to comply with rigorous manufacturing requirements make them strategic assets.

Building a Resilient Future for Advanced Therapies

The path from collection to treatment in CGT delivery is fragile, complex, and unforgiving. Any breakdown in that supply chain risks not only wasted product, but also lost treatment opportunities for patients who might have no alternative options. Blood centers bring decades of experience mitigating such risks; integrating such centers into CGT supply chains can reduce time, cost, and risk for therapy developers.

The biopharmaceutical industry doesn't lack in passion or capital for CGTs. However, it is facing a shortage of operationally ready, compliant, and distributed infrastructure that gets the right product to the right patient at the right time reliably and at a cost that the system can bear. As CGTs move toward broader adoption, a growing number of biopharmaceutical companies are recognizing that blood centers can be more than transfusion service providers. They are compliance-ready, biologics-handling specialists with a manufacturing mindset and community reach.

Community blood centers soon will become indispensable for the future of scaling advanced therapies safely, efficiently, and equitably. Such organizations have been working closely with the blood-products industry for decades. The fastest path to broad CGT access will be to plug into what already works, standardize interfaces, and scale. The building wave of partnership will be less about greenfield builds and more about tapping trusted institutions already embedded in our communities.

That future for CGTs will depend not only on scientific breakthroughs, but also on robust, decentralized, and resilient supply chains. Early adopters have found out that blood centers are already working with biomanufacturers in the blood-products industry. The next step for the biopharmaceutical industry is mainstreaming broad-based models to bring blood centers into the fold as full partners in delivering tomorrow's medicines.

References

1 Gazaille B. AABB Panel Highlights How Cell-Therapy Developers Can Draw Inspiration From Blood Centers. *BioProcess Insider* 24 April 2025; https://www.bioprocessintl.com/upstream-downstream-processing/aabb-panel-highlights-how-cell-therapy-developers-can-draw-inspiration-from-blood-centers.

2 Simmons GL. Bringing CAR T-Cell Therapies to Community Oncology Practices. *Targ. Ther. Oncol.* 14(16) 2025; https://www.targetedonc.com/view/bringing-car-t-cell-therapies-to-community-oncology-practices.

Lee Buckler *is senior vice president of advanced therapies at Blood Centers of America (BCA).* ***Jeff Wren*** *is vice president at the Association for the Advancement of Blood & Biotherapies (AABB). And* ***Kate Fry*** *is chief executive officer of America's Blood Centers (ABC). For inquiries, please contact bcar@ibcomms.agency.*

Integrating Quality by Design Principles into Gene-Therapy CMC Programs

Establishing Manufacturing Control and Comparability

Mo Heidaran

When describing biologics manufacturing, scientists long have said that "the process defines the product." Nowhere is that truer than in the context of cell and gene therapy (CGT) products. Unlike recombinant proteins, which often can be well characterized, CGTs are complex, variable, and highly dependent on biological source materials and process controls. Such complexity makes full product characterization impossible using quality control (QC) testing alone.

Unfortunately, some CGT industry representatives repeat the misleading assertion that "the process is not the product," implying that as long as a product passes QC and characterization tests, changes to manufacturing processes are inconsequential. For CGTs, that view is dangerously simplistic.

Each element of a biomanufacturing process, from raw materials and components to process parameters, can influence a final product's attributes. QC testing and characterization, though indispensable, cannot fully predict clinical performance or capture subtle shifts in a therapy's biological activity. That is why quality by design (QbD) must be embedded early in the development of CGT products. QbD builds a scientific foundation for understanding how process inputs and parameters drive product quality.

Figure 1: Prospective approach to identification and prioritization of clinically relevant cell and gene therapy (CGT) critical quality attributes (CQAs) using artificial intelligence (AI) tools. Such a process would be difficult to establish. It should be considered an aspirational model that could raise opportunities for expediting pre- and postapproval manufacturing changes.

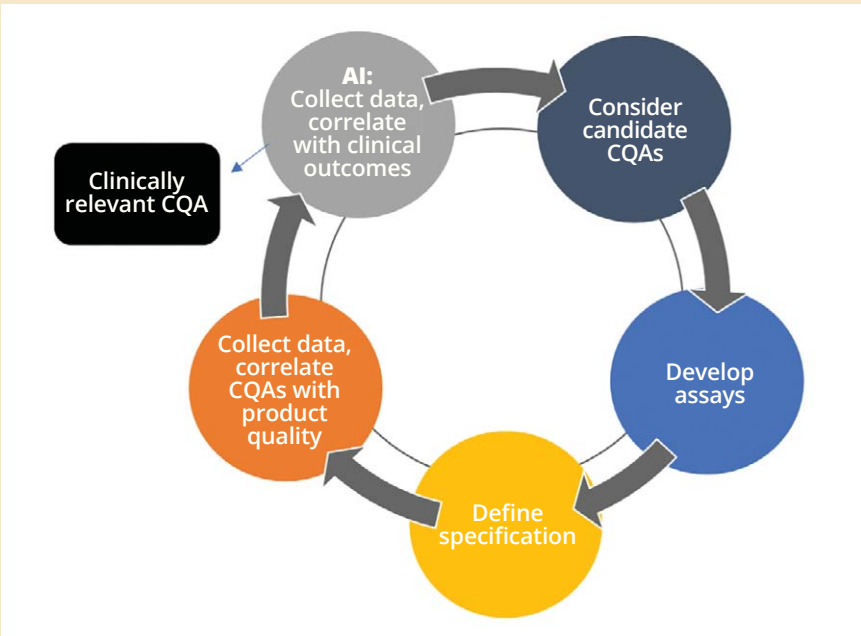

A QbD Framework for Gene-Therapy Manufacturing

What Is QbD? The International Council on Harmonisation of Technical Requirements for Pharmaceuticals for Human Use (ICH) defines *quality by design* as "a systematic approach to development that begins with predefined objectives and emphasizes product and process understanding and process control, based on sound science and quality risk management" (**1**). In simple terms, QbD means designing quality into the product from the start rather than testing for quality at the end of a process.

Core components of the QbD framework include

- *target product profiles* (TPPs), which define a product's clinical and quality objectives
- *critical quality attributes* (CQAs), or product properties that affect safety and efficacy (e.g., potency, purity, vector genome integrity)
- *critical process parameters* (CPPs), process variables that require tight control because they directly influence CQAs
- *key performance parameters* (KPPs), metrics independent of CQAs that track process health and consistency.

Together, those elements form the foundation of a science-based control strategy. The A-Gene initiative was one of the first efforts to adapt QbD concepts to gene-therapy manufacturing — years before formal guidance documents were issued (**2**). A-Gene demonstrated that applying QbD principles can significantly

reduce process variability, improve understanding, and accelerate regulatory alignment.

Building an Effective Manufacturing Control Strategy

A control strategy is the backbone of QbD implementation. For gene therapies, that includes

- input material controls — e.g., qualification of cell banks, plasmids, viral seeds, and raw materials
- process controls — in-process monitoring and control of transfection efficiency, vector concentration, culture conditions, and other CPPs throughout manufacturing
- analytical testing, such as characterization assays that evaluate CQAs for release and comparability
- process verification, or demonstration that a process consistently yields material with attributes that fall within defined control limits.

Control limits typically are structured into operating, alert, action, and specification ranges. A multitiered approach allows early detection of process drift before it affects product quality.

Establishing control limits and specifications — e.g., acceptance criteria, methods, and procedures — is extremely difficult for gene-therapy products. Most manufacturers justify acceptance criteria based on historical ranges. Consider potency assays: Because such assays typically are measured using cell-based or biological assays with inherent variability, acceptance criteria are set initially to wide ranges.

For most CGTs, overall acceptance criteria are not defined in terms of clinical effectiveness at any stage of development. Products that do not meet acceptance criteria or that are found to be in the low range for CQAs such as potency are not proven to be ineffective from a clinical perspective. For example, regarding products based on chimeric antigen receptor (CAR) T cells, there is generally no correlation between potency-assay results and clinical effectiveness. Thus, regulators have been receptive to setting acceptance criteria based on manufacturing capability, using testing to ensure manufacturing consistency rather than clinical effectiveness.

Linking CQAs to Clinical Relevance

A persistent challenge in CGT manufacturing is establishing which CQAs are clinically relevant. Potency provides an instructive example. For traditional biologics, potency assays often but do not always correlate well with clinical efficacy. In gene therapy, however, potency assays frequently are limited to measuring biological activity in vitro, which might not predict in vivo therapeutic effects. The US Food and Drug Administration (FDA) defines *potency* broadly as "the specific ability or capacity of the product to achieve a defined biological effect" (**3**). The biological effect is broadly interpreted as the ability of CGTs to function in vitro using a relevant biological assay without having regulatory expectations for a potency test to be correlated with clinical effectiveness. As a result, manufacturers often lack validated assays that reflect clinical efficacy with statistical confidence.

However, identifying CQAs that can be linked to clinical efficacy should not be just an aspirational goal. Before discussing design of experiments (DoE) methodologies as tools for defining a *design space* — the range in which product quality, as measured by CQAs, is not affected significantly — it is important to recall how CQAs are defined.

For most CGTs, the most difficult step is defining product quality in terms of biological activity. Identifying CQAs involves an iterative process in which candidate CQAs are defined initially using a matrix-based approach. For a hypothetical product based on adenoassociated virus (AAV) vectors, such attributes could be defined by measuring product purity (the proportion of empty to full AAV capsids), virus infectivity, or potency (as measured by transgene expression in an in vitro cell-based assay).

Ideally, such attributes would be measured during development and then correlated with product effectiveness during a clinical trial. But published results have not provided evidence that CQAs measured for AAV products (as defined by acceptance criteria) can be consistently correlated with final-product effectiveness. The reasons why could be manifold, but fundamentally, the lack of clear correlation reflects the complexity of AAV products' mechanism of action (MoA), which depends on factors including a patient's immune response and a product's efficiency in targeting the correct cell type in vivo.

Because CQAs are not necessarily predictive of in vivo product effectiveness, manufacturers should prioritize attributes that are highlighted during early risk assessment. That, in turn, can facilitate definition of CPPs using DoE. Because of such uncertainty, regulators have adopted a pragmatic approach, accepting CQAs based on risk assessment and scientific rationale while requiring manufacturers to tighten acceptance criteria as data are collected over time.

Figure 1 summarizes a recommended approach for prioritizing relevant CQAs (ones that could be linked to clinical effectiveness) during a product's development cycle. The first step involves identifying candidate CQAs, which is possible once a TPP and MoA have been determined fully. For a hypothetical AAV product, critical attributes might include infectivity, potency (as determined by assays of transgene expression and function), and empty:full capsid ratios. Those attributes, when measured using qualified assays, can be collected and correlated with clinical outcomes during a phase 1 study and, later, when clinical data from pivotal studies are unblinded before biologics license application (BLA) submission. Engaging in such an exercise would not be trivial; it would require considerable data collection and analyses supplemented by artificial intelligence (AI). In this context, AI should be viewed as a transformational tool to help scientists better assess and prioritize relevant CQAs linked to product effectiveness (**4**).

Defining CPPs and Linking Them to CQAs

DoE is a powerful tool for defining the space within which changes in process

parameters are not expected to influence product CQAs (**5**). Take the example of a typical CAR-T product. Process parameters that could affect CAR-T manufacturing include process temperature, culture-media components, and variables that are optimized to enhance cell expansion (such as process time, pH, concentration of toxic metabolites, and agitation rates).

Identifying CPPs that could affect product CQAs is the first step, followed by selecting appropriate methods to assess how those factors interact. Because it is virtually impossible to assess interactions among different factors experimentally, the CGT field has developed alternative approaches to conduct DoE. One of the most powerful approaches that I have used is *fractional factorial design*, which enables determination of negative and positive interactions between CPPs and product-quality attributes by testing a subset of all theoretical interactions in a matrix-based environment (**5**).

Staying within a configured design space provides control over manufacturing consistency. Thus, a design space can serve as a powerful tool for making manufacturing changes without requiring a full comparability study; such an approach has rarely been used in CGT manufacturing but is more common for other, better-defined biologics. In regulatory terms, identification of a design space for different CPPs is probably the most underused exercise in the CGT field. Understanding the design space is a useful way of determining "established conditions" within which manufacturing changes arguably would have no impact on a product's CQAs.

Establishing Comparability After Manufacturing Changes

Manufacturing changes are inevitable. Scale-up, automation, and process optimization often are introduced late in development as products advance toward commercialization. Each change must be evaluated to ensure product comparability regarding quality, safety, and efficacy.

Key guidance documents include

• FDA and European Medicines Agency (EMA) guidelines on comparability for CGTs and advanced-therapy medicinal products (ATMPs), respectively (**6–12**)

• ICH Q5E on *Comparability of Biotechnological/Biological Products* (**13**)

• ICH Q8–Q12, which provide frameworks for pharmaceutical development, risk management, and life-cycle management (**1, 14–17**)

• ICH M4Q(R1), which summarizes quality concerns in the Common Technical Document for pharmaceutical registration (**18**).

Those documents reinforce the principle that comparability is data driven. Regulators might require analytical, nonclinical, and sometimes even clinical data depending on the proposed change's potential impact.

Consider a hypothetical AAV-vector process that is moving from small-scale (2 L) to large-scale (200 L) production. Analytical comparability studies for that manufacturing change should examine

• vector titer and genome integrity (CQAs)

• transfection efficiency and harvest conditions (CPPs)

• impurity profiles and potency-assay results

• statistical evaluation based on equivalence testing or tolerance intervals (TIs) rather than traditional *t*-tests.

A structured approach to comparability assessment provides regulators with confidence that observed differences are within acceptable ranges and not clinically meaningful.

Analytical, Statistical, and Validation Considerations: Robust analytical and statistical methods are the foundation of reliable comparability and QbD implementation. All **analytical methods** used to measure CQAs must be fit for purpose and validated for accuracy, precision, specificity, and linearity. Because CGT assays often have higher variability than do other drug modalities, establishing appropriate acceptance criteria is essential.

Regarding **statistical approaches**, I recommend using equivalence testing or TIs to compare product lots across manufacturing changes. Avoid overreliance on *t*-tests, which often are misapplied to small, variable datasets. Apply multivariate statistical process control (MSPC) when multiple CQAs interact.

Establishing Equivalence with a Two One-Sided Test (TOST): CGT products generally have small datasets, often with sample sizes of three to five batches. TOST is the preferred method for showing equivalence because it is amenable to establishing similarity using small sample sizes (**5**). The formula used to establish equivalence acceptance criteria (EAC) is complex, but it is designed to factor in starting material variability, process and analytical variability, and additional factors based on historical standard deviation.

Another useful method is to establish comparability ranges, which frequently are calculated based on a statistical interval, such as a TI or minimum–maximum range. A TI can estimate a data range in which a specified portion (e.g., the central 90%) of units from the underlying population is assumed to be covered with a given degree of confidence (e.g., 95%). Comparability is established if all test batches fall within the 90%/95% TI computed from the reference batches.

Note that traditional paired *t*-tests are not appropriate for establishing similarity. A paired *t*-test often is used to determine whether data collected under two different conditions are different. Typically, the biopharmaceutical industry uses a *t*-test for comparability by rejecting the null hypothesis (which states that two populations are different). However, rejecting the null hypothesis of difference does not prove statistically that two populations are similar.

Sample-size calculation using an equivalence method allows for evaluation of small cohorts. Once an appropriate test such as a TOST has been selected, commercially available programs such as JMP software can use relevant inputs to determine sample size. For example, to calculate the sample size needed to establish comparability between products manufactured at two sites, statisticians might leverage historical standard deviation, estimated mean differences, and EACs for various quality attributes.

Challenges and Practical Recommendations

Implementing QbD in CGT programs remains difficult for several reasons.

Teams often have limited product and process knowledge early in development. Batch sizes tend to be small, and products show high variability. Correlation between in vitro assays and clinical results remains limited. And regulatory expectations continue to evolve.

Teams can address such challenges by

- introducing QbD before pivotal trials to enable data collection and process understanding prospectively
- engaging regulators proactively to align on CQA definitions and comparability plans
- using platform technologies and DoE approaches to evaluate process variables systematically
- planning for life-cycle changes early, recognizing that scale-up and automation are inevitable.

A Critical Enabler of CGT Quality, Safety, and Efficacy

QbD principles can be applied systematically to CGT manufacturing to establish robust control strategies and ensure product comparability throughout a product's life cycle. Unlike traditional biologics, CGTs are highly complex and variable, making full product characterization through QC testing alone insufficient. Thus, the manufacturing process itself defines the product, and process understanding becomes the foundation of quality.

Core components of QbD — e.g., TPP, CQAs, CPPs, and KPPs — can be integrated into science-based risk assessments and control strategies. Herein, I emphasized the clinical relevance of CQAs, the challenges of correlating potency assays with efficacy, and the need for statistical rigor when assessing comparability after manufacturing changes such as scale-up or implementation of automation.

Ultimately, QbD is not just a compliance exercise; it is a critical enabler of quality, safety, and efficacy in gene therapy. For CGTs, a process and product are inseparable, and a well-structured QbD framework ensures that both will evolve together under scientific and regulatory control.

References

1 ICH Q8(R2). *Pharmaceutical Development*. International Council on Harmonisation of Technical Requirements for Pharmaceuticals for Human Use: Geneva, Switzerland, 2009; https://database.ich.org/sites/default/files/Q8%28R2%29%20Guideline.pdf.

2 ARM/NIIMBL. *Project A-Gene: A Case Study-Based Approach to Integrating QbD Principles in Gene Therapy CMC Programs*. Alliance for Regenerative Medicine: Washington, DC, 2021; https://alliancerm.org/wp-content/uploads/2025/08/ALL-PROJECT-A-GENE-V10.pdf.

3 21 CFR 600.3. Biological Products: General — General Provisions — Definitions. *Code Fed. Reg*. 1 April 2011; https://www.govinfo.gov/app/details/CFR-2025-title21-vol7/CFR-2025-title21-vol7-sec600-3.

4 Di Cerbo V, et al. Artificial Intelligence, Machine Learning, and Digitalization Systems in the Cell and Gene Therapy Sector: A Guidance Document from the ISCT Industry. *Cytotherapy* 27(8) 2025: 903–909; https://doi.org/10.1016/j.jcyt.2025.05.003.

5 Haaland PD. *Experimental Design in Biotechnology* (1st Edition). CRC Press: Boca Raton, FL, 1989.

6 FDA-2023-D-2436. *Manufacturing Changes and Comparability for Human Cellular and Gene Therapy Products: Draft Guidance*. US Food and Drug Administration: Rockville, MD, 24 August 2023; https://www.fda.gov/media/170198/download.

7 EMA/CAT/499821/2019. *Questions and Answers: Comparability Considerations for Advanced Therapy Medicinal Products (ATMP)*. European Medicines Agency: Amsterdam, the Netherlands, 6 December 2019; https://www.ema.europa.eu/en/documents/other/questions-and-answers-comparability-considerations-advanced-therapy-medicinal-products-atmp_en.pdf.

8 EMA/CHMP/138502/2017. *Reflection Paper on Statistical Methodology for the Comparative Assessment of Quality Attributes in Drug Development*. European Medicines Agency: Amsterdam, the Netherlands, 26 July 2021; https://www.ema.europa.eu/en/documents/scientific-guideline/reflection-paper-statistical-methodology-comparative-assessment-quality-attributes-drug-development_en.pdf.

9 FDA-2011-D-0605. *Scientific Considerations in Demonstrating Biosimilarity to a Reference Product: Updated Recommendations for Assessing the Need for Comparative Efficacy Studies*. US Food and Drug Administration: Rockville, MD, 20 November 2025; https://www.fda.gov/media/189366/download.

10 *Guidance for Industry: Comparability Protocols — Chemistry, Manufacturing, and Control Information (Draft)*. US Food and Drug Administration: Rockville, MD, February 2003; https://www.fda.gov/files/drugs/published/Comparability-Protocols----Chemistry--Manufacturing--and-Controls-Information.pdf.

11 FDA-2013-S-0610. *Demonstration of Comparability of Human Biological Products, Including Therapeutic Biotechnology-Derived Products*. US Food and Drug Administration: Rockville, MD, 6 July 2005; https://www.fda.gov/regulatory-information/search-fda-guidance-documents/demonstration-comparability-human-biological-products-including-therapeutic-biotechnology-derived.

12 FDA-1995-D-0288. *Chemistry, Manufacturing, and Controls Changes to an Approved Application — Certain Biological Products: Guidance for Industry*. US Food and Drug Administration: Rockville, MD, 27 August 2021; https://www.fda.gov/regulatory-information/search-fda-guidance-documents/chemistry-manufacturing-and-controls-changes-approved-application-certain-biological-products.

13 ICH Q5E. *Comparability of Biotechnological/Biological Products Subject to Changes in Their Manufacturing Process*. International Council on Harmonisation of Technical Requirements for Pharmaceuticals for Human Use: Geneva, Switzerland, 18 November 2004; https://database.ich.org/sites/default/files/Q5E%20Guideline.pdf.

14 ICH Q9. *Quality Risk Management*. International Council on Harmonisation of Technical Requirements for Pharmaceuticals for Human Use: London, UK, 9 November 2005; https://database.ich.org/sites/default/files/Q9_Guideline.pdf.

15 ICH Q10. *Pharmaceutical Quality System: Scientific Guideline*. International Council on Harmonisation of Technical Requirements for Pharmaceuticals for Human Use: London, UK, 2015; https://www.ema.europa.eu/en/documents/scientific-guideline/international-conference-harmonisation-technical-requirements-registration-pharmaceuticals-human-guideline-q10-pharmaceutical-quality-system-step-5_en.pdf.

16 ICH Q11. *Development and Manufacture of Drug Substances (Chemical Entities and Biotechnological/Biological Entities)*. International Council on Harmonisation of Technical Requirements for Pharmaceuticals for Human Use: Geneva, Switzerland, 1 May 2012; https://database.ich.org/sites/default/files/Q11%20Guideline.pdf.

17 ICH Q12. *Technical and Regulatory Considerations for Pharmaceutical Product Lifecycle Management*. International Council on Harmonisation of Technical Requirements for Pharmaceuticals for Human Use: Geneva, Switzerland, 20 November 2019; https://database.ich.org/sites/default/files/Q12_Guideline_Step4_2019_1119.pdf.

18 ICH M4Q(R1). *The Common Technical Document for the Registration of Pharmaceuticals for Human Use: Quality*. International Council on Harmonisation of Technical Requirements for Pharmaceuticals for Human Use: Geneva, Switzerland, 12 September 2002; https://database.ich.org/sites/default/files/M4Q_R1_Guideline.pdf.

Mo Heiradan, *PhD, is chief regulatory scientist at Cellx Inc.; https://www.linkedin.com/in/heidaran.*

Development of a Closed-System Approach for Downstream Processing of Large Viruses

A Case Study for Preclinical and Clinical Applications

Tingting Ju, Salman Safdar, Ken Bui, Thomas Montague, and Nacole Lee

Large viruses such as poxviruses long have been used as vaccine vectors (**1**). Notably, vaccinia virus was administered for the prevention and eventual eradication of smallpox in 1980 (**1**). In addition to their application as vaccine vectors, poxviruses display oncolytic properties, which has led to their development as anticancer therapeutic agents in recent years (**2**). Despite their favorable immunoprofiles and promising oncolytic features, poxviruses present distinct manufacturing challenges, particularly under current good manufacturing practice (CGMP) conditions.

Viruses are biologically active only within a host; thus, for therapeutic applications, they must retain their ability to infect host cells. Sterilization of viral products is limited by their sensitivity to heat and radiation and by their inability to pass through conventional 0.2-µm sterilizing-grade filters. Such constraints eliminate common methods such as filtration, steam, and gamma-irradiation. Furthermore, therapeutic applications of virus products often demand one to two orders of magnitude higher viral titers than those of most vaccine applications (**3, 4**), intensifying downstream process demands.

In response to those obstacles, *closed-system processing* — complete elimination of environmental exposure throughout production processes — emerges as a critical strategy (**5**). However, such systems are uncommon in legacy downstream operations and require careful design to maintain aseptic integrity. We sought to address that need with a flexible, modular, and operationally closed process that uses custom-designed single-use assemblies. Below, we discuss the rationale, engineering considerations, and performance outcomes associated with implementing our process.

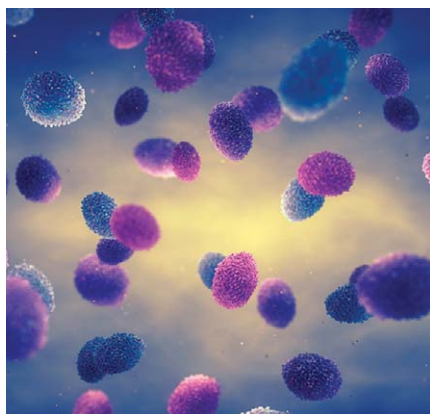

HTTPS://STOCK.ADOBE.COM

Rationale for Closed-System Design

For biologics, closed-system processing is essential to maintaining aseptic process conditions for preventing microbial, fungal, and particulate contamination. To eliminate environmental exposure and improve sterility assurance during downstream purification of poxviruses, we adapted our process to become flexible, modular, and operationally closed. Our solution applies custom single-use assemblies that can be adapted for large-scale aseptic manufacture of a breadth of poxviruses and other large viruses. We validated our strategy and resulting aseptic downstream production process through successful completion of several aseptic process simulation (APS) runs (see "APS" sidebar) and used the system successfully for multiple client CGMP batches.

Reduced cost (see the "Definitions" sidebar) is another advantage of closed systems. Production of biologics involving open transfer steps should be performed in highly controlled (grade A) environments such as biosafety cabinets (BSCs). Open-system control requires extensive environmental monitoring (e.g., settle plates, personnel monitoring, and equipment/room dynamic monitoring), whereas closed-system processes require only grade C or D environments with minimal environmental monitoring. In some cases, that can translate into significant facility-related savings of 30–40% (**4**).

Downstream Process Description

Downstream purification for poxviruses encompasses several unit operations: clarification, nuclease treatment, ultrafiltration/diafiltration (UF/DF) with tangential-flow filtration (TFF), excipient addition, and final filtration through a large-pore filter (≥1.2 µm). Scale-up for our downstream process, which initially was optimized for small-scale execution within a BSC, necessitated reengineering to ensure sterility, minimize manual manipulations, and maintain process robustness.

Table 1: Results of aseptic process simulation (APS) runs for a functionally closed large-scale poxvirus downstream-purification process; BDS = biological drug substance, NA = not applicable

Downstream Steps	Run 1	Run 2	Run 3	Run 4	Run 5	Run 6	Run 7	Run 8	Run 9	Run 10	Run 11
Clarified harvest sample	Pass	Pass	Pass	Pass	Pass	Pass	NA	NA	NA	Pass	NA
Postnuclease sample	Pass	Pass	Pass	Pass	Pass	Pass	NA	NA	NA	Pass	NA
Clarified harvest bulk	Pass	Pass	Pass	Pass	Pass	Pass	NA	NA	NA	Pass	NA
Postconcentration sample	Pass	Turbidity	Pass	Turbidity	NA	NA	Pass	Pass	Pass	NA	Pass
Prefiltration sample	Turbidity	Pass	Pass	Turbidity	NA	NA	Pass	Pass	Pass	NA	Pass
Final filtered sample	Pass	Turbidity	Pass	Turbidity	NA	NA	Pass	Pass	Pass	NA	Pass
BDS sample/bulk	Pass	Pass	Turbidity	Turbidity	NA	NA	Pass	Pass	Pass	NA	Pass

Challenges and Solutions for a Closed-System Transition

Ensuring Aseptic Integrity Throughout Downstream Processing: Downstream processing of poxvirus does not include a final sterilizing step due to the virus's large size; thus, we performed APS runs to evaluate the ability of our large-scale process to provide sterility assurance. Four initial APS runs were performed using tryptic soy broth (TSB) as a substitute for buffers and the product. Acceptance criteria for passing included an absence of turbidity at 14 days postincubation and compliance with sterility specifications for the final product.

Turbidity was detected in APS runs 1–4 using TSB, indicating microbial contamination. A root-cause analysis identified potential failure points, including the use of nonsterile components such as TFF cartridges and retentate reservoirs. Sampling techniques and excessive manual interventions also contributed to our unsuccessful attempts.

For those nonsterile components, we first considered steam sterilization to sanitize the TFF filters. However, effects of steam on filter pore size and performance can be difficult to predict and detect. Additionally, the filters' manufacturer did not have data to support steam sterilization. Validating a novel sterilization process is time-consuming and costly. Therefore, we implemented a functionally closed system (see "Definitions" sidebar) through chemical sanitization of the post-TFF flow-path assembly using 0.5 M sodium hydroxide.

We observed no turbidity in pre-TFF TSB volumes for all four initial APS runs using the functionally closed process. During clarification, depth filters were connected in tandem. Pressure and flow parameters used in the clarification step were well within recommended ranges from the depth-filter vendor. TSB subsequently was added to simulate nuclease addition. The resulting solution was mixed thoroughly, then placed under static hold for a predetermined period before sampling for turbidity. All TSB samples and remaining bulk at this step were subject to turbidity inspection. Results indicated that sterility assurance would be maintained during clarification and nuclease treatment.

Failures occurred after completion of the remaining downstream unit operations (TFF, final filtration, and excipient addition) (Table 1). Evaluation of those results and careful review of the functionally closed process revealed three potential sources of microbial contamination: the presence of nonsterile components (ineffective chemical sanitization using 0.5 M NaOH with overnight exposure), exposure to air during open-catch sampling, and a substantial number of manual manipulations.

Solution — Design and Implementation of a Fully Closed TFF System: It was clear that a functionally closed system could not provide adequate sterility assurance, particularly considering the potential for exposure of process fluid in a TFF assembly to the grade C environment. Therefore, we modified the TFF process to achieve a fully closed system that would provide high sterility assurance and increased processing efficiencies without diminishing product quality. Our modifications included the following:

- substitution of chemically sanitized components with gamma-irradiated, ready-to-use filters after a TFF vendor confirmed that irradiation had no known impact on pore size
- deployment of a custom-designed, fully enclosed, single-use flowpath assembly incorporating a gamma-irradiated retentate reservoir, pump chamber, and aseptic connectors
- integration of a 0.2-µm vent filter to maintain sterility while enabling air exchange outside a BSC and in a grade C environment
- introduction of a sterile sampling manifold to enable multiple sampling events in a grade C environment without compromising the aseptic state of TFF assembly.

To ensure performance of the irradiated TFF filter, we measured its normalized water permeability (NWP) in multiple CGMP-compliant production runs and found the NWP values to be satisfactory before moving on to the next step.

The redesigned system eliminated 51 manual connection steps, streamlined process execution, and converted TFF operations from a functionally closed system to a fully closed system. Note that this enabled critical operations to be performed outside a BSC, with welding and sealing of modules executed in a grade C environment. Use of gamma-irradiated TFF modules eliminated the chemical sanitization step, simplified operations, and shortened downstream-processing time.

Implementing a single-use flowpath with incorporated vent filters removed the need to assemble the TFF flowpath within a BSC, particularly because the original retentate reservoir was a carboy-style rigid plastic container rather than a soft bioprocessing bag. Because that reservoir was tall, many connections had to be made close to the ceiling of the BSC, which made it

Aseptic Process Simulation (APS)

APS is a valuable tool for evaluating aseptic manufacturing processes, demonstrating that asepsis can be achieved so long as sterility is maintained during execution (**11**).

In an APS run, all evaluated steps are executed using nutrient-rich microbial-growth–promoting media in place of buffers and products. Media are made to contact all product-contacting surfaces and exposed to the kinds of critical environment and process manipulations that products themselves will undergo (**11**).

After an APS run, all product-simulating media are incubated for seven days at temperatures that are optimal for bacterial and fungal growth. Any breach of the system (e.g., contaminants introduced during the process) will cause visible turbidity in the media. If no turbidity is observed, then the media enter growth-promotion testing, which involves inoculation with representative microorganisms to ensure that their growth is supported after processing. Simulated final products from the process also are tested for sterility as a confirmation to turbidity testing results. APS runs also can reveal weaknesses in facility design and maintenance, room qualification and environmental monitoring (EM) programs, aseptic practices and procedures, and operator training. Requalification of APS for manufacture of large viruses that cannot be sterile-filtered occurs at predefined intervals.

Overall, APS enables biomanufacturers to demonstrate the suitability and effectiveness of their aseptic processes to deliver sterile products both consistently and reproducibly (**11**). If sterility is not maintained, an effectively designed APS enables identification of potential contamination sources. It can even shine light on a company's overall quality procedures and practices.

difficult for operators to reach in and maneuver. In addition, the BSC was crowded with other bulky items such as braided tubing and a separate single-use pump chamber. Implementation of the custom single-use flowpath obviated the need for complex manipulations of bulky consumables inside a BSC.

The new fully closed TFF system not only provides significantly greater sterility assurance, but it also enables more efficient processing than does the functionally closed system through 40% reduction of APS setup and process times. Environmental monitoring requirements are lower because no open connections or transfers are made inside the BSC. Our fully closed system also eliminates the risk of leaks from manually installed fittings, and it saves time and expense by obviating the need for chemical sanitization.

Addressing Flow Rate and Shear Sensitivity: Our scale-up efforts revealed insufficient flow capacity and a risk of shear-induced virus degradation (**6–8**). The initial peristaltic pump we used could deliver only about 20 L/min; the APS run was modeled after a client's process requiring a TFF recirculation flow rate of ≈50 L/min. Therefore, we had to procure a higher-flow pump. At the desired operating speed, diaphragm pumps are better suited for handling shear-sensitive viral solutions because they generate relatively lower shear forces. Peristaltic pumps can create turbulent flow and generate high shear through their roller mechanisms.

Solution — Equipment Adaptation: Beyond the need for a fully closed TFF processing solution, our team faced two other important challenges during development of a large-scale downstream purification process for poxviruses.

The first challenge was to achieve a sufficiently high flow rate during the TFF step because the pumps available in house lacked the required capability. Our team procured a diaphragm pump with a maximum flow rate of 5000 L/h that was compatible with presterilized, single-use pump chambers. With no rotating parts that could cause particle shedding or heating at high flow, that pump provided gentle operation with low turbulence and shear.

Our second challenge was to ensure gentle mixing during nuclease digestion, thus preventing virus degradation from shear forces. So we used a mixing system that leverages magnetically driven levitating impellers within single-use bags. Engaged with a magnetic motor during installation, the impeller could deliver up to 500 rpm of mixing speed.

Modularization Using Existing Consumables: Many process-specific single-use bags and filters are not designed for closed processing. Their open connectors present a contamination risk.

Solution — Custom Extension Design: The mixer bag that we use does not come as a closed system. Therefore, we designed special extensions that could be added to a mixer bag inside a BSC before application. The extensions make the bag a closed module while enabling its connectivity to other modules by welding.

We applied the same strategy to many other system consumables, including bioprocessing bags (for buffers, products, samples, and waste) and the clarification filtration flowpath. Thus we were able to preserve flexibility and enable use of existing CGMP-qualified and/or process-specific consumables to build closed modules.

All connections and disconnections between modules were made using a tube welder and/or sealer in a cleanroom outside of a BSC (grade C environment). Special attention was given to the number of welds needed for each extension to ensure that the lengths of weldable tubing would be sufficient. For sampling steps, we used closed sampling bags with weldable tubing instead of open bottles. That also reduced contamination risk significantly.

We separated the construction of different modules (e.g., enclosing a central consumable such as a filter or bag with extensions) from their use in client-material production by scheduling those activities on different days. All closed modules were constructed before any product-containing material entered the cleanroom. That strategy significantly reduced contamination risk during the module-build phase and streamlined operations during project execution. As a result, APS execution time for the new fully closed process was 40% shorter than that for the functionally closed process.

Confirmation of Closed-Process Performance

We conducted seven APS runs (runs 5–11) to assess robustness of the fully

closed system, with no turbidity observed across any unit operations (Table 1). Our results demonstrate not only the effectiveness of the closed and modular design, but also the operational readiness of the resulting process for CGMP manufacturing.

By conducting confirmatory APS runs, we thoroughly tested all consumables, extensions, and predesigned assemblies while providing operators with an opportunity to refine their aseptic techniques. Although specific aseptic procedures and practices have been implemented to improve consistency and provide assurance, we recognize the importance of ongoing training to ensure that all operators have the necessary skills and expertise required to achieve robust manufacturing project execution. Interventions should include on-the-job training for proper use of all equipment and aseptic techniques. Operators also should participate in periodic requalification APS runs.

Broad Applicability and Future Potential

Sterility assurance remains a fundamental requirement for biopharmaceutical manufacturing, particularly for complex biologics such as large viruses that cannot be terminally sterilized. Assuring drug-product sterility is essential not only for regulatory compliance (**9, 10**), but also to ensure patient safety. Our fully closed downstream process offers a scalable, flexible, and cost-efficient platform solution that preserves product integrity and reduces contamination risks.

We adapted an existing downstream poxvirus process into a robust, large-scale, aseptic manufacturing process for viruses that are too large to pass through 0.2-µm sterilizing-grade filters, enabling its application to other similar products. The adapted process is CGMP-compliant and capable of consistently providing contamination-free purified products. It leverages the concepts of closed systems and modular design while using existing consumables with customized extensions and assemblies. Our process design allows for connection of different modules (e.g., mixers, filters, and waste and product bags) in multiple configurations, providing flexibility to accommodate specific project needs.

Now, process setup is simplified, manual manipulations are reduced, and aseptic conditions are maintained throughout downstream unit operations. Only certain preparation steps (such as addition of extensions to consumables) must be performed in a grade A environment. The process itself is implemented in a grade C environment, simplifying implementation and reducing operating costs.

We have demonstrated the ability of our closed downstream process to assure sterility for purified large-virus products. Following successful performance of multiple APS runs using TSB as a product substitute, our group successfully completed an engineering run and a large-scale CGMP poxvirus purification run for a client using the closed system. Moreover, the process has been applied to manufacture of a second virus in the poxvirus family.

In addition to its ease of use and assurance of sterility, the new downstream process is virus agnostic and suitable for purification of many distinct products, including large viruses that cannot be sterile-filtered. In the future, we will continue to optimize the process, broaden its application to other large-scale virus manufacturing platforms, and leverage its modular design to support further customization.

Definitions of Open, Functionally Closed, and Closed Systems

Open systems are process systems that expose products to surrounding environments during operations such as pipetting between containers, open-catch transfers, and making connections using regular triclamps or quick-disconnect (QDC) connectors. In such systems, the environment is controlled to minimize risks of product contamination. The process fluid often is sterile-filtered after completion of each process step (**5**).

A system is *functionally closed* when it is assembled to eliminate environmental exposure of product-contacting surfaces. Subsequently, the system undergoes disinfection or sterilization before product processing. Not all components in a functionally closed system are sterile at the assembly stage. Yet all product-contacting surfaces should be sterile when exposed to product-containing solutions (**5**).

A system is said to be *fully closed* when the following conditions are met:

- all components are sterile before assembly or introduction to the system
- assembly incurs minimal risk of introducing contamination
- closed state is maintained after assembly (all product-contacting surfaces are contained and separated from the immediate process environment)
- new elements are introduced without breaking the closed state (e.g., connecting to presterilized, single-use items using aseptic connectors) (**5**).

Success in Fully Closed Systems

The development of a closed-system downstream purification process for large, nonfilterable viruses represents a significant advance in aseptic biomanufacturing. Through thoughtful engineering, strategic use of existing consumables, and modular system design, we have addressed the challenges of sterility assurance at scale. Our approach offers a viable template for future viral-vector and oncolytic-virus manufacturing processes to ensure compliance, patient safety, and operational efficiency.

References

1 Baxby D. Poxviruses. *Medical Microbiology* (4th Edition). Baron S, Ed. University of Texas Medical Branch at Galveston: Galveston, TX, 1996.

2 Conrad SJ, Liu J. Poxviruses as Gene Therapy Vectors: Generating Poxviral Vectors Expressing Therapeutic Transgenes. *Meth. Mol. Biol.* 1937, 2019: 189–209; https://doi.org/10.1007/978-1-4939-9065-8_11.

3 Mastrangelo MJ, et al. Poxvirus Vectors: Orphaned and Underappreciated. *J. Clin. Invest.* 105(8) 2000: 1031–1034; https://doi.org/10.1172/JCI9819.

4 Chaurasiya S, Fong Y, Warner SG. Oncolytic Virotherapy for Cancer: Clinical Experience. *Biomedicines* 9(4) 2021: 419; https://doi.org/10.3390/biomedicines9040419.

*Continued on **page 35***

Monitoring and Control of Adenovirus Processes with Real-Time Multiangle Light Scattering

Adrian Apetri, Daniel Some, Frank Lubbers, and Robbert Haven

Over the past few years, we have reported on robust application of analytical techniques at different stages of biopharmaceutical research and development (R&D), including discovery (**1–3**), structural characterization studies (**4, 5**), and identity assay development (**6, 7**). The COVID-19 pandemic — during which robust interventions needed to be identified within extremely short timelines — made it clear that speeding up vaccine development is crucial to achieving pandemic-related public-health objectives. Here, we focus on an approach to accelerating bioprocess development by bringing analytical solutions directly to processes: specifically, using real-time multiangle light scattering (RT-MALS) for in-line or on-line multiparameter monitoring during downstream processing (DSP) of adenovirus (AdV) vectors.

AdV is one of the industry's primary vectors for gene delivery, whether for therapeutics or prophylactic vaccines. The Vaccines and Prevention unit of Johnson & Johnson (J&J) has used its proprietary AdVac platform to develop multiple products based on adenovirus, including vaccines against Ebola virus, Zika virus, respiratory syncytial virus (RSV), sudden acute respiratory syndrome coronavirus 2 (SARS-CoV-2), and human immunodeficiency virus (HIV) (**8–12**).

A primary difficulty in AdV DSP development and performance is the lack of a means for rapid determination of critical quality attributes (CQAs) such as identity, purity, and titer. Although ultraviolet-light (UV) spectroscopy can be used to monitor the presence of biomolecules in an eluting peak, that method provides little to no useful information about those CQAs. Hence, AdV DSPs are developed through extensive trial and error based on tedious off-line measurements. Common off-line techniques include dynamic light scattering (DLS) for particle-size determination (indicative of viral integrity or aggregation) and capillary-zone electrophoresis (CZE) for viral titer (**13**). Quality-based criteria for DSP unit operations often include large safety margins to account for variability in starting material, buffer composition, column aging, and other process parameters. Proceeding to the next process step can be delayed until off-line analyses have confirmed product quality and quantified the needed CQAs as inputs for subsequent unit operations. Safety margins and wait times for off-line analytics raise significant obstacles for development timelines, process productivity, profitability, and ultimately, accessibility of life-saving vaccines. RT-MALS offers a means for overcoming such challenges by providing instantaneous measurements of vector size and titer during downstream and fill–finish operations.

Figure 1: Integration of an ultraDAWN instrument for real-time multiangle light scattering (RT-MALS) and Observer software with preparative liquid chromatography (LC) for real-time feedback and control; CQA = critical quality attribute, UV = ultraviolet light

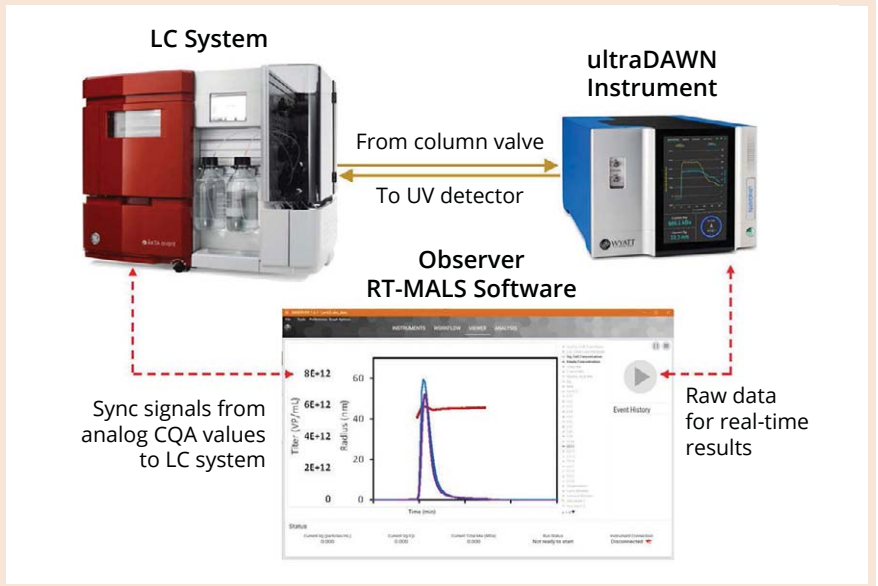

RT-MALS as a Process Analytical Technology (PAT)

RT-MALS operates on the same physical principles as standard MALS to measure

the molar mass and size of macromolecules as well as the size and physical titer of nanoparticles. But whereas instruments for standard MALS measurements typically are combined with analytical size-exclusion chromatography (SEC) (**14–16**), RT-MALS using an ultraDAWN instrument and Observer software (Waters) can be adapted for in-line use with bench-scale preparative liquid chromatography (LC) at flow rates up to 150 mL/min (Figure 1). For processes that operate at higher flow rates or take place in vessels, an auxiliary pump effects continuous on-line sampling. The ultraDAWN platform can import analog UV data and digital timing pulses from preparative-LC equipment as well as export signals to such systems for synchronization and process control. The RT-MALS technology also can accommodate high scattered intensities typically observed during AdV DSP, which would saturate standard MALS detectors.

RT-MALS can be applied as PAT in several biologics applications, including DSPs for proteins, nucleic acids, and viral vectors (**17, 18**). For small viral vectors, such as adenoassociated virus (AAV) particles, the technology can quantify genomic payload (empty:full capsid ratios) and titers of full and empty capsids (**19**). Other biopharmaceutical applications include monitoring of lipid-nanoparticle (LNP) encapsulation during manufacturing of messenger RNA (mRNA) products and of depolymerization or polysaccharide conjugation for pneumococcal vaccines (**20**).

Materials and Methods

AdV: We used an adenovirus serotype 26 (AdV26) active pharmaceutical ingredient (API). The composition of applied formulation buffers is not disclosed here; however, buffer components showed no interference with measurements (data not shown for brevity).

MALS: Because the process's high viral titer (>10^{12} viral particles (VP)/mL) generates high light scattering intensity, our team outfitted an ultraDAWN instrument with optical density (OD) 2 attenuators on detectors 2, 4, 6, 8, 10, 14, 16, and 18 to prevent saturation. Not all measurements required use of the attenuated detection angles. Particle concentration calculations were corrected for turbidity using the ultraDAWN system's Forward Monitor feature, which measures transmission through a flow cell.

RT-MALS technology can accommodate **HIGH SCATTERED INTENSITIES** typically observed during adenovirus downstream processing, which would saturate standard MALS detectors.

Preparative LC: AdV DSP included an ion-exchange (IEX) polishing step on an Äkta Pure 150 chromatography system (Cytiva) operated with a 20-mL column under Unicorn 7 control software at flow rates of 5–15 mL/min. Step-gradient elution was monitored by UV absorbance at 280 nm. The ultraDAWN instrument was plumbed in line between the UV and conductivity detectors, although it also could have been inserted between the column valve and UV detector or elsewhere.

Tangential-Flow Filtration (TFF): Our team constructed a bench-scale TFF system for AdV ultrafiltration/diafiltration (UF/DF) using peristaltic pumps, reservoirs monitored by electronic scales, and a hollow-fiber TFF cartridge. Retentate flowed at a rate of 600 mL/min. Sampling points were introduced through tee unions in the retentate and permeate lines, and the RT-MALS auxiliary pump was connected to one or the other line to draw a continuous slipstream to the ultraDAWN instrument. Then, the slipstream is recirculated to the main process flow.

Fill–Finish: For final dilution of purified material to drug-product concentration, we used a system comprising a mixing vessel, a pump for adding formulation buffer, and a recirculating pump for mixing. The RT-MALS auxiliary pump was connected to the recirculating line, where it drew a continuous slipstream to the ultraDAWN system and returned it to the recirculating line. The mixing vessel was loaded initially with 2 L of concentrated drug product. Stepwise dilutions were performed to a final volume of 14 L.

On-Line Analysis: Observer software was configured to acquire MALS data and report particle-size and concentration attributes, applying either in-line or on-line nanoparticle workflows depending on the specific process.

For prep-LC, the in-line nanoparticle workflow exchanged digital pulses and analog signals to enable synchronization and signaling with the Unicorn program. Data were acquired and attributes were reported at two-second intervals. Furthermore, a condition was set up in the Observer software to indicate when AdV product should be pooled. At the end of the run, Observer software integrated data over the expected pool to calculate average or total attribute values. Any region could be selected manually for such integration during postprocess analysis.

For UF/DF and fill–finish steps, the on-line nanoparticle workflow controlled an auxiliary pump to draw a slipstream from the process. Data were collected and attributes were reported at two-second intervals for TFF and at five-second intervals during fill–finish.

Off-Line Analysis: Fractions also were collected and analyzed off line. We used DLS for size determination and CZE for titer determination (**13, 21**).

Results and Discussion

IEX Polishing: AdV polishing was carried out by bind–elute IEX chromatography on an Äkta Pure 150 system (Cytiva). RT-MALS monitored column loading and washing as well as elution.

Column Loading — Dynamic Binding Capacity (DBC) and Impurity Flush: Loading is optimized such that viral vectors are retained on the column while impurities such as free proteins and nucleic acids flush through. To conserve product in this process, loading should cease upon column saturation.

Table 1: Comparison of in-line multiangle light scattering (MALS) with off-line capillary-zone electrophoresis (CZE) and dynamic light scattering (DLS) for viral titer and radii size, respectively, under different process conditions (R = mass-weighted radius, R_h = hydrodynamic radius, VP = virus particle)

	Test Conditions		Radius (nm)		Titer (VP/mL)	
Sample	Flow Rate (mL/min)	Load (Total VP)	RT-MALS (R)	DLS (R_h)	RT-MALS	CZE
AdVac vector 1	15	2.4×10^{13}	47.1 ± 2.4	47.6 ± 0.9	5.4×10^{11}	5.9×10^{11}
	5	2.4×10^{13}	45.7 ± 0.5	48.6 ± 0.2	7.3×10^{11}	6.1×10^{11}
	5	4.5×10^{13}	45.8 ± 0.7	48.6 ± 0.1	1.2×10^{12}	1.2×10^{12}
AdVac vector 2	15	1.8×10^{13}	45.0 ± 0.5	48.4 ± 0.7	1.0×10^{12}	8.2×10^{11}
	7.5	1.8×10^{13}	44.6 ± 3.5	47.7 ± 0.0	1.1×10^{12}	8.5×10^{11}
	7.5	1.8×10^{12}	43.3 ± 0.5	46.0 ± 0.4	1.5×10^{11}	9.1×10^{10}

Figure 2: Multiangle light scattering (MALS, black dashes) and ultraviolet-light (UV) spectroscopy (purple solid line) traces recorded during preliminary ion-exchange chromatography (IEX) polishing phases: conditioning (9–11 minutes), column loading (11–16 minutes), and wash (17–20 minutes); overall light scattering intensity (R_0) is the scattering signal extrapolated as a function of angle to 0°. Comparison of MALS and UV enables distinction of viruses versus free proteins and nucleic acids. (AU = absorbance units)

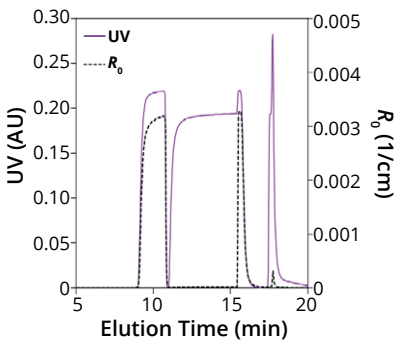

Figure 3: Viral titer (blue line and open circles) and viral-particle (VP) radii (red squares) from multiangle light scattering (MALS) analysis overlaid with ultraviolet-light (UV) spectroscopy (purple) during the elution phase; a 45-nm value of the radius is indicative of monomers. Radii and titer values averaged over the peak correlate well with off-line reference methods.

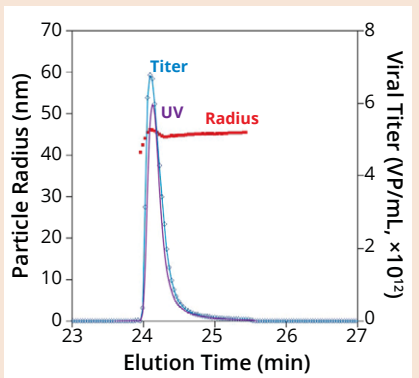

Figure 4: Viral-particle (VP) titer (blue open circles) and radii (red squares) from multiangle light scattering (MALS) analysis overlaid with ultraviolet-light (UV) spectroscopy (purple) during the elution and strip phases; the green band indicates when Observer software's trigger is activated for process control.

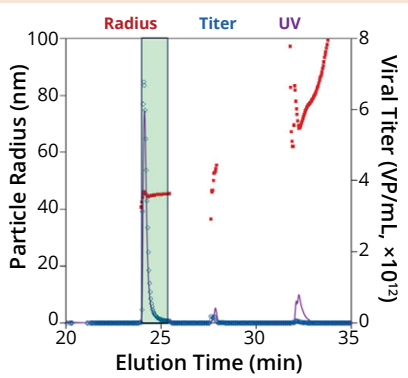

Although a UV detector typically is used to monitor molecules as they wash through a column, that method does not discriminate between product and impurities and hence is insufficient for optimizing AdV DSP. On the other hand, MALS intensity is responsive to the sixth power of a particle's radius, making it far more sensitive to viruses than to free macromolecules.

Figure 2 presents MALS and UV signals recorded during conditioning, column loading, and wash. During conditioning (9–11 minutes into the process), the system was flushed with load material, bypassing the column. Both UV and MALS signals are prominent at that point, meaning that relatively large particles with significant absorption passed through the detectors. At the beginning of the load phase (11–15 minutes), UV-active material (such as proteins and nucleic acids) washed through the column, as indicated by a rising UV signal. There was little scattering signal, suggesting that virus particles were adhering to the column and not reaching the detectors. At the end of loading (15–17 minutes), a jump in the UV signal correlates with the appearance of a substantial MALS signal. Thus, the column was fully saturated and had reached its DBC; subsequently loaded viruses would not bind to the column and would reach the detectors directly. In the wash phase (17–20 minutes), we again see an appreciable UV signal with almost no MALS counterpart, suggesting that primarily free molecules were dislodged from the column while viruses adhered.

In that operation, using RT-MALS alongside UV created a meaningful picture, enabling rapid process development and optimization. During manufacturing operations, RT-MALS can provide automated process control to overcome variations in titer and/or impurity load in feed material. For example, an automation system can be programmed to halt column loading when viral titers reach a preset value.

Elution — Size and Titer: Elution conditions are optimized to separate monomeric viruses from aggregates and free macromolecules. Following polishing, aliquots are normally sent to an analytical laboratory to confirm purity and titer, the latter measurements being needed to ensure optimal process parameters in subsequent UF/DF operations. Here, RT-MALS can monitor particle size to confirm the identity of monomeric AdVs and to ensure that monomers primarily are collected in an elution pool. Because RT-MALS determines titer at every data slice, results can be integrated over a collection period to provide immediate values for both VP/mL and total particles in a pool. Figure 3 shows particle-size and titer measurements from MALS along with the UV chromatogram obtained during elution.

We leveraged the Observer software's Trigger function to flag the presence of purely monomeric viruses, as determined by particle size. The function was set to activate as elution began. To prevent activation on arbitrary size values produced by noisy, low-

Close agreement in the obtained values suggests that implementation of RT-MALS should **ACCELERATE** adenovirus process development and enhance product quality while enabling a significant reduction to the number of off-line assays.

Figure 5: Tangential-flow filtration (TFF) system used for ultrafiltration and diafiltration (UF/DF) with on-line real-time multiangle light scattering (RT-MALS) analysis

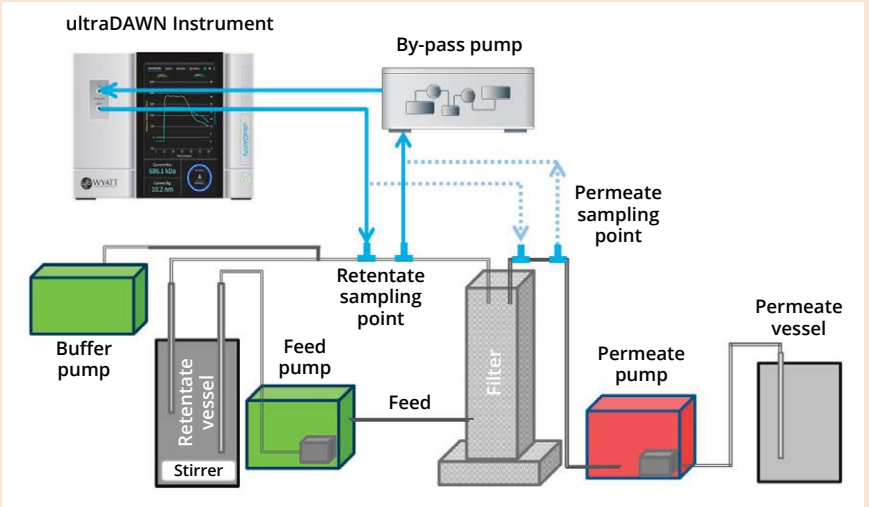

Figure 6: Real-time multiangle light scattering (RT-MALS) measurements of virus-particle (VP) radius and titer during a diafiltration run (DV = diafiltration volume)

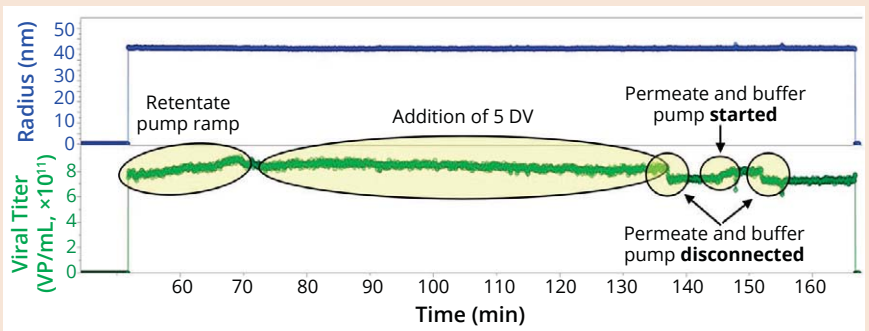

amplitude light-scattering signals, we configured the trigger to be kept "off" when overall light-scattering intensity (R_0) was below a predefined value. Specifically, the trigger conditions were

- measured particle radius = 40–50 nm
- R_0 > 3 × 10−4 cm^{-1}.

Figure 4 shows the region flagged upon applying these trigger conditions. The elution tail and later peaks produced during strip phases (containing aggregates or other large particulates) were not flagged, either because the MALS intensity was too low or because measured particle radii were out of range.

Comparison with Off-Line Analytics: During elution, a pool was collected and analyzed off line by reference methods: DLS for size and CZE for titer. Table 1 compares off-line values and RT-MALS results averaged over the trigger region for a series of purification runs. Those runs were performed at different flow rates and loading titers using two AdV constructs. As Table 1 shows, particle radii obtained by RT-MALS tracked well with those measured by DLS across the different conditions. The methods showed a small discrepancy in values — about 3 nm — that arises due to the different properties measured by the techniques. RT-MALS measures mass-weighted radii, whereas DLS estimates hydrodynamic radii. Furthermore, titers determined by RT-MALS and CZE were similar with differences of <30%, which represents reasonable variation between particle-concentration methods for process intermediates. Sources of variability include the specific range averaged by RT-MALS against the actual pooled range, the accuracy of optical parameters, the fact that CZE is a relative method whereas RT-MALS is an absolute method, and deviations in particle size calculated by RT-MALS (a 2% error in size leads to a 12% error in titer).

Close agreement in the obtained values suggests that implementation of RT-MALS should accelerate AdV process development and enhance product quality while enabling a significant reduction to the number of off-line assays.

UF/DF: For this step, we used a typical TFF system (Figure 5). RT-MALS sampling connections were set up on either the retentate or permeate line to monitor AdV particles continuously. Solution returned to the same line following measurement.

Retentate Monitoring: The bypass pump drew samples at 5 mL/min to the ultraDAWN instrument, which recorded average radii and titer values continuously at two-second intervals. Figure 6 presents those data with callouts indicating different process phases. The consistency of radius data across the run indicates no detection of virus-particle degradation, such as aggregation. Furthermore, although the titer data show some expected variation at pump flow-rate changes, values overall remain mostly consistent over the exchange of five diafiltration volumes. Such consistency provides clear proof that the operation proceeded as intended with no dilution or concentration of product.

Comparison with Off-Line Analytics: Several samples acquired during DF underwent off-line analysis and comparison with real-time data (Table 2). Once again, data obtained from RT-MALS and from the reference DLS and CZE methods correlate closely, and

Table 2: Comparison of real-time multiangle light scattering (RT-MALS) data with off-line results obtained with dynamic light scattering (DLS) and capillary-zone electrophoresis (CZE) reference methods for aliquots sampled at the indicated times; R = mass-weighted radius, R_h = hydrodynamic radius, VP = virus particle

	Radius (nm)		Titer (VP/mL)	
Time	RT-MALS (R)	DLS (R_h)	RT-MALS	CZE
81 min	45.1	48.2	8.6×10^{11}	6.6×10^{11}
97 min	45.3	48.0	8.4×10^{11}	7.1×10^{11}
112 min	45.4	48.0	8.2×10^{11}	6.6×10^{11}
134 min	45.2	48.4	8.2×10^{11}	6.3×10^{11}
141 min	45.2	48.7	7.3×10^{11}	5.8×10^{11}

Figure 7: Real-time multiangle light scattering (RT-MALS) RT-MALS plots of virus-particle (VP) radius (red circles) and titer (blue squares) during final product dilution; the increasing size values observed might have arisen from changes in refractive index of the solution over the dilution process.

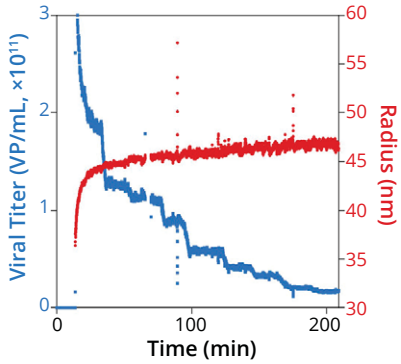

Figure 8: Measured and expected viral-particle (VP) titer during final dilution; real-time multiangle light scattering (RT-MALS, full circles), capillary-zone electrophoresis (CZE, open triangles), quantitative polymerase chain reaction (qPCR, open squares)

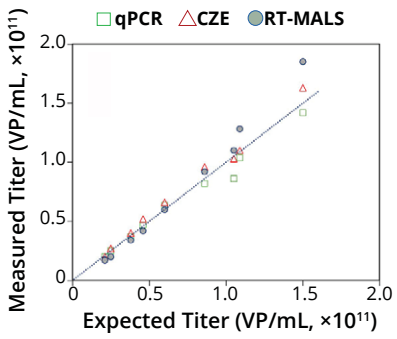

differences are consistent with those found for the chromatography runs: a 3-nm difference in radius values and a 20–30% difference in titers.

Permeate Monitoring: In other runs, RT-MALS monitoring served to detect viruses indicative of membrane fouling. No viral particles (or membrane fouling) were detected.

In this UF/DF step, drug substance typically is characterized before and after the process. It is unusual for development scientists to have relevant data during UF/DF unit operations. However, RT-MALS provided reliable, real-time data for monitoring process health and maintaining product quality.

Final Dilution: Concentrated product was diluted to a final concentration in the mixing system described above. Aliquots were removed periodically for off-line analysis by DLS, CZE, and quantitative polymerase chain reaction (qPCR, for viral titer in addition to CZE).

Figure 7 shows particle-size and titer measurements from RT-MALS over the stepwise dilutions, which manifest as incremental decreases in titer. An initially sharp and then slower increase in particle size is observed with the RT-MALS data over the dilution. That reflects the transition from drug-substance buffer to drug-product buffer. Those materials have substantially different refractive indices, influencing the angular fit of the scattering data. Because Observer software cannot change normalization constants during a run, those were calculated for the buffer present at the midpoint of dilution.

Those apparent variations in particle size are detrimental for titer analysis by RT-MALS. The calculated particle concentration is inversely proportional to the sixth power of the radius, so a nonlinear relationship can be expected between titer values from RT-MALS and expected titers or those measured by CZE or qPCR. Figure 8 shows such a relationship, especially for initial process steps (higher concentrations, right side of the graph), when buffer composition was still changing significantly.

Figure 9: Real-time multiangle light scattering (RT-MALS) traces of virus-particle radius (red circles) and overall light-scattering intensity (R_0, black squares)

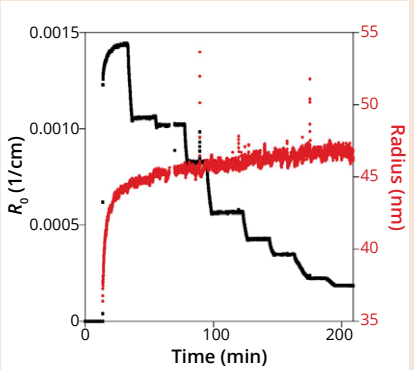

Nonlinearity and error in titer measurements due to changing buffer refractive index can be overcome by using R_0 values, which are plotted in Figure 9 along with measured radii. We convert those data to titer by multiplying RO values by a constant calibration factor determined for this step (which depends on particle size and buffer refractive index) to be 1.05×10^{-8} cm·VP/mL. Correlation to the expected titer is excellent, as seen in Figure 10. An added benefit of using R_0 with a calibration factor is the lower degree of noise relative to calculated titer, as is evident by comparing Figures 7 and 9.

As with UF/DF, standard protocols for final dilution steps provide no real-time monitor for CQAs and other product attributes, and aliquots must be transferred to an analytical laboratory for periodic analysis. That is not sufficiently timely for process control because deviations are caught only after the fact. On-line RT-MALS overcomes that limitation, enabling close monitoring of product quality and CQAs such as titer.

Conclusion

The aspiration to reduce time to market for life-saving biologics while boosting product yield highlights the need for real-time acquisition of CQAs and other product attributes. Real-time data capture and monitoring would help biomanufacturers to maintain product quality while increasing automation opportunities and providing for digitally interconnected unit operations with both feedback and feed-forward.

Figure 10: Viral-particle (VP) titer from multiangle light scattering (MALS) analysis results from multiplying particles' overall light-scattering intensity (R_0) by a constant factor of (1.05×10^{-8} cm·VP/mL); data closely match expected titer values, with a coefficient of determination (R^2) value of 0.999.

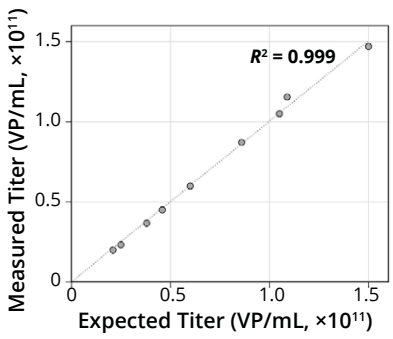

To accelerate time to market, DSP development teams and unit operations cannot wait weeks, days, or even hours for critical data. RT-MALS provides viral-vector CQAs on time scales of seconds to tens of seconds, speeding up process development, generating extensive process knowledge, and enabling direct control of process steps that may take place over minutes to an hour. RT-MALS, realized with technologies such as ultraDAWN MALS instruments and Observer software, could establish a new paradigm in PAT for DSP of viral vectors such as those produced by J&J's AdVac platform.

Acknowledgments

We express special thanks to Clara Perez Peinado for her extreme dedication in driving PAT efforts and advancing technology implementation. We also thank Andreia Allen, Marcus Valente, and Wouter den Dekker for their contributions to this work and Luca Martinelli for reviewing the manuscript.

References

1 Apetri A, et al. A Common Antigenic Motif Recognized by Naturally Occurring Human VH5-51/VL4-1 Anti-Tau Antibodies with Distinct Functionalities. *Acta Neuropathol. Commun*. 6, 2018: 43; https://doi.org/10.1186/s40478-018-0543-z.

2 van Ameijde J, et al. Enhancement of Therapeutic Potential of a Naturally Occurring Human Antibody Targeting a Phosphorylated Ser422 Containing Epitope on Pathological Tau. *Acta Neuropathol. Commun*. 6, 2018: 59; https://doi.org/10.1186/s40478-018-0562-9.

3 Nkolola JP, et al. Characterization and Immunogenicity of a Novel Mosaic M HIV-1 gp140 Trimer. *J. Virol*. 88(17) 2014: 9538–9552; https://doi.org/10.1128/JVI.01739-14.

4 Zhang H, et al. Structural Basis for Recognition of a Unique Epitope by a Human Anti-Tau Antibody. *Structure* 26(12) 2018: 1626–1634; https://doi.org/10.1016/j.str.2018.08.012.

5 Puchades C, et al. Epitope Mapping of Diverse Influenza Hemagglutinin Drug Candidates Using HDX-MS. *Sci. Rep.* 9, 2019: 4735; https://doi.org/10.1038/s41598-019-41179-0.

6 De Marco D, et al. Cell-Based Assay To Study Antibody-Mediated Tau Clearance by Microglia. *J. Visual. Experim*. 141, 2018: e58576; https://doi.org/10.3791/58576.

7 Crespo R, Koudstaal W, Apetri A. In Vitro Assay for Studying the Aggregation of Tau Protein and Drug Screening. *J. Visual. Experim.* 141, 2018: e58570; https://doi.org/10.3791/58570.

8 Bos R, et al. Ad26 Vector-Based COVID-19 Vaccine Encoding a Prefusion-Stabilized SARS-CoV-2 Spike Immunogen Induces Potent Humoral and Cellular Immune Responses. *NPJ Vaccines* 5, 2020: 91; https://doi.org/10.1038/s41541-020-00243-x.

9 Sadoff J, et al. Safety and Efficacy of Single-Dose Ad26.COV2.S Vaccine Against Covid-19. *New Engl. J. Med.* 384(23) 2021: 2187–2201; https://doi.org/10.1056/NEJMoa2101544.

10 Sadoff J, et al. Interim Results of a Phase 1–2a Trial of Ad26.COV2.S Covid-19 Vaccine. *New Engl. J. Med.* 384(19) 2021: 1824–1835; https://doi.org/10.1056/NEJMoa2034201.

11 Baden LR, et al. First-in-Human Evaluation of the Safety and Immunogenicity of a Recombinant Adenovirus Serotype 26 HIV-1 Env Vaccine (IPCAVD 001). *J. Infect. Dis*. 207(2) 2013: 240–247; https://doi.org/10.1093/infdis/jis670.

12 Barouch DH, et al. Characterization of Humoral and Cellular Immune Responses Elicited by a Recombinant Adenovirus Serotype 26 HIV-1 Env Vaccine in Healthy Adults (IPCAVD 001). *J. Infect. Dis*. 207(2) 2013: 248–256; https://doi.org/10.1093/infdis/jis671.

13 van Tricht E, et al. One Single, Fast and Robust Capillary Electrophoresis Method for the Direct Quantification of Intact Adenovirus Particles in Upstream and Downstream Processing Samples. *Talanta* 166, 2017: 8–14; https://doi.org/10.1016/j.talanta.2017.01.013.

14 Some D, et al. Characterization of Proteins by Size-Exclusion Chromatography Coupled to Multi-Angle Light Scattering (SEC-MALS). *J. Visual. Experim*. 148, 2019: e59615; https://doi.org/10.3791/59615.

15 Wen J, Arakawa T, Philo JS. Size-Exclusion Chromatography with On-Line Light-Scattering, Absorbance, and Refractive Index Detectors for Studying Proteins and Their Interactions. *Anal. Biochem*. 240(2) 1996: 155–166; https://doi.org/10.1006/abio.1996.0345.

16 Mogridge J. Using Light Scattering To Determine the Stoichiometry of Protein Complexes. *Meth. Mol. Biol*. 1278, 2015: 233–238; https://doi.org/10.1007/978-1-4939-2425-7_14.

17 Rajendar B, et al. Multi Angle Light Scattering as a Process Analytical Technology Tool for Real-Time Monitoring of Molar Mass of Protein-Polysaccharide Conjugate Fractions. *J. Chromatogr. Open* 2, 2022: 100045; https://doi.org/10.1016/j.jcoa.2022.100045.

18 Patel BA, et al. Multi-Angle Light Scattering as a Process Analytical Technology Measuring Real-Time Molecular Weight for Downstream Process Control. *mAbs* 10(7) 2018: 945–950; https://doi.org/10.1080/19420862.2018.1505178.

19 Haller FM, Some D. *AN8008: Real-Time Monitoring and Control of AAV Chromatographic Enrichment with RT-MALS* [application note]. Wyatt Technology: Santa Barbara, CA; https://www.wyatt.com/library/application-notes/an8008-real-time-monitoring-and-control-of-aav-chromatographic-enrichment-with-rt-mals.html.

20 Ralbovsky NM, et al. Process Analytical Technology for Real-Time Monitoring of Pharmaceutical Bioconjugation Reactions. *Org. Process Res. Dev.* 29(2) 2025: 353–362; https://doi.org/10.1021/acs.oprd.4c00399.

21 Mann B, et al. Capillary Zone Electrophoresis of a Recombinant Adenovirus. *J. Chromatogr. A* 895(1–2) 2000: 329–337; https://doi.org/10.1016/S0021-9673(00)00668-8.

Corresponding author ***Adrian Apetri*** *is scientific director for biophysics and process analytics in cell and gene therapy analytical development (aapetri@its.jnj.com),* ***Frank Lubbers*** *is a former scientist, and* ***Robbert Haven*** *is an associate scientist, all at Johnson & Johnson.* ***Daniel Some*** *is senior principal product manager for process analytical technology (PAT) at Waters Corporation.*

Exposing the F_0 Illusion in SIP

Why Sterilization Assurance Demands More

Naveenganesh Muralidharan, Alejandro Kaiser, Marc Pelletier, and Alexander Elkin

Steam-in-place (SIP) sterilization is essential in biopharmaceutical manufacturing for achieving microbial lethality standards. Often, the process is validated using overkill targets such as a sterilization lethality (F_0) value indicating a sterility assurance level (SAL) of 10^{-6} after application of saturated steam for 15–20 minutes at 121.1 °C. Although this approach is used widely in industry, it relies on temperature-sensor readings from outside of a process zone to confirm compliance. However, such measurements can be misleading if not coupled with other parameters. Sensors measure sterile-boundary steam temperature but cannot detect local reductions in wall temperature caused by residual air layers, which act as insulators and can be formed during sterilization cycles, especially in pipes that lack proper venting or sloping. Although axial steam displacement is rapid, radial diffusion toward pipe walls is slower and can leave persistent air films that reduce local lethality, even when measured steam temperature appears to be compliant. Thus, relying solely on sensor-based F_0 calculations brings a risk of overlooking such zones of sublethal exposure.

We examine the dynamics of axial and radial steam movement, friction factor and shear-stress effects on boundary-layer thickness, and the resulting impact on wall temperature and lethality. By introducing a "radial-access efficiency" (RAE) correction, it becomes clear that achieving genuine sterilization requires more than reaching an $F_0 \geq 12$ min at the sterile boundary. Rather, it demands adequate dwell times, effective venting strategies, and a sound pipe design to ensure full steam access and uniform microbial killing throughout a system.

Steam Flow Dynamics and Air Entrapment

During turbulent fluid flow inside a pipe, the overall motion of applied steam includes both axial movement (along the pipe) and random, chaotic eddies that support limited radial mixing. However, steam penetrates toward a pipe wall through a combination of radial convection and diffusion. Although convective eddies contribute to some cross-stream mixing, radial diffusion, governed by the slower mechanism of eddy diffusivity, remains dominant rather than bulk flow velocity (Figure 1A).

In SIP operations, air can remain trapped along pipe walls or in boundary layers because of incomplete displacement during the heat-up phase. Even with high axial steam velocity (e.g., 35 m/s) during that stage, steam can push rapidly through a pipe without ensuring removal of all air near the walls. It is important to consider how long fresh, pure steam takes to reach and replace air remaining in near-wall regions. Although steam flow provides continuous renewal, limited radial mixing and slow diffusion can leave thin air layers against the pipe wall. Such boundary layers act as insulators, lowering local temperatures and subsequent sterilization effectiveness even when sensors report adequate sterilizing temperatures overall.

Figure 1A illustrates that effect, with air collecting in the boundary layer that can develop into an unsterilized area if not properly purged during heat-up (**1**).

Axial displacement time (t_A) in the context of SIP operations is used to estimate how long it takes for steam to travel linearly (axially) through a pipe or vessel segment during the air-displacement phase (typically the heat-up phase of SIP):

Equation 1: $$t_A = L \div \vartheta$$

where ϑ represents steam velocity (e.g., 35 m/s) and L is pipe length (**1, 2**).

Convective Displacement Time: As illustrated by the helical arrows in Figure 1A, turbulent eddies carry steam radially toward the pipe wall while simultaneously sweeping it axially downstream. That bulk motion, known as *convective flow*, helps to drive steam into regions near the wall. However, due to the no-slip condition, velocity at the wall is effectively zero, allowing a thin boundary layer of residual air to persist.

Convective displacement time ($t_{r,Con}$) represents the time required for those radial eddies to push steam into the boundary layer and displace trapped air during heat-up. It is calculated using the following equation, in which Δz is the effective length of the mixing zone, D is the pipe diameter in meters, L is the pipe length in meters, and $\Delta z = (4DL)^{0.5}$ (**2**):

Equation 2: $$t_{r,Con} = (2 \times \Delta z \times t_A) \div L$$

Although convection accelerates mixing across most of a pipe cross-

section, it becomes ineffective near the wall where velocities approach zero. At that point, molecular diffusion becomes the dominant mechanism. Because diffusion is far slower than convection, additional time is needed for steam to penetrate the boundary layer and displace residual air completely.

Diffusion Displacement Time: Once convection can no longer drive mixing near the pipe wall, the final removal of air pockets is governed by diffusion. *Diffusion displacement time* ($t_{r,Diff}$) represents the time required for steam molecules to migrate from the pipe center line to the wall by radial eddy diffusion, as defined in Equation 3 below. Therein, E_r is the radial eddy diffusion coefficient, which equals $0.0518 \times D^{0.96}$ m²/s. That empirical correlation applies for nominal pipe sizes between 0.25 in. and 2 in. (**1, 2**).

Equation 3: $t_{r,Diff} = D^2 \div E_r$

From Flow Mechanisms to Numerical Modeling

The above section establishes the fundamental mechanisms by which steam displaces residual air in SIP systems — first axially, then radially by convection, and finally by diffusion. Together, those mechanisms explain why near-wall air pockets can persist despite rapid bulk steam flow. Now, we apply those flow principles to calculate the residual air-film thickness near a pipe wall under typical SIP conditions. By linking steam velocity, Reynolds number (*Re*), friction factor, and wall shear stress, we can characterize the turbulent boundary layer and determine how much air can remain trapped. That calculation will enable us to evaluate the effects of that air layer on wall temperature, heat transfer, and ultimately F_0, leading to an engineering-based correction model.

Residual Air-Film Thickness Near Pipe Wall: Although turbulent flow promotes mixing within most of the pipe, complete removal of residual air adjacent to the wall is a critical factor in SIP operations. That near-wall layer acts as a barrier to heat transfer, compromising sterilization performance.

At SIP conditions, saturated steam has very low kinematic viscosity and typically exhibits high *Re* values, resulting in fully developed turbulent flow with steep near-wall velocity gradients. Under such conditions, the skin-friction factor (f) is used to characterize wall shear stress and estimate the resulting thin, turbulent boundary layer.

Figure 1: (A) Convective flow and radial diffusion dynamics in piping during steam-in-place (SIP) operations; (B) comparing saturated steam and steam–air mixture to gauge misleading temperature readings in SIP (psig = gauge pressure in pounds per square inch, TT = temperature transmitter)

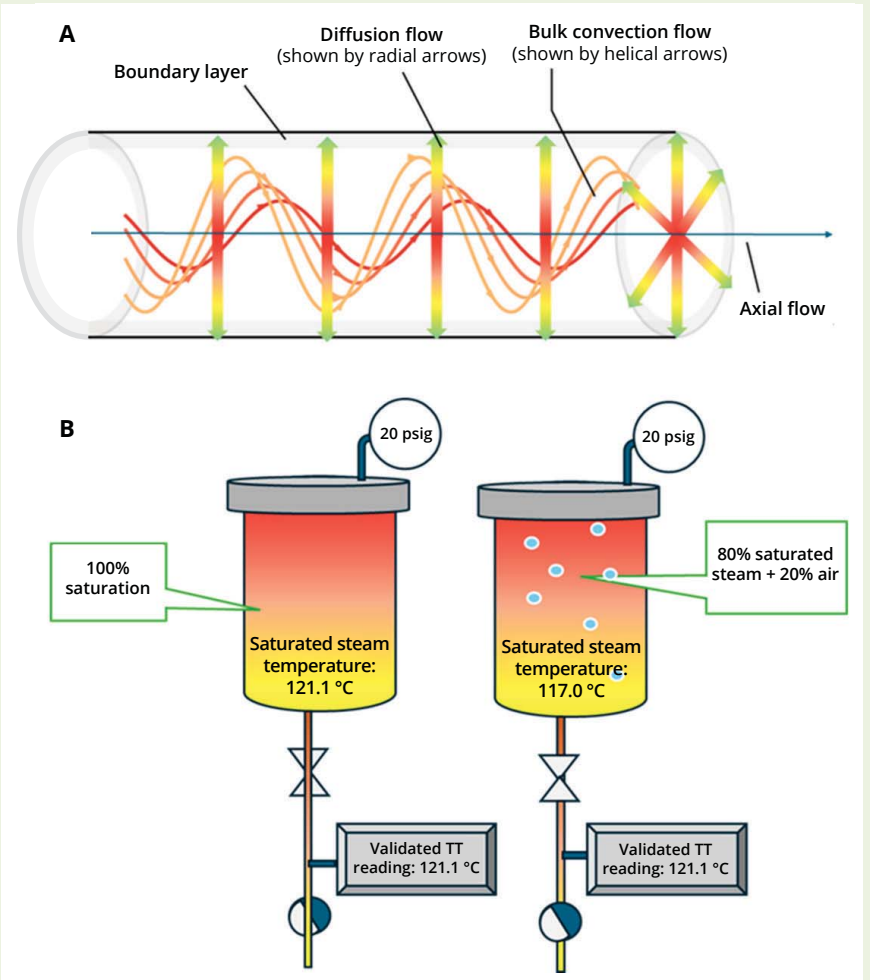

For turbulent flow in smooth pipes with flow regimes of $2100 < Re < 10^5$, Blasius estimates the friction factor as a function of *Re* as shown in Equation 4 (**3**). There, $v = 0.00002$ m²/s serves as the kinematic viscosity of steam, $\rho = 1.15$ kg/m³ is the steam density under ≈15.04 pounds per square inch gauge (psig) pressure in the system or 29.74 psi absolute pressure (15.04 psig + 14.7 psi atmospheric pressure), and $R = \vartheta D \div v$ (**4**):

Equation 4: $f \approx 0.0791 \times R^{-0.25}$

Friction factor also can be expressed as a function of wall shear stress (τ_w):

Equation 5:
$$f = 8\tau_w \div \rho\vartheta^2 \Rightarrow \tau_w = (f\rho\vartheta^2) \div 8$$

Wall shear stress governs the steam velocity gradient at a pipe wall according to Newton's law of viscosity, which states that a velocity gradient is proportional to the amount of shear stress divided by dynamic viscosity. Equation 6 expresses the characteristic near-wall region thickness (δ), with ϑ_s representing shear velocity (**6**):

Equation 6: $\delta \approx v \div \vartheta s$, where $\vartheta s = (\tau_w \rho)^{0.5}$

Temperature Gradient Across the Air-Filled Boundary Layer: In SIP operations, failure to remove residual air from the near-wall boundary layer results in both mass-transfer resistance (incomplete air displacement) and thermal resistance that reduces heat transfer to the pipe wall. Trapped air

Figure 2: Relationship between air fraction and steam temperature to calculate risk of sublethal exposure; F_0 = sterilization lethality, R^2 = coefficient of determination

Tank Diameter	Air Fraction	Actual Temperature	F_0 (Target = 12 min)
0.25 m	0.01%	126.0 °C	37.0
0.50 m	0.03%	126.0 °C	37.0
1.25 m	0.19%	125.9 °C	36.4
1.50 m	0.32%	125.9 °C	36.0
2.25 m	1.39%	125.4 °C	32.6
2.50 m	2.25%	125.1 °C	30.2
3.25 m	9.36%	122.3 °C	15.7
3.50 m	15.05%	120.0 °C	9.3

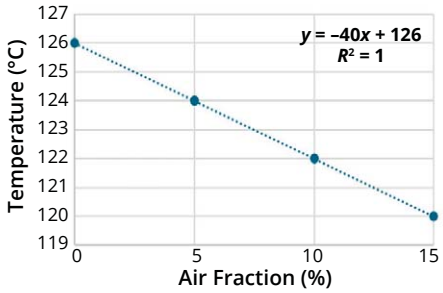

Figure 3: Relationship between air fraction and steam temperature to calculate risk of sublethal exposure; F_0 = sterilization lethality, t_{diff} = diffusion time

confined within the turbulent boundary layer acts as an insulator due to the low thermal conductivity of air (≈0.0264 W/m·°C) (**1**).

The temperature gradient across that air-filled boundary layer can be estimated using Fourier's law of conduction, as shown in Equation 7 below (**1**). There, Q represents the rate of heat transfer (W), A is the cross-sectional area perpendicular to the direction of heat flow (in square meters), $(Q \div A)$ = 1550 W/m^2 represents heat flux during SIP, k_c = 0.0264 W/m·°C represents the thermal conductivity of air, δ is air-layer thickness (m), T_{int} = 121.1 °C is the assumed steam-air interface temperature, and T_{wall} is the resulting pipe inner wall temperature.

Equation 7: $$Q/A = k_c \times ((T_{int} - T_{wall})/\delta)$$

Rearranging Equation 7 and solving for T_{wall} yields:

Equation 8: $$T_{wall} = T_{int} - (Q/A)(\delta/k_c)$$

Impact on F_0 Lethality: The F_0 value expresses the time in minutes at 121.1 °C (the standard reference temperature) required to kill a microbial population. As shown below, calculation of F_0 lethality is based on a decimal reduction time (*D-value*) representing the period required to reduce a microbial population by a factor of 10 at a temperature of 121.1 °C and a *z-value* representing the change in temperature needed to reduce a *D*-value by a factor of 10, often set to 10 °C for wet heat (**7**):

Equation 9: $$F_{0,wall} = \int_0^t 10^{\left(\frac{T_{wall} - 121.1}{z}\right)} dt$$

If the wall temperature (T_{wall}) is held constant during the dwell period (t_{dwell}), then that equation can be simplified:

Equation 10: $$F_{0,wall} = t_{dwell} \times 10^{\left(\frac{T_{wall} - 121.1}{z}\right)}$$

where the target ($F_{0,wall}$) is lethality at the pipe wall, 121.1 °C is the target SIP temperature, and T_{wall} represents the actual wall temperature due to trapped air.

Engineering-Based F_0 Correction Model: We introduce the RAE correction (Equation 11) to measure how effectively steam reaches and sterilizes near-wall areas during SIP.

Equation 11: $$RAE = t_{r,con} \div t_{r,diff}$$

If radial-diffusion displacement time ($t_{r,diff}$) is longer than the convective mixing time between steam and air ($t_{r,con}$), then steam will move on before completely purging the wall-adjacent air, increasing the risk of air entrapment and reducing sterilization effectiveness (**1, 2**). To adjust for limited steam penetration, a corrected F_0 value can be calculated based on RAE. If the convective mixing time required is greater than the diffusive radial displacement time required ($RAE \geq 1$), full lethality ($F_{0,target}$ = 12 min) is expected. If $RAE < 1$, then lethality is reduced proportionally as shown in Equation 12, reflecting incomplete displacement of air near the wall. This concept is especially relevant to complex piping geometries, such as tees, instrument branches, and short dead legs, in which steam can have suboptimal access and venting. In such regions, limited radial mixing can leave residual air pockets, making a correction factor important to prevent overestimation of sterilization lethality.

Equation 12:

$$\text{If } RAE \geq 1,\ F_{0,corrected} = F_{0,target};$$

$$\text{if } RAE < 1,\ F_{0,corrected} = F_{0,weighted};$$

$$F_{0,weighted} = F_{0,wall} + (F_{0,target} - F_{0,wall})(RAE)$$

- $RAE \geq 1$: Steam has sufficient time for radial access and sterilization of wall-adjacent regions. Residual air is purged, and full lethality is declared.
- $RAE < 1$: Steam exits before completing air displacement at the wall. Lethality is proportionally downgraded, bridging between actual thermal exposure and ideal target.

In Table 1, the comparative analysis across nominal pipe sizes (1/8 in. to 2 in.) with a 1-m length and 35-m/s steam velocity shows how axial, radial, and mixing times influence corrected lethality. The results highlight the risk of overestimating sterilization in larger pipes if steam access is not fully accounted for.

Air Trapping in Tank SIP

Noble developed Equation 13 based on boundary-layer diffusion theory and steam–gas mass-transfer principles (**1**). The equation calculates the fraction of noncondensable gas (air) remaining after the heat-up phase and present during the SIP dwell phase in vessels as a function of tank diameter. That fraction is quantified by modeling interfacial diffusion resistance as shown in Figure 2:

Equation 13:

$$f_a = C_{a,int} \times \left(\exp\left(\frac{\delta N_s}{c_n D_{gs}}\right) - 1\right) \times \frac{c_n D_{gs}}{\delta N_s} \times \frac{T_{std} R}{P_{std}}$$

Therein, $C_{a,int}$ = 0.0309 mol/m^3 is the interfacial concentration of air, D_{gs} = 0.003 m^2/s is the gas diffusion coefficient of steam, c_n = 0.88 mol/m^3 represents the molar concentration of steam, N_s = 0.01 mol/m^2 is molar steam flux, $\delta = D/2$ is the boundary-layer thickness, R = 8.314 J/(mol·K) is the universal gas constant, T_{std} = 298 K is the standard temperature, and P_{atm} = 1.015 × 10^5 Pa is standard atmospheric pressure.

Table 1: Impact of pipe inner diameter (ID) on steam mixing, wall temperature (T_{wall}), and corrected sterilization lethality ($F_{0,corrected}$) value in steam-in-place (SIP) systems; f = friction factor, RAE = radial-access efficiency, Re = Reynolds number, $t_{r,con}$ = convective mixing time between steam and air, $t_{r,diff}$ = radial-diffusion displacement time; δ = air-layer thickness, τ_w = wall shear stress

Pipe ID	$t_{r,con} \times 10^{-2}$	$t_{r,diff} \times 10^{-3}$	RAE	Re	$f \times 10^{-4}$	τ_w (kg·m^{-1}·s^{-2})	δ (mm) $\times 10^{-3}$	T_{wall}	$F_{0,corrected}$	$F_{0,weighted}$ (15 mins)[c]
1/8 in. (0.069 mm)	0.42 s	6.0 s	15.3	4763	96	1.70	14	120.4 °C	12.0[a]	12.9
1/4 in. (0.18mm)	2.0 s	9.0 s	5.4	9525	81	1.43	15	120.4 °C	12.0[a]	12.7
1/2 in. (0.37 mm)	7.0 s	13.0 s	1.9	19,050	68	1.20	16	120.3 °C	12.0[a]	12.5
1 in. (0.87 mm)	27.0 s	18.0 s	0.7	38,100	57	1.01	18	120.2 °C	11.3[b]	12.3
2 in. (1.87 mm)	108.0 s	26.0 s	0.2	76,200	48	0.85	19	120.2 °C	10.2[b]	12.1

[a] $F_{0,corrected}$ accounts for limited radial steam access using the radial-access efficiency (RAE) correction. When RAE ≥ 1, convective transport provides sufficient residence time for steam to access wall-adjacent regions fully. $F_{0,corrected}$ is taken as equal to the applied dwell time.

[b] When RAE < 1, radial heat transfer becomes diffusion limited, and sterilization lethality is reduced proportionally. In such cases, $F_{0,corrected}$ is calculated by weighting the wall-based lethality toward the target lethality in proportion to RAE, reflecting incomplete thermal exposure near the pipe wall.

[c] $F_{0,weighted}$ (15 min) represents the RAE-weighted effective lethality calculated at an extended dwell time of 15 minutes. Increasing dwell time from 12 to 15 minutes mitigates convective and diffusive transport limitations and results in effective lethality values that meet or exceed the target criterion across all pipe diameters. To simplify SIP design and to ensure robustness, a uniform dwell time of 15 min is recommended for all pipe sizes evaluated.

Parenteral Drug Association (PDA) *Technical Report 61* (TR 61) shows that even small amounts of residual air will reduce steam temperature during SIP. At 20 psig, temperature drops from ≈126 °C with 0% air to ≈120 °C with 15% air, following a linear trend as shown in Figure 2. By coupling Noble's boundary-layer diffusion model with empirically observed temperature reductions published in TR 61, F_0 calculation can account for air fraction persistence (**7**).

Air Removal from SIP Vessels

Limitations of Air Removal During Dwell Phase: Air removal during SIP relies on high steam flow and turbulence during the heat-up phase. During the dwell phase, steam flow is reduced drastically as low volumes of condensate form. Moreover, steam traps do not open as frequently as they do in heat-up, limiting gas-volume exchange and residual-air displacement. Because there is no active purging mechanism during the dwell phase, residual air can remain, especially in complex geometries such as tees and instrument branches where reduced momentum hinders complete air displacement. Even during heat-up, local mixing limitations can leave air in those regions, but the effect is more pronounced during the dwell phase because of its much-lower steam flow.

Comparing condensate generation between phases enables examination of that reduced gas movement. Page provides the following empirical models for condensate generation during heat-up ($C_{heat\text{-}up}$) and dwell (C_{hold}) phases, respectively (**8**):

Equation 14: $C_{heat\text{-}up} = 0.337V^{0.766}$, $R^2 = 0.99$

Equation 15: $C_{hold} = 0.09V^{0.51}$, $R^2 = 0.99$

Therein, C is expressed in pounds per hour, and V is given in liters. Compared with the equation for the heat-up phase, the dwell-phase equation has a much lower coefficient (0.09 as opposed to 0.337) and volume exponent (0.51 compared with 0.766). Those indicate both a reduced absolute condensate-formation rate and a weaker scaling proportion with vessel size. Further influencing that weaker scaling is the metal surface area:volume ratio, which decreases with increasing vessel size, with the effect of diminished heat transfer and condensate formation. Those observations support the understanding that condensate generation — and thus steam flow — is minimal during the dwell phase. Condensate load in that phase is just 1.1–3.3% of the heat-up load, confirming that steam flow during the dwell phase does not remove trapped air sufficiently.

Limitations of Passive Air Removal

Between Air and Steam: A common expectation is that air, being heavier than steam, will settle out of a vessel under gravity, leading to passive removal of trapped air over time. Although gravity does create stratification, that effect is weak because the density difference between the two gases is small at typical SIP temperatures and pressures: At 121 °C, steam ≈ 1.15 kg/m^3 and air ≈ 1.70 kg/m^3.

When steam is introduced from the top of a vessel during SIP, displacing air from the bottom relies on a gravity-driven hydrostatic pressure difference that is extremely low. For example, in a 10-m (≈33 ft) vessel, that density difference produces a hydrostatic pressure of only ≈0.0077 psi (**5**):

Equation 16:
$$\Delta P = \Delta\rho \times g \times H$$
$$= 0.034 \text{ lb/ft}^3 \times 33 \text{ ft}$$
$$\approx 1.12 \text{ lb/ft}^2 \approx 0.007 \text{ psi}$$

That pressure difference is negligible compared with typical SIP supply pressures of ≈20 psi needed to move steam through piping, vent valves, and equipment. Even static headspace pressure during SIP often exceeds 15 psi. Against such system pressures, a small hydrostatic head cannot reliably force air out of low points or dead zones, nor can it overcome flow resistance in nozzles, ports, and/or complex internal geometries. Thus, effective SIP system and process design demands that steam be introduced through high points and vented strategically to sweep air out of a system, with careful valve sequencing or toggling to prevent creation of multiple concurrent flow paths that could short-circuit the purge.

Figure 4: Proper condensate-drainage configuration in a steam-distribution system

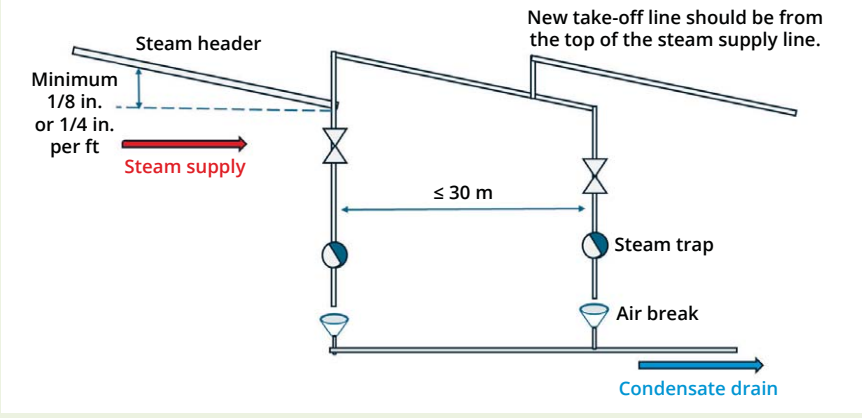

Air can stagnate in low-velocity regions and complex geometries such as capped nozzles, feed entries, horizontal piping runs, and instrument tees. Whereas properly designed pH/dissolved oxygen (DO) probe ports with flush-mounted O-rings generally prevent such dead zones, poorly designed and legacy instrument connections with recessed housings can create pockets in which air becomes trapped if not purged fully.

Limitations of Air Diffusion Through Steam in Dead Legs: In SIP systems, dead legs are stagnant zones with little or no steam flow. There, air removal depends on slow molecular diffusion. The diffusion time (t_{diff}) is given by Fick's second law as shown in Equation 17, in which L is the depth of the dead leg (m), and D_{eff} is the effective diffusivity of steam in air.

Equation 17: $t_{diff} = L^2 \div D_{eff}$

Dead-leg length has a profound impact on diffusion time, and although that needed time could be accommodated with a longer heat-up phase, the effectiveness of air removal by diffusion alone can remain unreliable in practice (Figure 3). Additionally, long dead legs require increased heat-up times that create operational challenges. Without active convective steam flow, cool air pockets can persist, delaying or preventing uniform temperature distribution and compromising sterility assurance. Therefore, relying solely on F_0 values during heat-up without verifying air removal can be insufficient, especially when multiple dead legs are present throughout a system. Best practice calls for temperature measurement with a resistance temperature detector (RTD) in representative dead-leg locations during SIP validation to confirm adequate heat penetration and sterility assurance.

Minimum Dwell Time as a Mitigation Strategy

Residual air near pipe walls and in vessel bottoms reduces surface steam contact and prevents those areas from reaching full sterilization temperature, risking sublethal exposure. Steam tends to stratify above dense air, which settles at the bottom of a vessel if not expelled fully. Note that microbial inactivation is not driven by temperature alone, but also by enthalpy transfer from condensing saturated steam. At 121 °C, it releases ≈2200 kJ/kg of latent heat during condensation, which is in addition to sensible heat. By contrast, air at the same temperature contributes only sensible heat, with a specific heat capacity of ≈1.0 kJ/kg·K. Heating 1 kg of air from 25 °C to 121 °C provides ≈100 kJ of energy. That >20-fold difference allows even thin residual air layers to block condensation at the vessel surface and thus protect microorganisms of lethal enthalpy exposure, despite sensors indicating compliant bulk temperatures.

To achieve $F_0 \geq 12$ minutes in large pipes (≥1 in.) and vessels with limited mixing, we recommend a minimum 15-minute dwell period with effective venting to ensure full thermal penetration and lethality. In smaller pipes (0.5 and 0.75 in.), although the RAE correction might show sufficient purging of air, steam paradoxically can push upward into the pipe, not allowing adequate space for air to move downward and be expelled against the steam force. Thus, the air becomes trapped in place. In such cases, a minimum dwell period of ≈15–20 minutes often is applied as a conservative strategy to promote full thermal penetration and lethality. The actual requirement can differ with pipe size (e.g., 0.5-in. or 0.75-in. lines), venting efficiency, and mixing conditions. Accordingly, our recommendation should be treated as a practical guideline rather than a fixed limit, with validation studies using RTDs placed at worst-case locations to confirm adequacy for each system.

System Design for Uniform Sterilization

Isobaric Nature of SIP and Temperature Monitoring: SIP operates as an inherently isobaric process during the dwell phase, with pressure held constant to maintain saturated steam conditions across a system. Steam flow is minimal, and no significant pressure drop occurs through fixtures such as spray devices. According to the 2024 American Society of Mechanical Engineers Bioprocessing Equipment (ASME-BPE) standard, temperature sensors located within a sterile boundary ideally should reflect consistent readings within a narrow band of ±2 °C. That range accounts for calibration error, instrument accuracy variance, and signal translation rather than actual system-pressure fluctuations. Deviations beyond that margin typically indicate localized steam condensation, poor thermal distribution, or mechanical design deficiencies, all of which compromise sterilization assurance. Because microbial kill depends on enthalpy delivered through condensation rather than temperature alone, confirming consistent saturated conditions at all sensor locations is critical.

Steam-Supply and Drainage-System Design: Maintaining steam gauge pressures between 15.0 and 24.4 psig establishes a practical sterilization range. Within that window, steam saturation temperatures remain ≈121–130 °C — low enough to obviate prolonged dwell times for lethality at the lower end, but not so high as to risk

thermal degradation of elastomer system components.

The 2024 ASME BPE standard recommends that, during dwell time, all temperature sensors within the sterile boundary should differ by no more than ±2 °C. However, when contrasted with the tighter calibration tolerances defined in the British Standards Institution (BSI) BS EN 285:2006 +A2:2009 standard for autoclave chambers — ±0.5 °C for sterilization-system temperature sensors and ±5 kPa (±0.73 psig) for pressure gauges — practical experience shows that all temperature sensors can be maintained within ±1.0 °C.

Operating below 15 psig of saturated steam pressure will allow steam temperatures to fall below 121 °C. Under such conditions, achieving the required F_0 value for sterilization might require prolonged dwell times, increasing cycle duration and potentially compromising process efficiency.

Operating above 24.4 psig of saturated steam pressure will raise steam temperatures above 130 °C, which is beyond the operational temperature limit of most elastomers.

Steam pressure showing temperatures **above saturation correlation** indicates the presence of superheated steam. In that state, it fails to condense readily on surfaces, reducing the latent heat transfer that is essential for killing microbes. Superheated steam also increases risk for thermal degradation of sensitive elastomeric components.

Thus, as shown in Figure 4, **good drainage-system design** calls for

• an adequate line slope — all SIP lines should have a slope of at least 1/8 in. per ft. (or ideally 1/4 in. per ft.) to facilitate proper condensate drainage (**10**)

• strategic placement of condensate drop lines — install condensate drop lines at intervals of no more than 30 m along steam-supply and process-fluid flow lines within sterile boundaries; the new take-off line should come from the top of the steam-supply line to prevent condensate collection (**9**).

Single Steam Source During Dwell (Recommended): It is advisable to use multiple steam sources during the initial heat-up phase of SIP, especially for large vessels and/or complex piping systems. Such an approach enhances the speed and uniformity of heat distribution, reducing cold-spot risk and improving air displacement. However, during the dwell phase, only one steam source is recommended. Using a single inlet helps to maintain steady-state, unidirectional flow while preventing introduction of pressure fluctuations and flow disturbances. Thus, a single-inlet design helps to stabilize pressure and temperature, supporting consistent holds and uniform sterilization conditions, both of which are critical for meeting F_0 requirements and validating sterilization efficacy.

Figure 5: (A) Impact of drop-leg geometry and instrumentation placement on effective steam-in-place (SIP) condensate removal; (B) a two-step SIP design with dedicated steam traps to prevent backflow and ensure sterilization integrity (D = pipe diameter, d = inner diameter, TT = temperature transmitter)

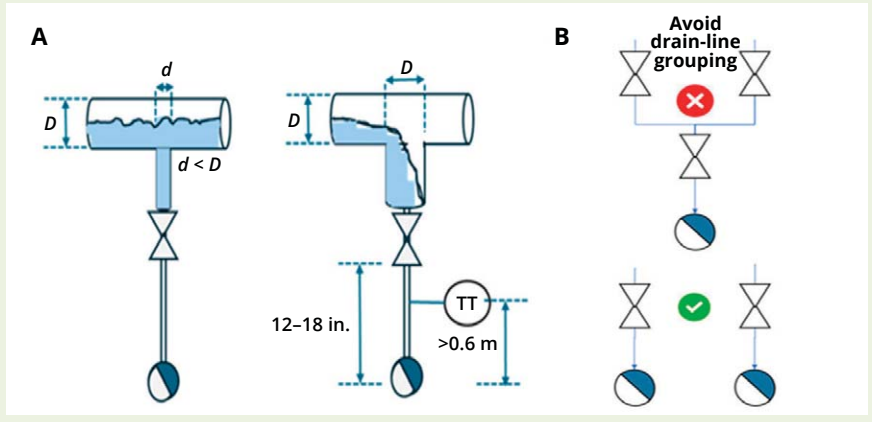

Condensate Management and Instrumentation: Steam traps should be installed at least 1 m below an RTD to ensure effective gravitational drainage and prevent condensate backpressure during SIP operations. Such backpressure can cool a system temperature element below required levels. The 1-m distance should provide sufficient hydrostatic pressure (≈0.1 bar or 1.4 psi) to move condensate reliably through the trap, even under low-flow conditions during the dwell phase. A taller vertical leg also helps to prevent pooling and backflow of condensate into the sterile boundary, which otherwise could lead to thermal buffering, cold spots, and inconsistent sterilization performance. Moreover, a vertical leg allows for proper flash-steam separation, reducing vapor interference and ensuring uninterrupted flow through the trap (**9**).

Temperature sensors should be positioned ≈12–18 in. above the steam trap to allow for consistent condensate build-up and accurate thermal monitoring (Figure 5A). At that height, a sensor will be submerged in hot, stable condensate rather than exposed to fluctuating steam or flash vapor, which can distort readings. Because of its thermal mass, condensate has a more uniform temperature profile than that of steam, thus providing a more reliable indication of an SIP system's sterilization status. Such placement also ensures that a sensor is located within a buffered zone that minimizes the influence of trap cycling and enhances the accuracy of temperature-hold verification during validation studies (**10**).

Avoid Drain Line Grouping: Do not group multiple drain lines into a single steam trap (Figure 5B). Each drop line should have its own dedicated trap to prevent cross-contamination and backflow (**9**).

An Insulated Condensate Leg Prevents Heat Loss: An insulated condensate leg can hinder effective drainage during SIP operations by trapping heat and preventing natural condensate cooling (Figure 6). Normally, condensate removal is driven not only by gravity, but also by a temperature differential: Compared with warmer legs, cooler legs promote faster separation and drainage of condensate from steam. Thus, a leg without insulation loses heat to the surrounding environment, allowing condensate to cool and drain more effectively. However, insulation retains heat within the leg, keeping the temperature closer to that of the steam line. That effect slows the cooling

Figure 6: Effect of insulation on condensate leg performance — promoting drainage efficiency and temperature accuracy in a steam-in-place (SIP) system (α = differential, F_{drain} = rate of condensate drainage, ρ = density, T = temperature, TT = temperature transmitter)

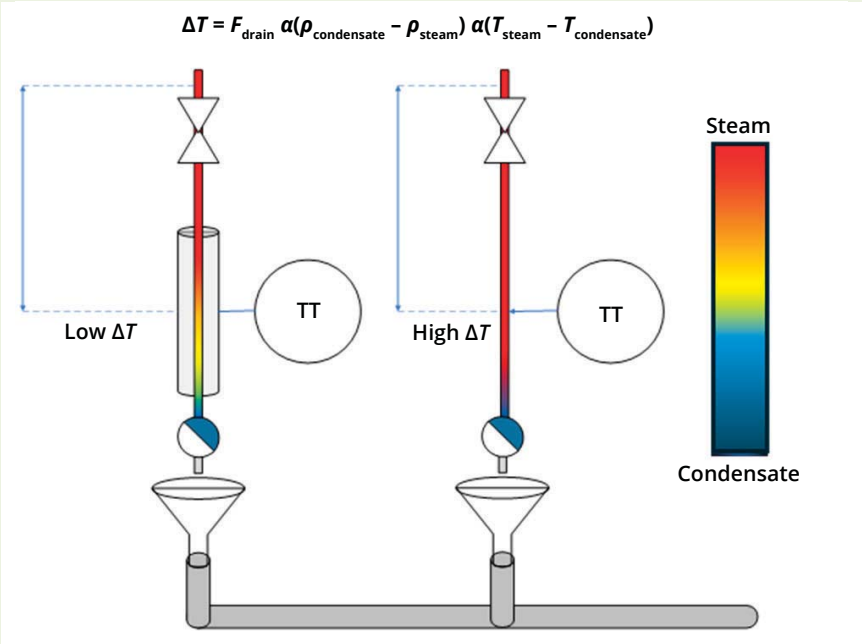

process and can cause flash steam to form or retained vapor pressure to impede flow. Condensate can accumulate as a result, leading to inconsistent temperature readings and potential air entrapment or cold spots — all of which compromise sterilization assurance. Therefore, we recommend removing insulation from the condensate leg to support efficient condensate removal and improve SIP effectiveness (**11, 12**).

Cooling of the condensate leg is essential to increasing the temperature differential between steam and condensate, which drives both gravitational drainage and steam-trap actuation. If insulation retains heat, the condensate remains warmer than it otherwise would, reducing temperature change and slowing drainage. **Equation 18** models the rate of heat loss (**2**):

$$Q = q \times A \times t$$

in which Q is total heat loss (J), q is heat flux (W/m^2), A is the pipe surface area (m2), and t is the time (s). Noble reports q values of 15,150 W/m^2 and 344 W/m^2 for noninsulated and insulated stainless-steel pipes, respectively, under these assumptions:

- pipe diameter: 0.5 in. (0.0094 m inner diameter, ID)
- pipe length: 1 m
- steam velocity: 35 m/s
- gauge pressure: 20 psig (≈2.36 bar)
- steam temperature: ≈121 °C
- ambient temperature: ≈25 °C
- overall heat transfer coefficient (U) for steam-to-air transfer with insulation: ≈16.1 W/m^2·°C (**1**).

For a 1-m long, 0.5-in. pipe, the surface area (A) = $\pi \times D \times L$ = $\pi \times 0.0094$ m $\times$ 1 m = 0.0295 m^2 (**1**). Based on that figure, the following equations calculate the amount of heat lost over a minute for noninsulated and insulated pipes, respectively:

Equation 19: $Q_{noninsulated}$ = 15,150 W/m^2 × 0.0295 m^2 × 60 s = 26.8 KJ

Equation 20: $Q_{insulated}$ = 344 W/m^2 × 0.0295 m^2 × 60 s = 0.61 KJ

The rate of condensate drainage (F_{drain}) depends on the temperature difference between saturated steam and condensate. As condensate cools, that ΔT increases, enhancing gravitational drainage and triggering trap actuation. If insulation retains heat, then condensate remains warmer, the rate of temperature change decreases, and drainage slows:

Equation 21: $F_{drain}\, \alpha(T_{condensate} - T_{steam})$; $\Delta T = T_{condensate} - T_{steam}$

In SIP systems, effective condensate removal is essential to maintaining uniform sterilization conditions. Insulating a condensate leg limits heat loss that otherwise would facilitate condensate separation and drainage. The results are decreased condensate density, increased vapor retention, and reduced drainage velocity, which collectively compromise temperature uniformity and increase the risk of cold spots, trapped air, and submerging of the temperature element in condensate. Additionally, there is a risk of developing superheated liquid condensate that fails to use the designed steam-trap mechanism for liquid removal. Therefore, insulation should be avoided on condensate legs. Removing insulation enhances heat dissipation, supports fast and complete drainage, and contributes directly to SIP-cycle effectiveness and reliability.

Excessive Distance Between the Sterile-Boundary Valve and Steam Trap: Steam traps use thermal elements that open when they cool (condensate present) and close when they sense hot steam. A long, insulated vertical drop leg can hold a tall column of hot condensate (trapped condensate thermal load) that keeps the trap's sensor warm such that it never cools to its opening temperature. The trap stays shut while condensate builds above it, leading to uneven temperatures and uncertain sterilization. Moreover, probes sitting in pooled condensate can give false low readings or unstable values, complicating validation.

To reduce such risks, keep the leg short and place the temperature probe ≈1 m below the sterile-boundary valve and ≈0.6 m above the steam trap. Such placement should keep probes out of pooled liquid, enabling sensing of process-zone steam temperature. The following equation estimates the mass (m, in grams) of condensate formed due to heat loss during SIP when a condensate line is insulated. Here, we assume the latent heat of condensation (h_{fg}) to be 2.2 × 10^6 J/kg (**2**).

Equation 22: $m = Q \div h_{fg} = (q \times A \times t) \div h_{fg} = (q \times \pi \times D \times H \times t) \div h_{fg}$

For a 1-m line with a diameter of 0.5 in., m = (344 W/m^2 × 0.0295 m^2 × 60 s) ÷ (2.2 × 10^6 J/kg) = 0.28 g.

For a 5-m line with a diameter of 0.5 in., m = (344 W/m^2 × 0.1975 m^2 × 60 s) ÷ (2.2 × 10^6 J/kg) = 1.85 g.

Those calculations demonstrate that potential condensate load scales proportionally with vertical leg length — in this case, a 5× increase in line length results theoretically in a 5× higher condensate generation. That does not mean a line always fills entirely with condensate. For instance, a 100-m line is not assumed to contain 100× more condensate at all times. Rather, the calculation highlights the increased thermal load that longer legs can impose, which in turn raises the risk of exceeding a steam trap's discharge capacity if backpressure or poor drainage occurs. Retained liquid acts as a persistent heat sink, interfering with uniform heating and sterilization if not managed properly.

Moreover, sensors located in trapped condensate can register artificially low temperatures due to localized cooling. Such readings could trigger false alarms and introduce uncertainty in sterilization validation. Maintaining proper steam-trap placement in the vertical leg length ensures effective drainage, stable temperature control, and validatable SIP performance.

A Holistic Approach to Sterility Assurance

Achieving F_0 ≥ 12 minutes at 121.1 °C long has been deemed the cornerstone of SIP validation. However, our analysis demonstrates that F_0 alone cannot guarantee sterilization: Residual air can still prevent saturated steam from contacting all surfaces, compromising sterility assurance.

We recommend a more holistic approach: Use F_0 calculations and microbial-spore strip testing to demonstrate lethality verification as supporting checks, but also confirm saturated steam conditions and apply a minimum dwell period of 15–20 minutes. This integrated strategy should make SIP validation more scientifically robust and operationally reliable.

References

1 Noble PT. Modeling Transport Processes in Sterilization-in-Place. *Biotechnol. Prog.* 8(4) 1992: 275–284; https://doi.org/10.1021/bp00016a003.

2 Sherwood TK. *Mass Transfer.* McGraw-Hill: New York, NY, 1975.

3 Bird RB, Stewart WE, Lightfoot EN. *Transport Phenomena* (revised 2nd ed.). Wiley: Hoboken, NJ, 2009.

4 Çengel YA, Ghajar AJ. *Heat and Mass Transfer: Fundamentals and Applications* (5th ed.). McGraw-Hill Education: New York, NY, 2015.

5 Bansal RK. *A Textbook of Fluid Mechanics and Hydraulic Machines* (9th ed.). Laxmi Publications: New Delhi, India, 2010.

6 Harvey AH. T*hermodynamic Properties of Water: Tabulation from the IAPWS Formulation 1995 for the Thermodynamic Properties of Ordinary Water Substance for General and Scientific Use (NISTIR 5078).* National Institute of Standards and Technology: Boulder, CO, October 1998; https://www.nist.gov/system/files/documents/srd/NISTIR5078.htm.

7 *PDA Technical Report No. 61: Steam in Place.* Parenteral Drug Association: Bethesda, MD, 2013; https://store.pda.org/TableOfContents/TR6113_TOC.pdf.

8 Page GW, Kral R. Designing a Shorter Vertical Leg for Sanitary Steam Traps. *BioPharm Int.* 19(9) 2006; https://www.biopharminternational.com/view/designing-shorter-vertical-leg-sanitary-steam-traps.

9 *Technical Brief TB011ENOO: Principles of Steam-in-Place.* MilliporeSigma: Billerica, MA, 2003; https://www.sigmaaldrich.com/deepweb/assets/sigmaaldrich/product/documents/269/118/tb011en00.pdf.

10 Johansen C. *SIP: Avoid Errors and Achieve Stable Sterility in Pharma and Food.* Alflow Scandinavia: Vejen, Denmark, 2026; https://www.alflow.dk/en/sip-to-avoid-validation-errors-and-ensure-sterility.

11 Lutkewitte KJ. *An Overview of Steam-In-Place.* Steriflow Valve: Cincinnati, OH; https://www.steriflowvalve.com/wp-content/uploads/2019/06/SIP_WhitePaper.pdf.

12 P-101-A1. *Steam Conservation Guidelines for Condensate Drainage.* Armstrong International: Three Rivers, MI, 2016; https://www.armstronginternational.com/wp-content/uploads/Broch_SteamConservationGuidelines_P101D_EN_20-20190501.pdf.

Corresponding author and BPI editorial advisor ***Naveenganesh Muralidharan*** *is founder of Bench2Batch CMC Life Cycle Partners; naveen@bench2batch.com.* ***Alejandro Kaiser*** *is founder of Kaiser Global Engineering.* ***Marc Pelletier*** *is bioprocess equipment (BPE) chair and senior fellow in bioprocess design at CRB. And corresponding author* ***Alexander Elkin*** *is an engineer in the manufacturing science and technology (MSAT) group at AGC Biologics; aelkin@agcbio.com.*

Continued from page 21

5 Le Merdy S, Dufossé C. A Step Closer to Closure in Bioprocessing. *BioPharm Int.* 37(4) 2021: 4–10; https://biopharminternational.com/view/a-step-closer-to-closure-in-bioprocessing.

6 Makovitzki A, et al. Evaluation of a Downstream Process for the Recovery and Concentration of a Cell-Culture-Derived rVSV-Spike COVID-19 Vaccine Candidate. *Vaccine* 39(48) 2021: 7044–7051; https://doi.org/10.1016/j.vaccine.2021.10.045.

7 Wolf T, et al. The Effects of High Shear Rates on the Average Hydrodynamic Diameter Measured in Biomimetic HIV Gag Virus-Like Particle Dispersions. *Front. Bioeng. Biotechnol.* 12, 2024; https://doi.org/10.3389/fbioe.2024.1367405.

8 Grein TA, et al. Aeration and Shear Stress Are Critical Process Parameters for the Production of Oncolytic Measles. *Front. Bioeng. Biotechnol.* 7, 2019: 78; https://doi.org/10.3389/fbioe.2019.00078.

9 *Sterile Drug Products Produced by Aseptic Processing — Current Good Manufacturing Practice: Guidance for Industry.* US Food and Drug Administration: Rockville, MD, 2004; https://www.fda.gov/regulatory-information/search-fda-guidance-documents/sterile-drug-products-produced-aseptic-processing-current-good-manufacturing-practice.

10 EMA/CHMP/CVMP/QWP/850374/2015. *Guideline on the Sterilisation of the Medicinal Product, Active Substance, Excipient and Primary Container.* European Medicines Agency: Amsterdam, the Netherlands, 2019; https://www.ema.europa.eu/en/documents/scientific-guideline/guideline-sterilisation-medicinal-product-active-substance-excipient-and-primary-container_en.pdf.

11 Ghosh M. *Aseptic Process Simulation (Media Fill)* [presentation]. Parenteral Drug Association, Southern California Chapter, Aseptic Processing and Sterilization Event: Irvine, CA, 7 November 2019; https://www.pda.org/docs/default-source/website-document-library/chapters/presentations/southern-california/2019-aseptic-day/aseptic-process-simulation-(media-fill).pdf?sfvrsn=12.

Salman Safdar *is downstream manufacturing manager,* ***Ken Bui*** *is GMP central services manager,* ***Thomas Montague*** *is director of operational excellence and continuous improvement,* ***Nacole Lee*** *is senior director of manufacturing, and corresponding author* ***Tingting Ju*** *(tingting.ju@ablinc.com) is manufacturing technical operations (MTO) manager at Advanced BioScience Laboratories (ABL), 9800 Medical Center Drive D, Rockville, MD 20850; https://ablinc.com.*

Supporting a Maturing Modality

Large-Volume Manufacturing of Mesenchymal Stem Cells

Brian Gazaille, with Khang Luu and Irana Coletti Malaspina

Mesenchymal stem/stromal cells (MSCs) are making headway in biopharmaceutical development pipelines. Khang Luu and Irana Coletti Malaspina (both field application scientists at Corning Life Sciences) explain that such cells were used initially to tamp down immune responses in cases such as graft-versus-host disease (GvHD) and osteoarthritis. Researchers have since discovered that MSCs differentiate into several therapeutically valuable cell types, secrete molecules that contribute to tissue repair, and exhibit anti-inflammatory properties that enable safe allogeneic administration. Thus, developers are investigating MSCs and MSC-derived exosomes for treatment of chronic wounds and inflammatory diseases. MSCs also naturally infiltrate tumors, opening up possibilities for engineering MSCs to deliver therapies to cancer cells.

Despite clinical progress, large-volume MSC manufacturing remains difficult. I corresponded with Luu and Malaspina to learn about efforts to increase the scalability of MSC production. Their combined responses are below. With multiple MSC candidates knocking on the door to commercialization, the industry needs advanced cell-culture technologies that will support the modality's maturation.

Corning HYPERStack vessels deliver high-density culture of mesenchymal stem cells (MSCs) with optimized gas exchange and a minimal footprint.
(HTTPS://WWW.CORNING.COM)

Improving Yield and Quality

My impression is that producing large quantities of MSCs remains challenging. What factors hamper MSC production? Historically, biological constraints have limited large-scale production. Suboptimal culture components — such as low-grade media, reagents, and consumables — can impair MSC growth from the outset. Cells expanded with nonoptimal materials often show reduced proliferative capacity and inferior overall performance in subsequent passages. Poor environmental conditions also can cause MSCs to deviate from their intended lineage, leading to unwanted differentiation and compromising product quality and consistency.

Production techniques must be tailored to a facility's infrastructure, staffing levels, scale of operation, and end goals, whether the objective is producing MSCs or harvesting their secreted factors. Maximizing yield depends heavily on workflow optimization and equipment that can process cells gently enough to preserve their physical integrity, biological characteristics, and potency.

Long-term stability raises difficulties, too. MSCs are highly sensitive to storage conditions, temperature fluctuations, and handling, all of which can compromise their viability and therapeutic function.

What quality markers should be monitored during production, and why is it difficult to preserve them? Guidelines from the International Society for Cell & Gene Therapy (ISCT) clearly define required MSC surface markers and biological functions. Such characteristics can be fully assessed only at the end of production, so release testing is required to confirm MSC identity, purity, and functional quality. Moreover, each batch must undergo quality control (QC) testing after production to ensure that it meets specifications.

During process validation, critical quality attributes (CQAs) must be

established in alignment with regulatory expectations. Manufacturers must demonstrate that a process will produce MSCs that consistently meet release criteria despite the inherent biological variability of cell-based products.

A major impediment is the current lack of validated secreted biomarkers that can be analyzed from a culture environment to predict final MSC quality. Throughout manufacturing, MSCs remain sensitive to changes in their culture environments, so they can differentiate inadvertently into non–stem-cell phenotypes if conditions are not carefully maintained.

Many developers apply a quality by design (QbD) approach to address such challenges. A QbD strategy emphasizes designing and optimizing a robust production process — e.g., using a reliable cell source and high-quality reagents and culture materials — to increase the likelihood that MSCs will meet quality requirements during final QC and release testing.

What parameters should sponsors prioritize during MSC expansion? Manufacturers should emphasize conditions that support consistent cell growth, preserve stem-like characteristics, and minimize variability across scale-up steps. Expansion typically follows a seed-train approach, moving from small vessels such as T flasks to larger systems such as Corning HYPERStack vessels and CellCube systems. At each transition, scientists should monitor contamination, cell morphology, and yield; a well-controlled process should produce relatively stable yields across scales, with only minor variations. Significant fluctuations often signal underlying issues with culture health or process stability.

A well-controlled culture environment is equally important. Manufacturers should use reliable, high-quality consumables and reagents, ensuring that supplements are fresh and consistent in grade. When possible, media formulations should be designed specifically for MSC expansion. Sponsors also should limit passage numbers to preserve MSC "stemness." Doing so requires a well-qualified master cell bank (MCB) and monitoring of CQAs throughout expansion.

To maintain cell viability and potency throughout manufacturing, downstream-processing and fill–finish equipment must handle cells gently. Moreover, MSC-aggregate formation should be managed carefully through appropriate process controls. Factors such as confluency at harvest, environmental conditions, media composition, harvest reagents, and agitation parameters all play a role in preventing aggregation, which can diminish cell quality and performance.

What equipment formats can help to address MSC scalability concerns? Platforms such as Corning CellSTACK culture chambers, HYPERStack vessels, and CellCube systems can be used for both scale-out and scale-up strategies depending on how your process begins and what your production goals are. Such systems provide reliable, well-characterized environments for MSC culture and have been adopted widely throughout the industry because they meet diverse application and product needs.

MSC yield requirements can differ substantially depending on route of administration, dosing frequency, disease indication, and patient population. Such variables determine required cell numbers per batch and thus whether to scale up or out. Companies also must ensure that CQAs remain stable throughout production. Scale-up approaches (e.g., expanding into CellCube systems) are often a good choice for products that require large quantities of cells and/or long-term storage. When small batches are needed at high frequencies for immediate use, scale-out approaches (with Corning HYPERStack vessels or CellSTACK culture chambers) might be the better option.

Amid variability in demand, modular technologies (including CellSTACK chambers, HYPERStack vessels, and CellCube systems) can provide flexible scaling options by enabling adjustment of total culture surface area while maintaining a consistent growth environment. Such flexibility supports predictable, reproducible MSC expansion and helps manufacturers align their production strategies with therapeutic, regulatory, and operational requirements.

How much does vessel-surface treatment influence MSC expansion? It has a significant impact because MSCs are adherent cells. Depending on your culture conditions, particularly when using serum-free media, specialized technologies such as Corning's CellBIND surface might be necessary to ensuring robust adhesion and optimal growth. When MSCs must be grown in three-dimensional spheroid formats, such as for enhanced exosome production, ultralow-attachment (ULA) surfaces are required to prevent cell adherence. Even among standard treatments, variations in surface chemistry and manufacturing among brands can lead to differences in attachment efficiency, affecting MSC growth rates and expansion performance.

Are you aware of promising developments in the MSC field? Japanese regulatory authorities recently approved two therapies derived from induced pluripotent stem cells (iPSCs). In addition to marking global firsts for the field, those approvals signal growing regulatory confidence in advanced cell based therapeutics and highlight increasing momentum behind next-generation stem-cell technologies. Such progress not only underscores the maturation of the cell-therapy industry, but also provides important insights for future development and commercialization pathways related to MSC-based therapies and other regenerative treatments.

Brian Gazaille *is managing editor of* BPI*; brian.gazaille@informa.com.* ***Khang Luu,*** *PhD, is a field applications scientist for Southeast Asia, and* ***Irana Coletti Malaspina,*** *MSc, is a field application scientist for South America from Corning Life Sciences.*

Global HCP Profiling and Quantification by Native Digestion and LC-MS Analysis

Johanna Barnhill, Timothy Licknack, Stephen Stahlschmidt, Brinkley Thornton, and Jared Isaac

Host cell proteins (HCPs) are process-related impurities that can diminish biopharmaceutical stability and efficacy or elicit a harmful immune response. HCP levels typically are measured through enzyme-linked immunosorbent assays (ELISAs), which are useful for purification process development, in-process sample testing, lot-release testing, and quality control (QC). Although ELISA is highly sensitive, it does not discern the identity of HCPs contributing to its immunological signal.

Analytical methods such as liquid chromatography coupled to mass spectrometry (LC-MS) can be used to identify and quantify individual HCPs. To overcome the massive dynamic range of drug substance (DS) samples, native digestion is performed to digest HCPs preferentially relative to the monoclonal antibody (mAb) or therapeutic protein (**1**). For subsequent HCP quantification, three major strategies have been reported: measuring relative to the drug product (DP), to spiked-in proteins, and to spiked-in peptides. Here, we describe development and qualification of the inSPECt relative quantification strategy, which uses native digestion, high-resolution MS, and quantification relative to spiked-in protein standards.

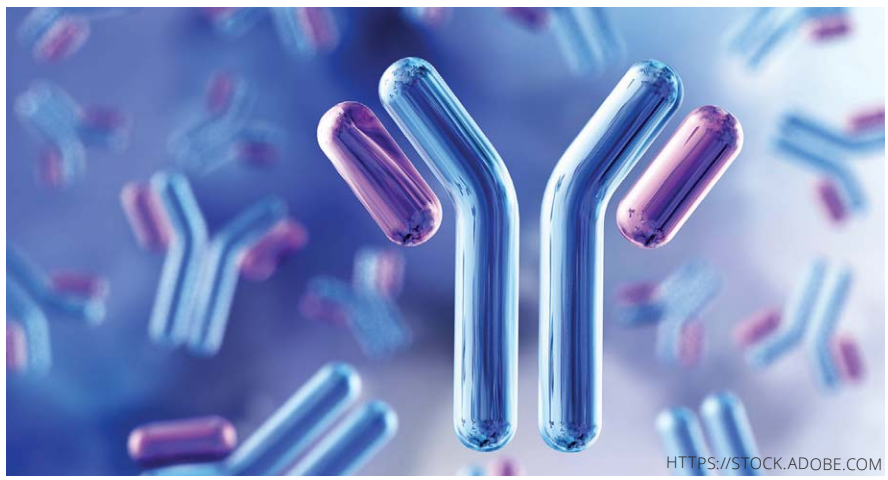

Global LC-MS Analysis

Global HCP profiling measures the approximate abundance of dozens to thousands of HCPs simultaneously by comparing their signals to those of spiked-in protein standards at known concentrations. A Cygnus protein standard (CPS) was spiked into NISTmAb reference standard (Agilent, 5191-5744). Then, proteolytic digestion was performed without protein solubilization or cysteine reduction/alkylation to enrich HCPs. The resulting peptides were separated on a 50-cm octadecyl (C18) column on a Vanquish Neo ultrahigh-performance liquid chromatography (UHPLC) system coupled to an Obritrap Eclipse mass spectrometer (Thermo Fisher Scientific) for data-independent acquisition (DIA) followed by data analysis using the CHIMERYS search algorithm (MSAID) implemented in ProteomeDiscoverer software version 3.3 (Thermo Fisher Scientific).

Results revealed a strong, linear relationship between the concentration of individual CPS proteins and their measured abundance. Analytical precision was demonstrated at 10–500 parts per million (ppm), with the coefficient of variation (CV) of all triplicate injections being <18%. In all four curves, coefficient of determination (R^2) values for individual CPS proteins were >0.95. The linear relationship was used to calculate a median response factor (RF) to estimate concentration in ppm from the measured abundance. Deviation between the estimated and known CPS concentration determines a linear range of 10–500 ppm with a limit of detection (LoD) of 0.2–8 ppm.

Because the NISTmAb standard has been analyzed extensively, we compared the HCPs identified and quantified during method qualification with previously published results (**2**). With only 6 µg of protein digest injected, 51 HCPs were identified in all three replicates, 29 of which were above the method LoD of 5.3 ppm. In

Table 1: Top four host cell proteins (HCPs) in NISTmAb material; HCP values obtained using data-independent acquisition (DIA), gas-phase fractionation (GPF)–DIA, data-dependent acquisition (DDA), and DDA–field asymmetric ion-mobility spectrometry (FAIMS) were averaged from Beaumal et al. (**2**) and compared with calculated values from our study. (ppm = parts per million)

HCP	Beaumal et al.	InSPECt MS
Fructose-bisphosphate aldolase A	189 ppm	240 ppm
Fructose-bisphosphate aldolase C	84 ppm	83 ppm
Protein disulfide-isomerase A6	83 ppm	148 ppm
Glucose-6-phosphate isomerase	32 ppm	87 ppm

multiple studies, four HCPs dominated the total HCP mass of the NISTmAb material: fructose bisphosphate aldolase A, fructose bisphosphate aldolase C, protein disulfide-isomerase A6, and glucose-6-phosphate isomerase. Beaumal et al. present the most thorough analysis of NISTmAb material using four acquisition variants of DIA and data-dependent acquisition (DDA) (**2**). The authors' mean reported levels are highly similar to those that we obtained (Table 1). The inSPECt method also quantified 11 extremely low-abundance HCPs (<1 ppm) that were identified in Beaumal et al.

HCP concentrations in the NISTmAb material are biased by the native digestion HCP enrichment strategy, and although the similarities in HCP estimates are promising (Table 1), testing the performance of the inSPECt method for HCPs of a known concentration will determine its accuracy. To that end, we spiked several concentrations of recombinant HCPs into the NISTmAb, serving as DS matrix. Three HCPs were mildly underestimated in the 100–1000 ppm range with acceptable accuracy and precision (Table 2). Those three HCPs are known to be problematic in final DSs, and knowledge of their approximate concentration would be useful in ensuring a safe, effective therapeutic.

Figure 1: Cygnus protein standard (CPS) calibration curve; the linear relationship was measured between known CPS concentration and measured CPS protein abundance. Each colored point represents an individual CPS protein, and the red line is the median used to generate the response factor.

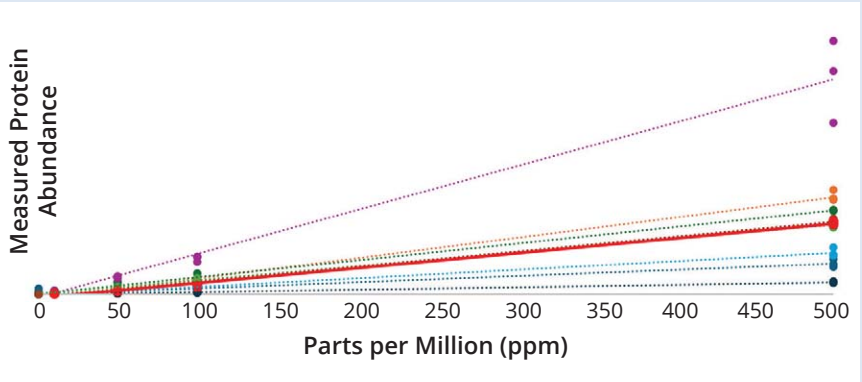

Table 2: Host cell protein (HCP) spike and recovery; potentially problematic HCPs were spiked into NISTmAb material (used as drug substance) and measured using the inSPECt method. Accuracy (%Error) and precision (coefficient of variation, %CV) were calculated at three concentrations.

	100 ppm		500 ppm		1000 ppm	
HCP	%Error	%CV	%Error	%CV	%Error	%CV
Lysosomal phospholipase A and acyltransferase	–26%	2%	–32%	2%	–34%	4%
Clusterin	6%	3%	–5%	3%	–11%	6%
Glutathione S-transferase P1	–23%	5%	–27%	2%	–31%	7%

Highly Sensitive HCP Quantification

Our results support the utility of the inSPECt method for highly sensitive HCP quantification. The spiked-in protein standards (CPS) display a strong, linear response across a broad range spanning at least two orders of magnitude (Figure 1). Detection limits were measured in sub- or low-ppm concentrations depending on the DS matrix. Known HCPs were measured close to their expected value both as endogenous HCPs within NISTmAb material and as spiked-in HCP standards. The InSPECt method should be used in HCP profiling of downstream bioprocessing samples.

References

1 Huang L, et al. A Novel Sample Preparation for Shotgun Proteomics Characterization of HCPs in Antibodies. *Anal. Chem.* 89(10) 2017: 5436–5444; https://doi.org/10.1021/acs.analchem.7b00304.

2 Beaumal C, et al. Advanced Mass Spectrometry Workflows for Accurate Quantification of Trace-Level Host Cell Proteins in Drug Products: Benefits of FAIMS Separation and Gas-Phase Fractionation DIA. *Proteomics* 23(16) 2023: 2300172; https://doi.org/10.1002/pmic.202300172.

Johanna Barnhill *is senior associate scientist,* ***Timothy Licknack*** *is a mass spectrometry scientist,* ***Stephen Stahlschmidt*** *is an associate scientist,* ***Brinkley Thornton*** *is a chromatography and mass spectrometry technician, and corresponding author* ***Jared Isaac*** *(jared@cygnustechnologies.com) is director of chromatography and mass spectrometry, all at Cygnus Technologies, 1523 Olde Waterford Way, Leland, NC 28451; https://www.cygnustechnologies.com.*

HCP inSPECt MS quantification service is now available from Cygnus Technologies. Contact techsupport@cygnustechnologies.com to discuss your projects.

ADC Platform Process Development Using Variable Pathlength Technology

Fiona Ford, Melissa Nixon, and Bérengère François

Antibody–drug conjugates (ADCs) are biomolecules — usually monoclonal antibodies (mAbs) — that are bound to a small drug molecule through a chemical linker. ADCs are targeted therapies; the mAb portion homes to an antigen on a cell and delivers the drug to the appropriate site. Although most such therapies address cancer indications, the field is widening to incorporate other disease targets. Protein concentration and drug:antibody ratio (DAR) can be used to monitor manufacturing from start to end.

Aspects of ADC Manufacturing

Tangential flow filtration (TFF) commonly is used during biomolecules purification. Small molecules are removed with a permeate, whereas large molecules are retained and recirculated back to the batch with a retentate (Figure 1). TFF typically consists of two operational modes: diafiltration (DF) and ultrafiltration (UF). *Diafiltration* removes small molecules with a permeate while maintaining batch concentration. For ADC manufacturing, DF is used to exchange buffers and/or conjugated proteins into a new buffer system and to remove unwanted small molecules. *Ultrafiltration* is the process of concentrating biomolecules. Buffer permeates the filter while large molecules (e.g., proteins and conjugates) are retained, decreasing batch volume and increasing protein concentration.

A fixed number of diavolumes (DVs) is used to assess free-drug clearance and buffer exchange with samples taken at specified intervals. However, data analysis occurs retrospectively, creating a delay between experimental work and data analysis. That practice also might use unnecessary time and resources because free-drug clearance can be obtained before the specified number of DVs has been processed. Alternatively, free-drug clearance might not be achieved within the designated number of DVs, necessitating a repeat of experimental work. Therefore, the number of DVs used must be reliable and defined during development.

Figure 1: Illustration of tangential-flow filtration (TFF) process

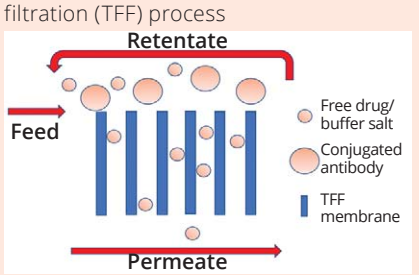

During UF, protein concentration must be monitored accurately to achieve the correct drug concentration. Typically, material samples are taken after UF. However, off-line analysis can be time-consuming and delay processes. Additionally, operators generally will have no indication of whether proteins pass through the filter membrane until off-line analysis, creating risk for significant losses or further delays.

One solution is to use in-line ultraviolet–visible light (UV-vis) spectroscopy to measure protein and drug concentrations, provided that the drug exhibits absorbance in the UV-vis region. However, traditional in-line UV-vis sensors suffer from limited dynamic ranges because UV-vis absorbance depends on both concentration and optical pathlength. Similarly, fixed-pathlength sensors often saturate at high concentrations when the total absorbance exceeds a sensor's detection limit.

Variable pathlength technology (VPT) is a patented tool for UV-vis spectroscopy and uses the slope spectroscopy equation, derived from the Beer–Lambert law. The PATsmart SoloVPE and FlowVPX systems from Repligen use VPT to find optimal absorbance rates and measure 5–10 datapoints at progressively smaller pathlengths to create a slope. The system then calculates concentration with a user-provided material extinction coefficient. With the in-line FlowVPX instrument, such measurements are taken every ≈10 seconds to monitor concentration and DAR in real time. With analog output signaling enabled, the system creates a feedback loop to control the process automatically without operator intervention.

Case Study

The study sought to monitor protein concentration and DAR in the feed line during DF and UF, monitor free-drug clearance in the permeate line, and compare FlowVPX data with those obtained from established SoloVPE methods (**1**). To achieve those objectives, two FlowVPX systems were used: one installed on the feed line to monitor DAR and ADC concentration, and one on the permeate line to follow drug clearance.

Materials and Methods: The team used a Masterflex pump and size 16 Masterflex tubing (Avantor). A Pellicon 3 cassette with Biomax polyethersulfone

Figure 2: Experimental set-up; TFF = tangential-flow filtration, VPX = FlowVPX system

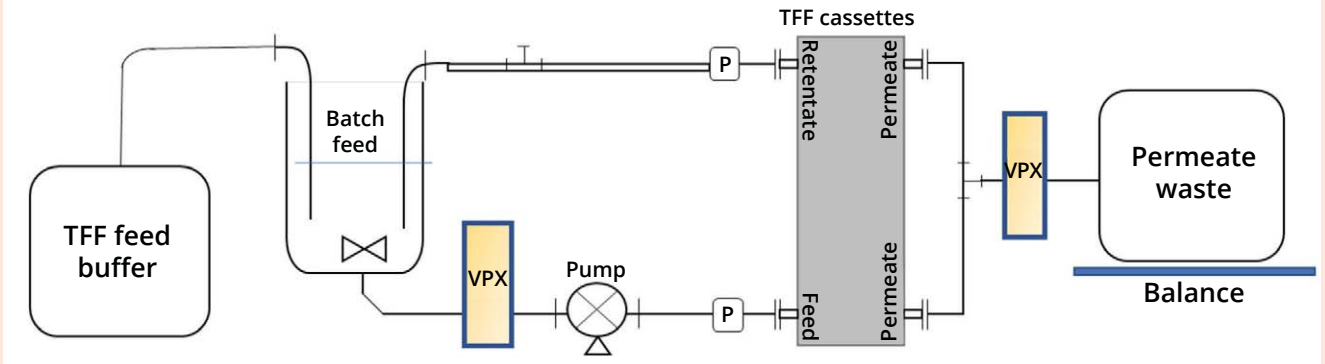

(PES) membranes at 30 kDa (MilliporeSigma) was used to conduct TFF. To monitor pressure, the team used a PendoTECH pressure sensor (Mettler Toldeo). Two FlowVPX systems using FlowVPX 3-mm single-use flow cells and one SoloVPE system were tested. Analog signals in the FlowVPX system were not used for this study. Data were recorded with CTech ViPER ANLYTX software.

The ADC used in this study was composed of a mAb conjugated to a drug and commercially available linker at a concentration of 5 mg/mL. The resulting DAR was 4. The ADC solution was spiked with 1.1 mM drug solution targeting 3.2 equivalents (eq) of free drug, mimicking typical free drug at conjugation and allowing clearance of free drug to be monitored. Protein concentration was adjusted by controlling the amount of feed buffer added to the batch during DF. The FlowVPX system monitored protein concentration in real time. Figure 2 depicts the system setup.

Protein concentration can be calculated by rearranging the Beer–Lambert law ($A = \varepsilon \times c \times l$) (**Equation 1**) to create **Equation 2:** $c = A \div (\varepsilon \times l)$, where A is absorbance, ε is the molar extinction coefficient, c represents concentration, and l is pathlength. When taking a dilution factor (DF) into account, that equation becomes $c = (A \times DF) \div (\varepsilon \times l)$ (**Equation 3**).

To calculate DAR, the molar concentrations of the drug (c_{drug}) and protein (c_{mAb}) must be calculated by simultaneous equations, wherein λ(drug) is the drug-linker wavelength:

Equation 4:

$$c_{mAb} = (A_{280}\varepsilon_{drug}^{\lambda(drug)} - A_{\lambda(drug)}\varepsilon_{drug}^{280}) \div [(\varepsilon_{mAb}^{280}\varepsilon_{drug}^{\lambda(drug)} - \varepsilon_{mAb}^{\lambda(drug)}\varepsilon_{drug}^{280}) \times l\,]$$

Equation 5:

$$c_{drug} = (A_{280}\varepsilon_{mAb}^{\lambda(drug)} - A_{\lambda(drug)}\varepsilon_{mAb}^{280}) \div [(\varepsilon_{drug}^{280}\varepsilon_{mAb}^{\lambda(drug)} - \varepsilon_{drug}^{\lambda(drug)}\varepsilon_{mAb}^{280}) \times l\,]$$

The DAR is given by this equation: $DAR = c_{drug} \div c_{mAb}$ (**Equation 6**).

Slope spectroscopy alters the Beer–Lambert Law by moving the pathlength term (l) to the left-hand side of the equation: $A \div l = \varepsilon \times c$ (**Equation 7**).

The linear equation from the regression of absorbance against pathlength data can be written as **Equation 8:** $A = m \times l + b$, where m is the slope of the regression line and b is the y-intercept of the linear equation. The units of the slope term in the regression equation are absorbance/pathlength and thus are expressed as Abs/mm. That dimensional equality enables direct replacement of ($A \div l$) with the slope term m from Equation 8. This substitution yields the slope spectroscopy equation: $m = \varepsilon \times c$ (**Equation 9**).

Absorbance against pathlength data obtained by the FlowVPX system create a linear regression, which can be used to calculate sample concentration as shown in Equation 9. Then, each concentration measurement is plotted on a graph in the software, allowing real-time monitoring of concentration over time.

In addition to the slope value, the FlowVPX linear regression analysis provides a coefficient of determination (R^2), which indicates linearity of measured data and thus confirms compliance with the Beer–Lambert law. That parameter serves as a real-time, built-in quality check for all measurements taken by the FlowVPX system. SoloVPE data were collected using the same method parameters as those for the FlowVPX system. Samples were analyzed in triplicate.

Results and Discussion

Drug Clearance: 5-mg/mL ADC solution was added to the feed vessel and recirculated to establish baselines for protein concentration and free drug (≈40 minutes). Free drug (1.1 mM, 3.2 eq) was used to spike the batch and mimic typical free drug during conjugation, artificially increasing DAR from 4 to 7. ADC concentration and DAR spiking were monitored by the FlowVPX system on the feed line. FlowVPX data collected from the permeate line indicated when the spiked drug started to pass through the permeate. Free-drug clearance then was monitored as the data from the permeate line showed a decrease in UV-vis absorbance.

Figure 3 shows data collected from the permeate (TOP) and feed (BOTTOM) lines with absorbances at two wavelengths. The red and green lines represent free-drug and ADC absorbance, respectively. In the permeate line, the drug began to clear ≈15 minutes postspike with a maximum at ≈130 minutes postspike. Drug absorbance then decreased over the next 100–150 minutes (≈2 DVs), indicating drug clearance. The area between the red curve and the x-axis represents the total cleared drug quantity. About 70% of the drug was cleared within 2 DVs. Clearance rate typically decreases as the concentration of free drug species decreases, and full clearance often is seen at 8–10 DVs.

Drug spike in the feed line was measured before 50 minutes. The trend was marked by a sharp increase in drug absorbance. Throughout DF, the difference between ADC and drug

Figure 3: ViPER software graph readout of permeate (TOP) and feed (BOTTOM) line data; the red line represents free drug concentration, whereas the green line represents antibody–drug conjugate (ADC) concentration. (DV = diavolume)

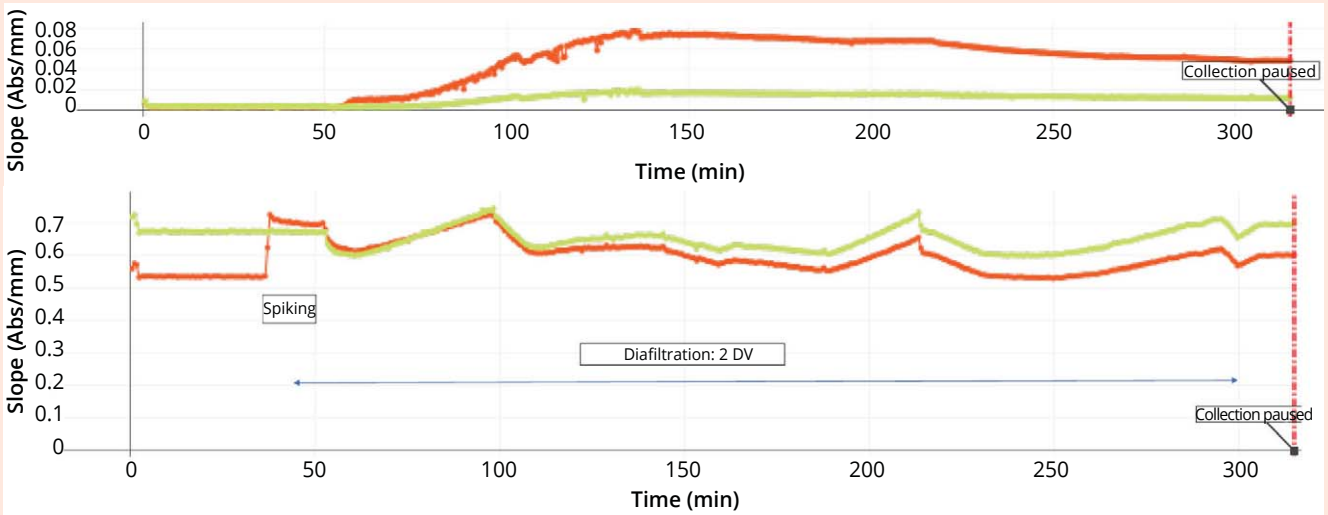

slopes gradually widened due to free-drug clearance. Figure 4 compares DAR data against cycle counts; one cycle is equal to one concentration measurement. The spike was indicated by an increase in DAR from 4 to 7. Final DAR was 4.8 after 2 DVs.

Protein concentration was controlled during DF by using a line marked on the vessel to help maintain the batch level with buffer addition. Samples were taken from the vessel at specified points and analyzed using a previously developed SoloVPE method to enable comparison of the two datasets (**1**). SoloVPE and FlowVPX data are shown in Table 1. Agreement between the two systems was calculated by **Equation 10:**

$$\textit{Agreement} = (\textit{FlowVPX data} \div \textit{SoloVPE data}) \times 100\%$$

ADC Concentration: In a separate run, the team assessed the FlowVPX system's ability to monitor protein concentration. A known amount of ADC was added to the vessel followed by concentration and dilution phases. Each concentration was performed by opening the permeate line with the buffer feed pump turned off. Table 2 lists an overview of concentration and dilution steps. Each step was monitored by the FlowVPX system in the feed line; samples were taken from the retentate line due to low batch volume for comparison with the SoloVPE system. Table 3 lists reported protein concentrations with theoretical values. Figure 5 shows FlowVPX real-time data during concentration and dilution.

Figure 4: Drug:antibody ratio (DAR) plotted against cycle counts

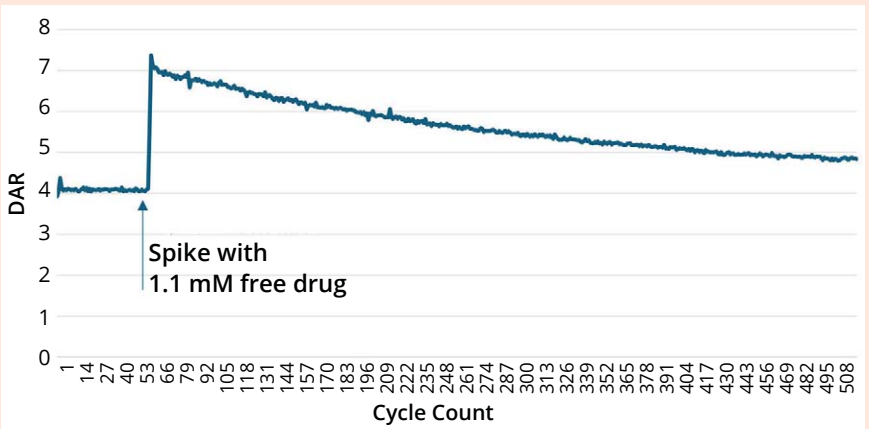

Table 1: Protein concentration data acquired with FlowVPX and SoloVPE systems; DF = diafiltration, DV = diavolume, eq = equivalents

Sample Stage	Protein Concentration		Agreement Between Systems
	FlowVPX System	SoloVPE System	
Initial recirculation	4.35 mg/mL	4.35 mg/mL	100.0%
After 3.2 eq drug spike	4.05 mg/mL	4.10 mg/mL	98.8%
DF, during first DV	3.98 mg/mL	4.01 mg/mL	99.3%
DF, after first DV	3.80 mg/mL	3.81 mg/mL	99.7%
DF, after second DV	4.30 mg/mL	4.65 mg/mL	92.5%
After final concentration	4.40 mg/mL	4.40 mg/mL	100.0%

Theoretical protein concentrations only can be calculated accurately if the batch volume is known. Concentration (c) and volume (v) are related by **Equation 11:** $c_1 \times v_1 = c_2 \times v_2$.

Theoretical protein concentrations were calculated for samples UF1, UF2, and UF6. UF6 was overconcentrated in error by 5%, which accounts for the slightly higher FlowVPX data compared with theoretical values. Discrepancies between calculated and measured protein concentrations could be explained by slow flow rates. Additionally, the batch might not have been completely homogeneous when samples were taken.

FlowVPX measurements typically fell between 90% and 110% of corresponding SoloVPE measurements, showing good agreement between the two systems. Homogenization of the concentrated samples can be affected by low flow rates; therefore, samples were taken

Figure 5: Real-time FlowVPX data during concentration and dilution steps; the red line represents free drug concentration, whereas the green line represents antibody–drug conjugate (ADC) concentration.

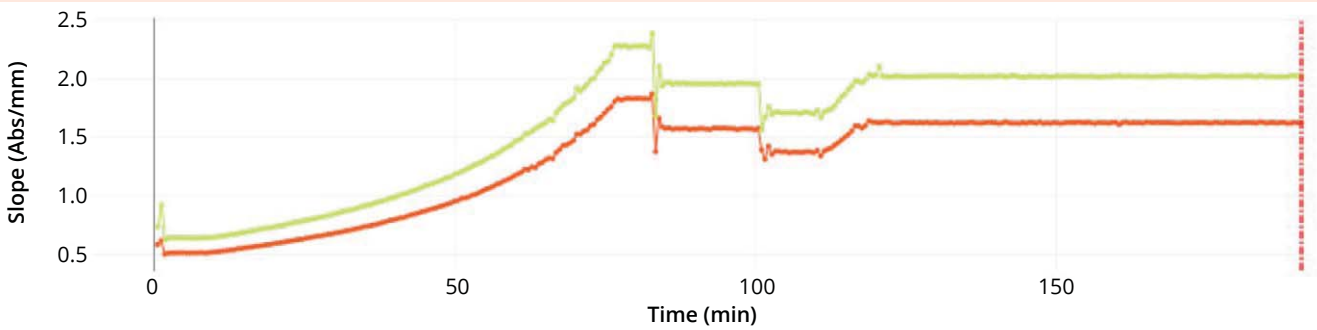

Table 2: Ultrafiltration (UF) steps; ADC = antibody–drug conjugate

Action	Sample Reference
ADC added and recirculated to mix with buffer	UF1
UF batch concentration	UF2
Further UF batch concentration	UF3
Batch diluted with 10-mL buffer	UF4
Batch further diluted with 10-mL buffer	UF5
Batch concentrated, 10-mL buffer removed	UF6

Table 3: FlowVPX and SoloVPE ultrafiltration (UF) data; Conc. = concentration, Contrib. = contribution, mAb = monoclonal antibody, NA = not applicable

Sample	Protein Concentration			Agreement Between FlowVPX and SoloVPE data
	Theoretical	Measured FlowVPX Data	Measured SoloVPE (Total Conc., mAb, and Drug Contrib.)	
UF1	4.16 mg/mL	4.12 mg/mL	–	–
UF2	8.50 mg/mL	9.59 mg/mL	10.39 mg/mL	92.3%
UF3	NA[a]	12.59 mg/mL	NA[b]	NA
UF4	11.93 mg/mL[c]	12.56 mg/mL	NA[b]	NA
UF5	10.07 mg/mL[c]	10.99 mg/mL	11.05 mg/mL	99.5%
UF6	12.60 mg/mL[c]	12.96 mg/mL	11.69 mg/mL	110.9%

[a] Theoretical concentration could not be calculated because the batch volume was unknown.
[b] No sample taken.
[c] Theoretical concentration calculated based on previous FlowVPX data. Differences between UF4 and UF6 theoretical values are due to sampling (removal of material), inaccurate collection of 10 mL with permeate at UF4, and differences between measured readings.

before complete homogenization. FlowVPX data (Figure 5) match expected changes in concentration. Protein concentration changed gradually during the TFF process and decreased sharply when buffer was added to dilute the batch.

Conclusion

This study demonstrates that the FlowVPX System can be a useful tool during ADC process development and manufacturing. Free-drug clearance can be monitored in real time, reducing the overall time required and providing cost savings when developing robust TFF processes.

By enabling real-time monitoring of critical parameters, the FlowVPX system significantly reduces the time required for data turnaround and process validation, allowing manufacturing teams to make immediate, informed decisions. In-line measurements avoid the need for extensive off-line analysis and simplify the transfer of robust processes to manufacturing environments. Batch-volume control also improved during DF. The FlowVPX system can reduce the complexity of monitoring long TFF operations and shorten timelines.

The FlowVPX system can facilitate comprehensive process understanding by providing continuous monitoring of DAR and mAb concentration during TFF. Prompt feedback on process conditions supports swift troubleshooting and effective optimization of UF and DF processes. In this study, drug clearance was monitored with the FlowVPX system, enabling determination of the optimum number of DVs for removal of unwanted molecules. Constant monitoring is instrumental in large-scale processing to identify issues that arise, such as leaks or membrane fouling. Overall, implementing the FlowVPX system in ADC manufacturing offers efficient sample management, reduced costs for operation and consumables, rapid feedback and data turnaround, and constant product quality monitoring.

Acknowledgments

We thank Priya Arora (head of development, Piramal Pharma Solutions), Irene Perez (process development manager, Piramal Pharma Solutions), and Joe Ferraiolo (director of bioanalytics applications, Repligen Corporation) for their contributions to this study.

Statement of Interest

Research detailed here received technical support from Repligen. The authors affirm that Repligen's involvement in the research did not influence the presentation of results or conclusions drawn in this manuscript.

Reference

1 Nixon M, François B, Validation of ADC Platform for Protein Concentration and the Drug-Antibody Ratio (DAR) Using Variable Pathlength Technology. *ADC Rev. J. ADCs* 5 December 2023; https://www.adcreview.com/articles/validation-of-adc-platform-for-protein-concentration-and-the-drug-antibody-ratio-dar-using-variable-pathlength-technology.

Fiona Ford *is a protein scientist, and* ***Melissa Nixon*** *is senior analytical development scientist, both at Piramal Pharma Solutions, Earls Road, Grangemouth, Stirlingshire, FK3 8XG, UK.* ***Bérengère François*** *is bioanalytics field application specialist (EU manager) at Repligen Corporation; 41 Seyon Street, Building 1, Suite 100 Waltham, MA 02453.*

Putting the Genie Back into the Bottle

How Controlled Freezing Preserves Integrity of Bottled Biologics

Claus Exenberger

The integrity of high-value biologic products necessitates a consistent and controlled cold chain during storage and transport. Such substances are thermally unstable; thus, freezing, cold storage, and thawing impose significant stresses on their integrity. If improperly managed, those stresses can compromise activity or even create harmful degradation products. Robust cold-chain control is therefore essential to preserving product quality, identity, purity, and potency. Although single-use bags have become increasingly common as primary packaging for drug substances, single-use bottles remain widely used in biomanufacturing.

Figure 1: Post-freezing change in dye concentration (%) for top and bottom levels of bottles with uncontrolled freezing technologies (adapted from **1**).

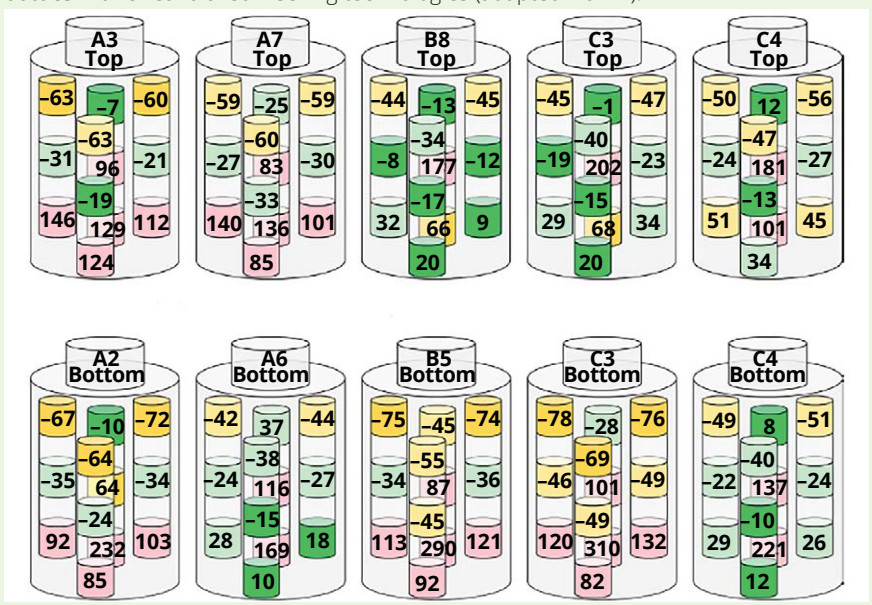

Role of Bottles in Biomanufacturing

Bottles are used routinely, from aliquoting and intermediate storage to final bulk drug-substance handling. However, their rigid and bulky geometry introduces distinctive technical challenges. Unlike flexible, two-dimensional (2D) bags, which exhibit low water columns, bottles have comparatively high volume:surface area ratios, resulting in slower and less homogeneous heat transfer. Delays in removing heat from a container's liquid center can influence freezing.

Bottles typically are frozen upright, which shapes how ice fronts propagate. That factor can limit scalability and increase the need for specialized equipment to ensure consistent and reproducible freeze profiles.

Mechanisms and Risks: Freezing biologics involves more than simply lowering temperature. In such a complex thermodynamic process, for example, protein solutions can supercool below their equilibrium freezing point before ice nucleation initiates. Once nucleation begins, the release of latent heat temporarily stabilizes temperature until solidification advances. During that progression, several stability risks emerge in parallel. *Cryoconcentration* occurs as the forming ice phase consists of nearly pure water, resulting in a progressive enrichment of proteins, salts, and buffering components in the remaining unfrozen fraction.

The resulting increase in local solute concentrations can promote protein denaturation or aggregation, and shifts in pH can disrupt protein structures further. As ice fronts develop, newly generated ice–liquid interfaces can adsorb proteins and induce unfolding; trapped air bubbles introduce additional interfacial stresses that compromise molecular stability.

In bottles, uncontrolled freezing frequently produces a characteristic "volcano effect." As ice fronts advance from the side walls and bottom, inward expansion forces the remaining solute-rich liquid toward the center and upward, which forms a cone-shaped region of concentrated material.

Blast Freezing Improves Thermal Performance

To mitigate non-uniform freezing with bottles, manufacturers increasingly use *blast freezing* (also known as *convective freezing*), which manipulates high-velocity airflow to remove heat more efficiently compared with static freezing. By stabilizing and

homogenizing cold-air distribution, blast freezing minimizes thermal gradients that otherwise would exacerbate cryoconcentration.

Single Use Support's RoSS.BLST blast freezer is a modular, protocol-driven system that uses high-volume airflow to ensure uniform temperature distribution, supporting controlled cooling to –80 °C. Its design enables biomanufacturers to tailor freezing profiles to individual drug substances, which can improve reproducibility during technology transfers. The system can hold bottles of 30 mL to 10 L and has a loading capacity of up to 192 2-L bottles per run.

Impact on Quality

The Management Center Innsbruck and Single Use Support performed blast-freezing tests to understand cryoconcentration of solutes within bottles (**1**). A surrogate solution of sucrose, NaCl, and phosphate buffers was supplemented with Naphthol Blue Black dye (MilliporeSigma) to visualize concentration gradients throughout the frozen matrix. Analysis revealed pronounced heterogeneity; deviations in dye concentration exceeded 80% in certain regions of each bottle (Figure 1). Conductivity and dye absorbance were consistently higher in lower and middle bottle segments than in upper segments. Such results demonstrate that liquid cores solidified last, indicating solute migration during the final phase of freezing.

In extreme cases, cryoconcentration differed by >300% between top and bottom sections. Those results demonstrate the extent to which uncontrolled freezing can distort solute distribution. Visual inspection confirmed the presence of the characteristic volcano effect (Figure 2). Such results underscore the need for controlled-rate freezing to minimize solute redistribution.

Controlled Blast Freezing for Product Integrity: Controlled-rate freezing (ideally within –0.1 to –0.5 °C per minute) helps to stabilize the phase transition and reduces the severity of cryoconcentration (**2, 3**). The RoSS.BLST blast freezer applies optimized airflow patterns to limit formation of uncontrolled ice fronts and to promote uniform solidification throughout bottles. Comparative testing showed that dye — and thus solute — distribution was homogeneous under controlled conditions. Conductivity measurements also differed less across different bottle sections, demonstrating consistent distribution of components. The resulting ice morphology was uniform, reducing structural stresses (e.g., air bubbles and cracks) that denature proteins.

Figure 2: Comparison of volcano effects in bottles occurring in uncontrolled freezing and consistent distribution in controlled freezing (adapted from **1**); CC = cryoconcentration

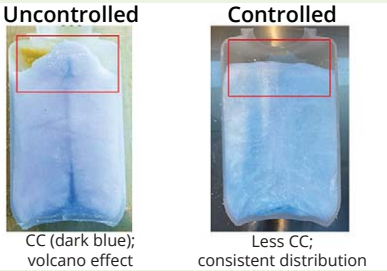

Ensuring container–closure integrity during cold-chain operations is crucial for safety and efficiency. Bottle caps or attached single-use assemblies can become brittle when frozen. Single Use Support's Bottle RoSS container provides robust secondary protection for bottle caps and tubing assemblies. It offers a tamper-evident barrier for safe handling of diverse bottle formats and reduces the likelihood of product loss.

Operational and Sustainability Efficiency: Beyond product quality, controlled blast freezing also addresses process efficiency and decarbonization. With a best-in-class ratio of chamber volume to overall footprint, the RoSS.BLST blast freezer offers a compact solution for high-density loading in manufacturing facilities. It contributes sustainability initiatives by using natural refrigerants (R290 and R170) with reduced global-warming potential. Natural refrigerant charges remain <500 g, eliminating the need for additional room-safety measures. The system also supports controlled thawing with integrated shaking for uniform temperature distribution.

Conclusion

As batch sizes and molecule sensitivity increase, uncontrolled freezing is no longer a tolerable risk. Maintaining safe freezing of biologics in bottles requires a holistic, end-to-end strategy that encompasses automated filling, controlled freezing, secure cold storage, and temperature-monitored transport. Combining modularity, compatibility, sustainability, and good manufacturing practice (GMP) readiness, controlled blast-freezing systems help process engineers perform reliable and efficient technology transfers. Aligning such systems with Annex 1 expectations and ensuring compatibility across bottle suppliers transforms a longstanding bottleneck into a dependable, high-quality manufacturing step. With advanced controlled-freezing technologies, biomanufacturers finally can put the "genie" back into the bottle for reliable primary packaging of sensitive biologics and cold-chain processes.

References

1 Exenberger C. *How Blast Freezing Affects the Quality of Bottled Drug Substance: Test Results and Insights.* Single-Use Support: Kufstein, Austria, 25 September 2025.

2 Minatovicz B, et al. Large-Scale Freeze-Thaw of Protein Solutions: Study of the Relative Contributions of Freeze-Concentration and Ice Surface Area on Stability of Lactate Dehydrogenase. *J. Pharm. Sci.* 112(2) 2023: 482–491.

3 Singh SK, et al. Large-Scale Freezing of Biologics. *BioProcess Int.* 11(10) 2009: 32–44.

Claus Exenberger *is technical product owner for freeze/thaw systems at Single Use Support GmbH, Endach 36, 6330 Kufstein, Austria; sales@susupport.com; https://www.susupport.com.*

BioProcess International

by informa

BPI eBooks provide focused discussions on emerging therapeutic modalities and critical aspects of biomanufacturing and biopharmaceutical business.

Highly targeted and gated, BPI's eBook series focuses on the emerging technologies and therapies transforming bioprocess research, development, and manufacturing. Every month, BPI eBooks provide sponsors with the opportunity to connect their expertise to targeted themes while delivering highly qualified lead generation. And new topics are sure to be added throughout the year.

MONTH	THEME
January	Outsourcing
February	Scale-Up; Quality and Analytics
March	Emerging Modalities; Continuous Bioprocessing
April	Sustainability; Downstream Processing
May	Bioconjugates and ADCs; Process-Related Impurities
June	Chromatography; Manufacturing Capacity
July	AI, Automation, and Industry 4.0
August	Allogeneic Cell Therapies; Tech Transfer; BPI Theater at BIO; Industry Benchmark Report
September	Product-Related Impurities; Downstream Intensification
October	Autologous Cell Therapies; QA/QC
November	Bioreactors and Continuous Processes; Bioregions: Europe
December	Gene Therapies; Upstream Processing

Contact the editors for more information:
Brian Gazaille (brian.gazaille@informa.com)
Sarah Stefancin (sarah.stefancin@informa.com).

Browse the complete archive online at
https://bioprocessintl.com/ebooks/

For more information, download our media kit.

Coatings in Cleanroom Design

Empowering Safe and Sterile Environments for Making Life-Saving Medicines

Sharon Lee

Biopharmaceutical manufacturing operates at the intersection of strict regulatory compliance and groundbreaking innovation. At the heart of the industry are *cleanrooms*: highly controlled environments that are designed to ensure sterility, minimize contamination, and protect the integrity of life-saving therapies. Although much focus for cleanrooms centers on ventilation systems and filtration, an important yet often-overlooked element is high-performance coatings. When applied to floors, walls, ceilings, and other surfaces, such coatings are foundational to the functionality and reliability of cleanrooms and the aseptic processes that they house. The ability of specialized coatings to withstand chemical exposure, facilitate surface cleaning, and maintain durability under rigorous conditions makes them vital to cleanroom design. Here's how high-performance coatings empower biopharmaceutical facilities to achieve compliance and operational excellence.

High-performance coatings are specialized protective materials — e.g., epoxies, polyurethanes, and polyaspartics — that are designed to withstand harsh industrial and/or commercial environments. Unlike standard paint, they offer superior resistance to abrasion, corrosion, ultraviolet rays, chemicals, and extreme temperatures. These coatings are used on steel structures, machinery, concrete floors, and pipelines, as well as in marine or aerospace applications, to prevent degradation and extend asset life. In the biopharmaceutical industry, such materials most often are applied to cleanroom flooring, walls, and other surfaces. Favored for helping to create seamless, nonporous, and hygienic environments, epoxy flooring systems are the most common coated surfaces in pharmaceutical cleanrooms. Epoxies offer high chemical resistance to disinfectants and superior durability. Polyurethane and methyl methacrylate (MMA) coatings are also frequently used for specific high-traffic or rapid-curing needs.

Managing Compliance in a Complex Regulatory Landscape

Biopharmaceutical manufacturers operate within a tightly regulated industry, adhering to current good manufacturing practices (CGMPs) and guidelines from authorities such as the US Food and Drug Administration (FDA) and the European Medicines Agency (EMA) to ensure product quality and consumer safety. Cleanrooms in biomanufacturing facilities must meet stringent sterility and hygiene standards, and the surfaces within those environments play a pivotal role in ensuring regulatory compliance. High-performance coatings are engineered specifically to help companies meet such needs by creating smooth, nonporous surfaces that prevent microbial growth by eliminating gaps where contaminants could hide. Those surfaces need to withstand repeated exposure to harsh cleaning protocols involving aggressive disinfectants, sterilants, and other cleaning chemicals.

HTTPS://STOCK.ADOBE.COM

By delivering those essential elements, high-performance coatings help biomanufacturers minimize contamination risk, comply with regulations, and prevent costly disruptions caused by noncompliance and/or contamination incidents.

Minimizing Downtime and Maximizing Efficiency

In biopharmaceutical manufacturing, even brief periods of downtime can disrupt production schedules and jeopardize product delivery. High-performance coatings are designed to enhance operational efficiency and minimize disruptions by enabling rapid turnaround and supporting environmental-sustainability initiatives. Coatings with rapid cure times, such as MMA and polyurethane, provide for timely installation and maintenance, reducing facility downtime during repairs and shutdowns. Engineered to withstand heavy foot traffic and machinery as well as repeated chemical exposure, coatings such as epoxies can reduce the frequency of surface repairs or replacements. And many coatings come in water-based formulations with low levels of volatile organic compounds

(VOCs) that still maintain high performance. Such formulations align with the industry's growing focus on environmental responsibility. By optimizing operational uptime and extending the lifespan of cleanroom surfaces, high-performance coatings can help biomanufacturers safeguard their production schedules, ensure product quality, and protect their outgoing supply chains.

Meeting the Challenges of Cleanroom Design

Cleanrooms present distinctive needs that require precision-engineered solutions. High-performance coatings are tailored to meet the specific needs of biopharmaceutical environments. Seamless flooring systems eliminate cracks, seams, and joints where contaminants could collect, ensuring a hygienic and sterile environment. Chemical-resistant protective finishes for walls and ceilings resist stains, abrasions, and harsh cleaning agents to maintain their integrity over time. For facilities where static electricity can pose safety or contamination risks, specialized coatings can dissipate static charges and contribute to both operator safety and product quality. Such adaptabilities enable high-performance coatings to address the unique operational, environmental, and safety challenges of each cleanroom application.

The Future of Coatings in Biopharmaceutical Manufacturing

As biopharmaceutical manufacturing evolves, the role of coatings continues to expand. Emerging technologies, such as microbially resistant coatings, are offering new ways to help reduce contamination risks and extend maintenance cycles. Future-proofing cleanroom design includes prioritizing high-performance coatings. By investing in such solutions, biomanufacturers can enhance the safety of their facilities, ensure compliance with evolving regulations, and stay ahead in an increasingly demanding industry. High-performance coatings are more than just a finishing touch; they are a foundational component of cleanroom design. By promoting sterility, durability, and compliance, they empower biomanufacturers to deliver life-saving products with confidence.

Further Reading

Sandle T. Cleanroom Decontamination: Application of Hydrogen Peroxide Vapor Following Maintenance Activities. *BioProcess Int*. 13 May 2025; https://www.bioprocessintl.com/facility-design-engineering/cleanroom-decontamination-application-of-hydrogen-peroxide-vapor-following-maintenance-activities.

Gazaille B, et al. Beyond Traditional Microbiology Testing: Developing a Comprehensive Strategy for Microbial Control and Detection. *BioProcess Int*. 30 September 2025; https://www.bioprocessintl.com/qa-qc/beyond-traditional-microbiology-testing-developing-a-comprehensive-strategy-for-microbial-control-and-detection.

Sandle T. Establishing Microbiological and Particulate Controls When Reworking a Sterile Drug Product. *BioProcess Int*. 19 September 2023; https://www.bioprocessintl.com/qa-qc/establishing-microbiological-and-particulate-controls-when-reworking-a-sterile-drug-product.

Sandle T. A Case Study in Environmental Monitoring: Reviewing Incubation Times Upon Recovery of Microorganisms. *BioProcess Int*. 21 March 2023; https://www.bioprocessintl.com/qa-qc/a-case-study-in-environmental-monitoring-reviewing-incubation-times-upon-recovery-of-microorganisms.

Scott C. Introduction: Practicalities of Aseptic Processing for Modern Biological Drug Products. *BioProcess Int.* 21 March 2023; https://www.bioprocessintl.com/fill-finish/introduction-practicalities-of-aseptic-processing-for-modern-biological-drug-products.

Sandle T. Risk Considerations for Aging Pharmaceutical Facility Cleanrooms. *BioProcess Int.* 21 May 2021; https://www.bioprocessintl.com/facility-design-engineering/risk-considerations-for-aging-pharmaceutical-facility-cleanrooms.

Nieuwenhuizen P. Aseptic Considerations in Formulation, Fill and Finish: Choosing Between Barrier and Isolator Technologies. *BioProcess Int.* 30 September 2021; https://www.bioprocessintl.com/fill-finish/aseptic-considerations-in-formulation-fill-and-finish-choosing-between-barrier-and-isolator-technologies.

Sandle T. Expanding Considerations in Cleaning Validation: Risks Posed By Indirect Product-Contact Surfaces on Pharmaceutical Equipment. *BioProcess Int.* 20 October 2022; https://www.bioprocessintl.com/validation/expanding-considerations-in-cleaning-validation-risks-posed-by-indirect-product-contact-surfaces-on-pharmaceutical-equipment.

Sharon Lee *is the North American pharmaceutical market segment manager for Sherwin-Williams Protective & Marine, 101 West Prospect Avenue, Cleveland, OH 44115; https://industrial.sherwin-williams.com/na/us/en/protective-marine.html. She has been in the coatings market for over 16 years and is active in local International Society for Pharmaceutical Engineering (ISPE) and Association for Materials Protection and Performance (AMPP) chapters.*

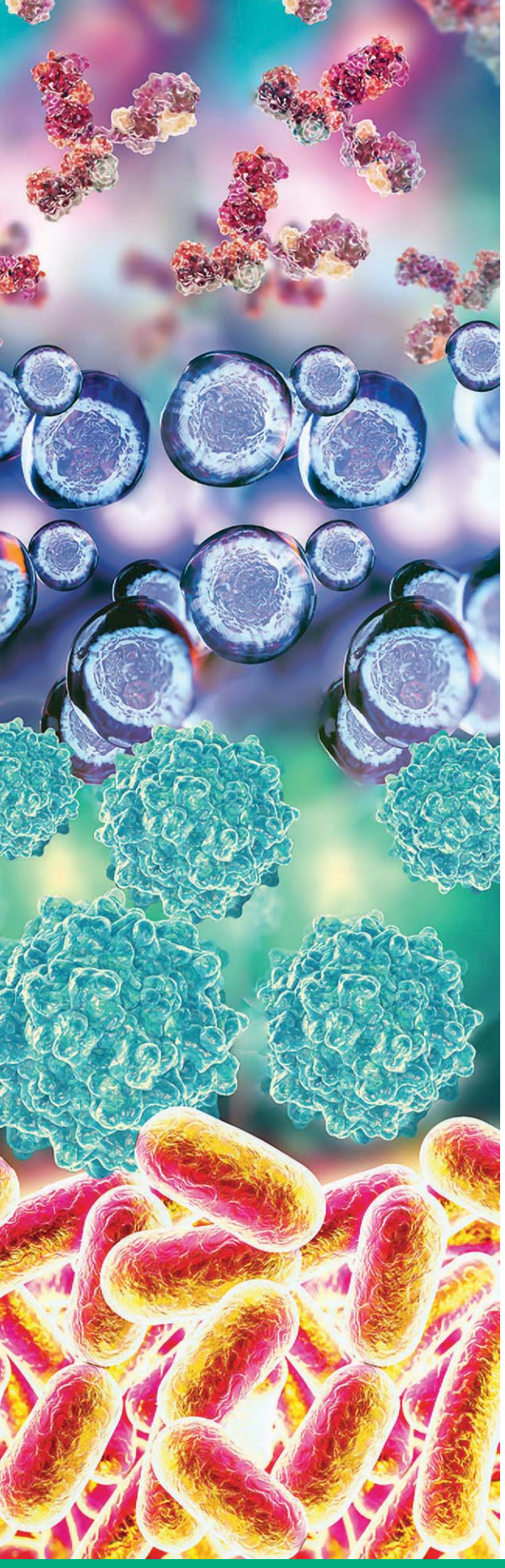

FUJIFILM
Value from Innovation

As **Partners for Life**, our CDMO services and life science solutions support therapeutics from discovery to commercialization.

Our CDMO Modalities

- Mammalian Cell Culture
- Microbial Fermentation
- Cell & Gene Therapy
- Vaccines

FUJIFILM
FUJIFILM Biotechnologies

Contact us to discuss your project and learn how we can be Partners for Life.

fujifilmbiotechnologies.fujifilm.com

Partners for *Life*

Bora Biologics

BUILT FOR COMMERCIAL

engineered for scale

JOIN US

Bio International Convention

June 22–25, 2026 | San Diego, CA

Visit us at Booth #5307

Schedule time with our team

bd@borabiologics.com

BIO 2026 • BPI THEATER

Engineering Commercial Readiness

Aligning Scale, Geography, and Launch Risk

Mike Alston Jr.

Executive Director of Operations

JUNE 23, 2026

10:45 AM – 11:15 AM

Immediately following the Keynote